

Berichte

zur Polar-
und Meeresforschung

653
2012

Reports
on Polar and Marine Research



Joint Russian-German Polygon Project
East Siberia 2011 - 2014: The expedition Kytalyk 2011

Edited by
Lutz Schirrmeister, Lyudmila Pestryakova,
Sebastian Wetterich and Vladimir Tumskoy
with contributions of the participants



ALFRED-WEGENER-INSTITUT FÜR
POLAR- UND MEERESFORSCHUNG
in der Helmholtz-Gemeinschaft
D-27570 BREMERHAVEN
Bundesrepublik Deutschland

ISSN 1866-3192

Hinweis

Die Berichte zur Polar- und Meeresforschung werden vom Alfred-Wegener-Institut für Polar- und Meeresforschung in Bremerhaven* in unregelmäßiger Abfolge herausgegeben.

Sie enthalten Beschreibungen und Ergebnisse der vom Institut (AWI) oder mit seiner Unterstützung durchgeführten Forschungsarbeiten in den Polargebieten und in den Meeren.

Es werden veröffentlicht:

- Expeditionsberichte
(inkl. Stationslisten und Routenkarten)
- Expeditions- und Forschungsergebnisse
(inkl. Dissertationen)
- wissenschaftliche Berichte der
Forschungsstationen des AWI
- Berichte wissenschaftlicher Tagungen

Die Beiträge geben nicht notwendigerweise die Auffassung des Instituts wieder.

Notice

The Reports on Polar and Marine Research are issued by the Alfred Wegener Institute for Polar and Marine Research in Bremerhaven*, Federal Republic of Germany. They are published in irregular intervals.

They contain descriptions and results of investigations in polar regions and in the seas either conducted by the Institute (AWI) or with its support.

The following items are published:

- expedition reports
(incl. station lists and route maps)
- expedition and research results
(incl. Ph.D. theses)
- scientific reports of research stations
operated by the AWI
- reports on scientific meetings

The papers contained in the Reports do not necessarily reflect the opinion of the Institute.

The „Berichte zur Polar- und Meeresforschung“
continue the former „Berichte zur Polarforschung“

* Anschrift / Address

Alfred-Wegener-Institut
für Polar- und Meeresforschung
D-27570 Bremerhaven
Germany
www.awi.de

Editor:

Dr. Horst Bornemann

Assistant editor:

Birgit Chiaventone

Die "Berichte zur Polar- und Meeresforschung" (ISSN 1866-3192) werden ab 2008 als Open-Access-Publikation herausgegeben (URL: <http://epic.awi.de>).

Since 2008 the "Reports on Polar and Marine Research" (ISSN 1866-3192) are available as open-access publications (URL: <http://epic.awi.de>)

Joint Russian-German Polygon Project
East Siberia 2011 - 2014: The expedition Kytalyk 2011

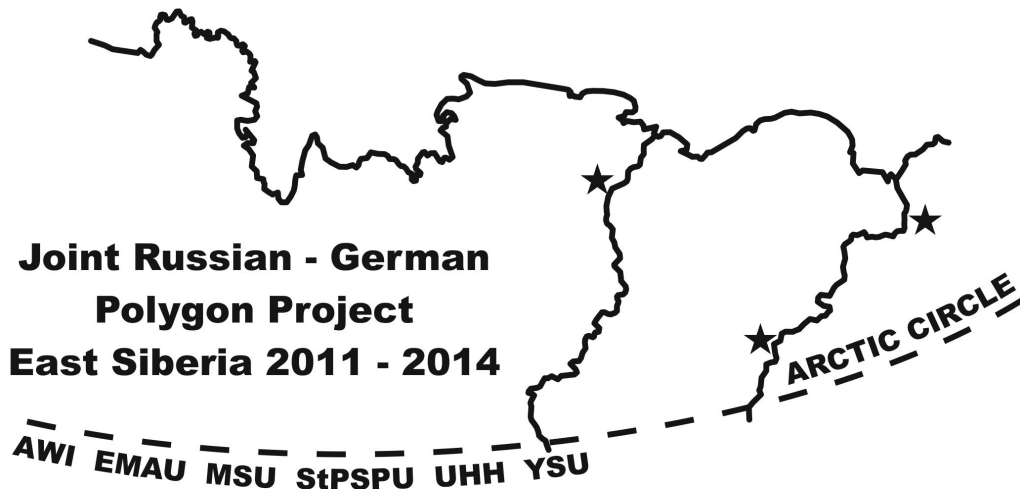
Edited by

**Lutz Schirrmeister, Lyudmila Pestryakova,
Sebastian Wetterich and Vladimir Tumskoy**

with contributions of the participants

Please cite or link this publication using the identifier
hdl: 10013/epic.40369 or <http://hdl.handle.net/10013/epic.40369>

ISSN 1866-3192



July 01 – September 05, 2011

Kytalyk, Indigirka Lowland, East Siberia

Russian expedition leaders:

Prof. Lyudmila Pestryakova
Yakutsk Federal University
Belinsky st., 58, 677000 Yakutsk, Russia

Dr. Vladimir Tumskoy
Department of Geocryology, Faculty of Geology,
Moscow State University
Vorob`evy Gory, 119992 Moscow, Russia,

German expedition leader:

Dr. Lutz Schirrmeister
Alfred Wegener Institute for Polar and Marine Research
Department of Periglacial Research
Telegrafenberg A5, 14473 Potsdam, Germany

CONTENT

Chapter 1	Introduction	1
	Lutz Schirrmeister & Lyudmila Pestryakova	
Chapter 2	Study area, geological and geographical characteristics	5
	Vladimir Tumskoy & Lutz Schirrmeister	
Chapter 3	Monitoring of a polygon site (KYT-1)	11
	Andrea Schneider & Lutz Schirrmeister	
Chapter 4	Ecological studies of polygonal ponds	24
	Andrea Schneider, Lyudmila Pestryakova & Lutz Schirrmeister	
Chapter 5	Limnological and sedimentological studies	41
	Viktor Sitalo & Dmitry Subetto	
Chapter 6	Records from the model polygon LHC-11 for modern and palaeoecological studies	51
	Annette Teltewskoi, Juliane Seyfert & Hans Joosten	
Chapter 7	Pedological studies of various polygon sites	61
	Fabian Beermann & Lyubov Kokhanova	
Chapter 8	Permafrost exposures	71
	Lutz Schirrmeister & Vladimir Tumskoy	
Chapter 9	Drill holes and pits around Kytalyk	79
	Vladimir Tumskoy & Evgenya Zhukova	
Chapter 10	Moss collection	94
	Andrea Schneider	
Chapter 11	Cryolithological studies in the middle Berelekh area	96
	Vladimir Tumskoy & Evgenya Zhukova	
References		113

Appendix 1	Coordinates of study sites in the Kytalyk area	117
Appendix 2	List of hydrobiological samples Andrea Schneider	119
Appendix 3	Plant taxa from vegetation transect KYT-1 Andrea Schneider	126
Appendix 4	List of moss and lichen samples Andrea Schneider	129
Appendix 5	Plant collection and peat cores from LHC-11 Annette Teltewskoi	136
Appendix 6	Data of soil studies (field analytics) Fabian Beermann	138
Appendix 7	Samples from permafrost deposits Lutz Schirrmeister & Evgenya Zhukova	145
Appendix 8	Water, ice and rain samples Lutz Schirrmeister, Andrea Schneider & Evgenya Zhukova	148
Appendix 9	Water salinity in surface water and texture ice Vladimir Tumskoy	153

1. INTRODUCTION

Lyudmila Pestryakova & Lutz Schirrmeister

1.1 Scientific motivation

Patterned ground of the polygonal tundra yields sensitive indicators of environmental and climate change. Polygon ponds, mires and cryosols are typical components of arctic Siberian wetlands underlain by permafrost.

Within the frame of the joint German-Russian DFG-RFBR project „Polygons in tundra wetlands: state and dynamics under climate variability in Polar Regions (POLYGON)“ and the BMBF project „Joint German-Russian laboratory for studies of environmental dynamics in the terrestrial Arctic (Biological Monitoring - BioM)“, field studies of recent and of Quaternary environmental dynamics were carried out in the Indigirka lowland in summer 2011.

Using a multidisciplinary approach, several stages of polygonal systems were studied (chapter 4) as modern tundra habitats in the surrounding of the WWF station Kytalyk at the Berelekh River, a tributary of the Indigirka River (Fig. 1-1). The floral and faunal associations of the polygonal tundra landscape were described (chapters 5, 10). Ecological, hydrological, meteorological, limnological (chapters 3, 5), pedological (chapter 7) and cryological (chapters 8, 9) features were analyzed in order to evaluate modern environmental conditions and their essential controlling parameters. A monitoring program was carried out to measure changes of air, water and ground temperatures as well as water conductivity, water level and soil moisture and to collect water, zooplankton, phytoplankton and ostracod samples (chapter 3). In addition, exposures, pits and drill cores were studied to understand the cryolithological structures of frozen ground and to collect samples for detailed paleoenvironmental research of the Quaternary past (chapters 8, 9). Cryolithological studies of Yedoma sites and thermokarst depressions were also conducted in the area of the middle Berelekh reaches (chapter 11). Our studies were realized in coordination with Dutch groups from the Vrije Universiteit, Faculty of Earth and Life Sciences in Amsterdam, and the University Wageningen. This report contains systematical description and documentation of field data and observations with all basic information for future analysis of sample collections and interpretation of field data.

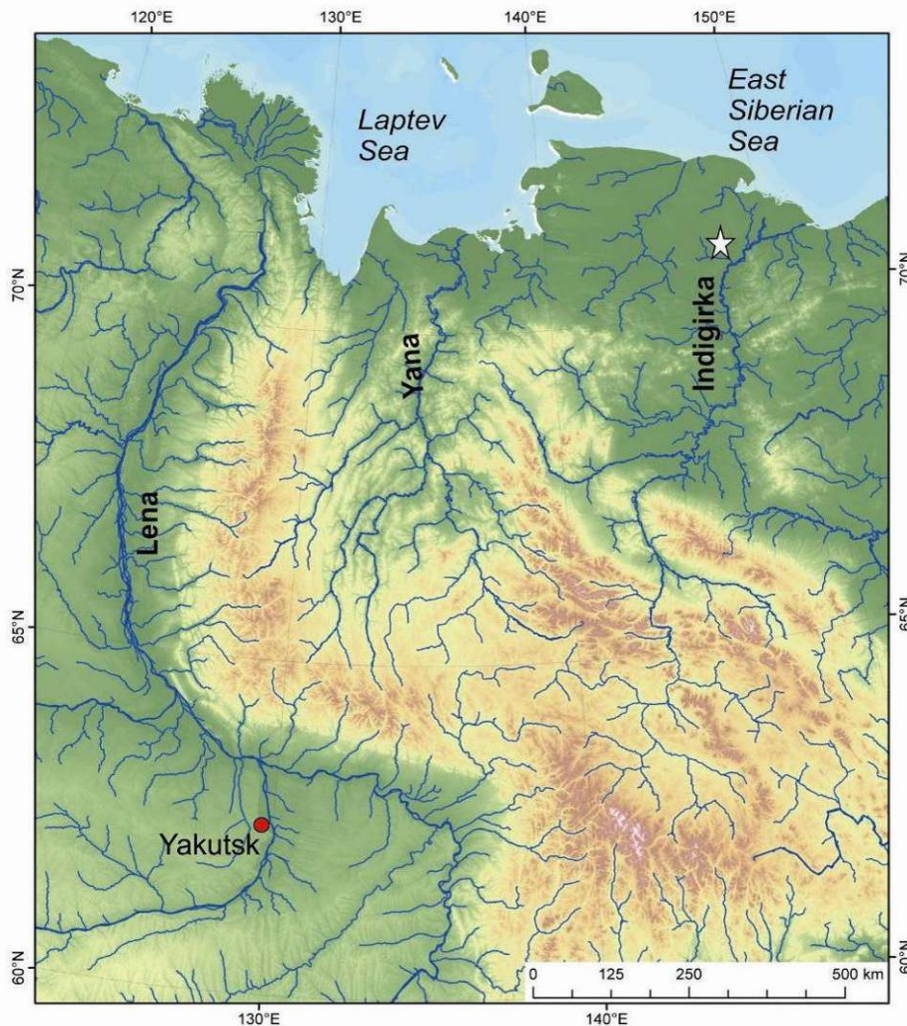


Fig. 1-1: Position of the study area in the Indigirka lowland marked by a white star. DEM compiled by G. Grosse (University of Alaska, Fairbanks, AK).

1.2 Expedition itinerary and general logistics

Field studies in the vicinity of the Kytalyk station and along the Berelekh River were performed from July 14th to August 28th 2011. In total 12 colleagues (6 Germans, 6 Russians) from six different institutes and universities (Tab. 1-1, Fig. 1-2) participated on the expedition. A first group started already in the beginning of July to prepare the expedition in Yakutsk. A second group worked in the field from mid of July to mid of August (Tab. 1-2). The route of the groups was from Moscow via Yakutsk and Chokurdakh by airplane. The travel to the Kytalyk station was continued by boat along the Berelekh River (Fig. 2-1).

The expedition would not have been successfully without the support of several Russian and German institutions and authorities. In particular, we would like to thank the Committee of Nature Conservation in Chokurdakh (Yevgeni Yanyigin, Tatyana Gavrilovna), the North-Eastern Federal University “M.K. Ammosov” (Mikhael Cherosov) and Alexei Pestryakov, our most important logistic support in Yakutsk.

Tab. 1-1: List of participants.

Participant	Competence	Affiliation	E mail
Lyudmilla Pestryakova	Russian coordinator, Phytoplankton	University Yakutsk	lapest@mail.ru
Zina Atlasova	Zoobenthos	University Yakutsk	
Andrea Schneider	Polygon monitoring, ostracod sampling	AWI Potsdam	andrea.schneider@cms.huberlin.de
Lutz Schirrmeister	German expedition, leader, Quaternary geology	AWI Potsdam	lutz.schirrmeister@awi.de
Fabian Beerbaum	Soil science, nutrients	University Hamburg	Fabian.Beerbaum@uni-hamburg.de
Hans Joosten	Mire ecology	University Greifswald	joosten@uni-greifswald.de
Annette Teltewskoi	Vegetation studies	University Greifswald	nette11@gmx.net
Juliane Seyfert	Polygon mapping	University Greifswald	juliane.seyfert@stud.uni-greifswald.de
Viktor Sitalo	Limnology	Herzen University St. Petersburg	sitalo_viktor@mail.ru
Lyubov Kokhanova	Soil ecology	Moscow State University	lubasik10@yandex.ru
Vladimir Tumskoy	Russian expedition leader, Cryolithology	Moscow State University	vtumskoy@rambler.ru
Evgenya Zhukova	Geomorphology,	Moscow State University	checkedz@gmail.com

Tab. 1-2: Time table of the expedition Kytalyk 2011.

Date	Location	Activity
01.07. 2011	Berlin	Departure of the 1 st group
02.07. 2011	Yakutsk	Arrival of the 1 st group
03. to 12.07. 2011	Yakutsk	Expedition preparation
13.07. 2011	Yakutsk to Chokurdakh	Travel by airplane
14./15.07. 2011	Chokurdakh to Kytalyk	Travel by boat
15.07. 2011	Kytalyk	Begin of field work
19.07. 2011	Kytalyk	Arrival of the 2 nd group
11.07. 2011	Kytalyk	Departure of the 2 nd group
27.08. 2011	Kytalyk	End of field work
28.08. 2011	Kytalyk to Chokurdakh	Return by boat
29.08. 2011	Chokurdakh to Yakutsk	Return by airplane
30.08. to 04.09. 2011	Yakutsk	Post expedition processing
05.09. 2011	Yakutsk	Departure of the 1 st group
05.09. 2011	Berlin	Arrival of the 1 st group



Fig. 1-2: The participants of the expedition "Kytalyk 2011"; from the bottom left to top right: L. Koshanova, F. Beermann, A. Schneider, E. Zhukova, J. Seyfert, L. Schirrmeister, H. Joosten, V. Tumskoy, V. Sitalo, A. Teltewskoi, downright: L. Pestryakova, top right: Z. Atlasova.

2. STUDY AREA, GEOLOGICAL AND GEOGRAPHICAL CHARACTERISTICS

Vladimir Tumskoy & Lutz Schirrmeister

The study area of the expedition “Kytalyk 2011” was located in the flood plain and the adjacent thermokarst affected lowland along the Berelekh River 28 km northwest of the settlement Chokurdakh. The Berelekh River is well-known because of the Berelekh “mammoth cemetery” that exists upstream of the river (Vereshchagin, 1977; Vereshchagin & Ukrainseva, 1985; Mochanov, & Fedoseeva, 1996; Pitulko 2011). In the lower stream, after Dzhelon-Sise Highland, which is oriented in NW direction, the river runs for about 80 km in east direction along the Allaikhovski Highland (Fig. 2-1).

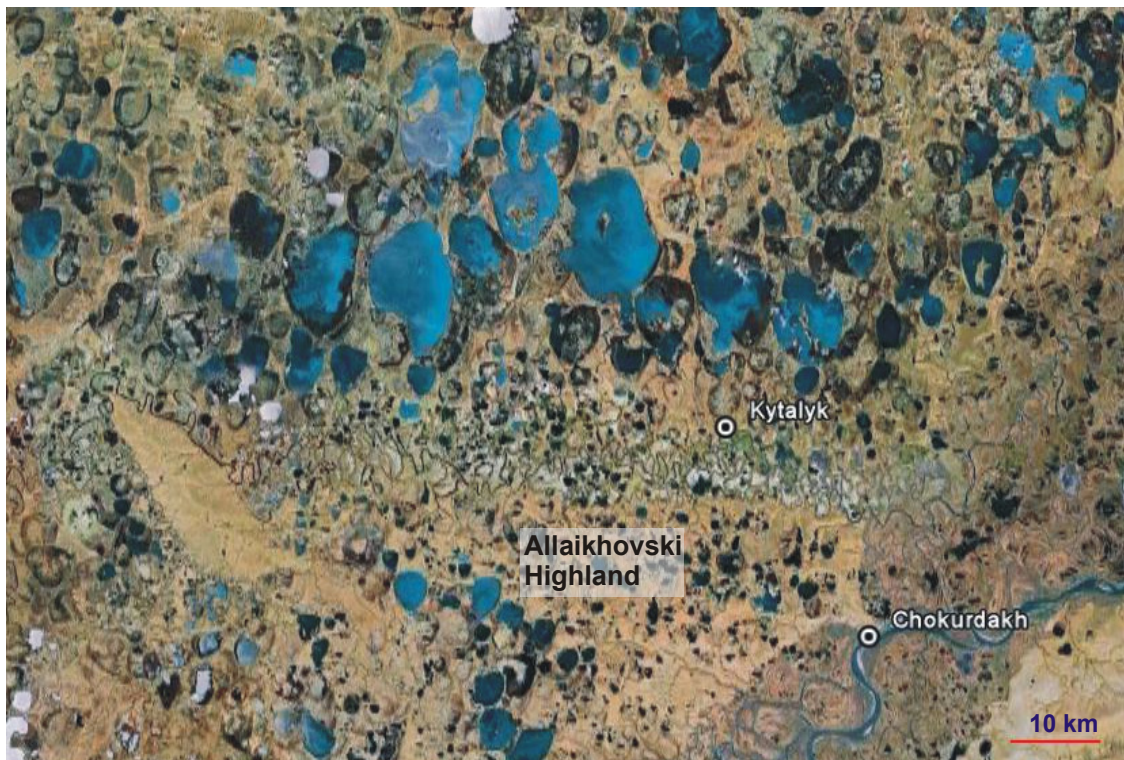


Fig. 2-1: The study region of the Expedition “Kytalyk 2011” in the lower reaches of the Berelekh River near Chokurdakh.

The vegetation is described as a tussock-sedge, dwarf shrub, moss tundra (Rivas Martinez, 2007). According to meteorological data (Chokurdakh, WMO 21946) the climate is characterized by $T_{\text{July}} +9.7^{\circ}\text{C}$, $T_{\text{January}} -36.6^{\circ}\text{C}$, $T_{\text{Mean}} -14.2^{\circ}\text{C}$, and $p_{\text{ann}} 350$ mm. The permafrost temperature in the region is stated at -4 to -6°C (CAVM Team 2003) and the permafrost thickness is mapped to be between 200 to 300 m (Geocryological Map, 1991)

Pre-Quaternary deposits in the study region were found at the left bank of the Indigirka River forming the Kondakovski Hills. The village Chokurdakh is located on sandstone rocks, visible on bank exposures of the Indigirka. In addition, Paleogene to Neogene gravelly sands form the base of the Dzhelon-Sise Highland and occur northwest of this elevation in small terrain steps near the Tastakh Lake (Ovander & Rybakova, 1985). Most of the study region is covered by Quaternary permafrost deposits. The major landscape elements in the Berelekh River valley are:

1. Flood plain and terraces of the Berelekh River, its branches and tributaries;
2. Yedoma hills composed of middle to late Pleistocene Ice Complex deposits (Lavrushin, 1963; Kaplina et al., 1980);
3. Alas depressions with initial and secondary thermokarst lakes formed at the end of the Lateglacial and during the Holocene, which were connected with the accumulation of Alas Complex deposits and of numerous pingo hills.

A separate non typical relief with specific landscapes represents the neotectonical formed Dzhelon-Sise Highland as well as the hills near the Tastakh lake (see chapter 11).

The W-E oriented Berelekh River valley is 4 to 7 km wide in the lower reaches. Because of the very low bias of the valley bottom, the river channel is strongly meandering. Only when flowing into the large Indigirka River valley the direction of the Berelekh River changes to NE. In the lower reaches, the Berelekh River valley is bounded to the south by the Allaikhovski Highland (about 70 m a.s.l.) and to the north by an alas plain that contains several Yedoma hills of 20 to 30 m height (Fig. 2-1). The Allaikhovski Highland consists of middle and late Pleistocene deposits. The upper 30 to 40 m of these sequences are composed of ice-rich Ice Complex deposits (Kaplina et al., 1980). This affected the development of thermokarst processes and the formation of numerous thermokarst lakes.

The hydrology of the Berelekh River is controlled by the essential influence of the Indigirka River, the low biases of the valley bottom, the position of the upper reaches in the Polousnyi Ridge, and the occurrence of continuous permafrost. During winters some segments in the upper and the middle reaches of the river are frozen down to the bottom reducing the river runoff (Mukhin & Tolstov, 1960). The spring flood is long and high-connected with the latitudinal position of the river valley and the back-flooding by the Indigirka River. The high-water level is about 3 to 4 m. The water depth near Kytalyk amounts 5 to 8 m and increases near the cut banks to 10 to 15 m. Because of the low river bias and the low alas level, the increasing water level results in strong inundations and a broadening of the river channel to 200 m and more. The water level drops down only during the second half of July but could be delayed until the beginning of August as observed in 2011.

Because of the specific permafrost dynamics the formation of numerous lake-like waters (in Russian "Layda") were observed. They usually represent lakes of secondary thermokarst origin, which are flooded during high waters. Therefore, the river channels are not well-pronounced, and also after the water level sinks, a lot of remaining lakes are connected with the river trough wide channels. In addition, after dropping of the water level, numerous decameters-wide sandbanks appear at convex banks of the river branches, which are covered by Equisetum and grass. Such a

sandbank is located at the right river bank about 0.8 km above the station Kytalyk (see chapter 9).

The Berelekh valley is characterized by an indistinct shape of the terrace levels. The height of the flood plain amounts 3 to 4 m, the first terrace above the flood plain is 7 to 10 m and the second terrace 15 to 20 m high. But these levels are much more pronounced in the upper and the middle reaches.

The bottom of alas depressions is situated at 4 to 6 m height. Therefore, the flood plain level and the alas bottom level have often the same altitude and cannot be well differentiated without specific studies.

The river flood plain is often separated from the sandbanks by stripes of 2 to 3 m high willow shrubs and additionally shaped by alternating deeper boggy and higher shrubby stripes. In addition, the flood plain area is characterized by polygonal frost crack systems of about 20x20 m size. Polygon centers contain ponds or are boggy.

Circular alas depressions represent one of the major relief elements in the Berelekh area with diameters of ≥ 15 km. These depressions are considered to be former thermokarst lakes, which were drained in several stages forming alas terraces. As different lakes were drained in various times, the number and height of alas terraces are inconsistent in different depressions.

Major studies of the expeditions occurred in the area of the Kytalyk station, which is located in southernmost part of an alas depression (Fig. 2-2). This depression with a diameter of 5.5 km is weakly elongated in meridional direction. Two major levels with 1 to 1.5 m height difference could be distinguished. The upper level covers the southern part of the depression. The lower level represents the circular boggy surface in the alas center, which probably drained last. An additional alas level about 1 m higher as the upper level was observed only below the eastern Yedomá ridge (Fig. 2-2). Polygonal structures are distributed on all alas levels which are clearly shaped in the moist areas of the alas periphery and in marginal area of the lower level. The mean size of polygons amounts 15x20 to 20x20 meters. Here the development of modern ice wedges and of the polygonal relief continues including the formation of polygon walls. In other places, the degradation of polygon walls is visible that results in the formation of linear pond above thawing ice wedges. Intrapolygonal ponds do not exist there.

Pingos of 20 m height and more are characteristic for the alas depression of Kytalyk as well as for other thermokarst depressions in the study region. In addition separate elevated areas of 1 to 3 m height and 150 to 200 m in diameter were observed, which could be considered as initial pingo forms.

The Kytalyk alas is drained by the Konsor-Syane River, which flows from north to south through the entire alas and discharges into the Berelekh River (Fig. 2-2). The Konsor-Syane River cuts some high pingos in the lower alas level from which one is described in chapter 8.

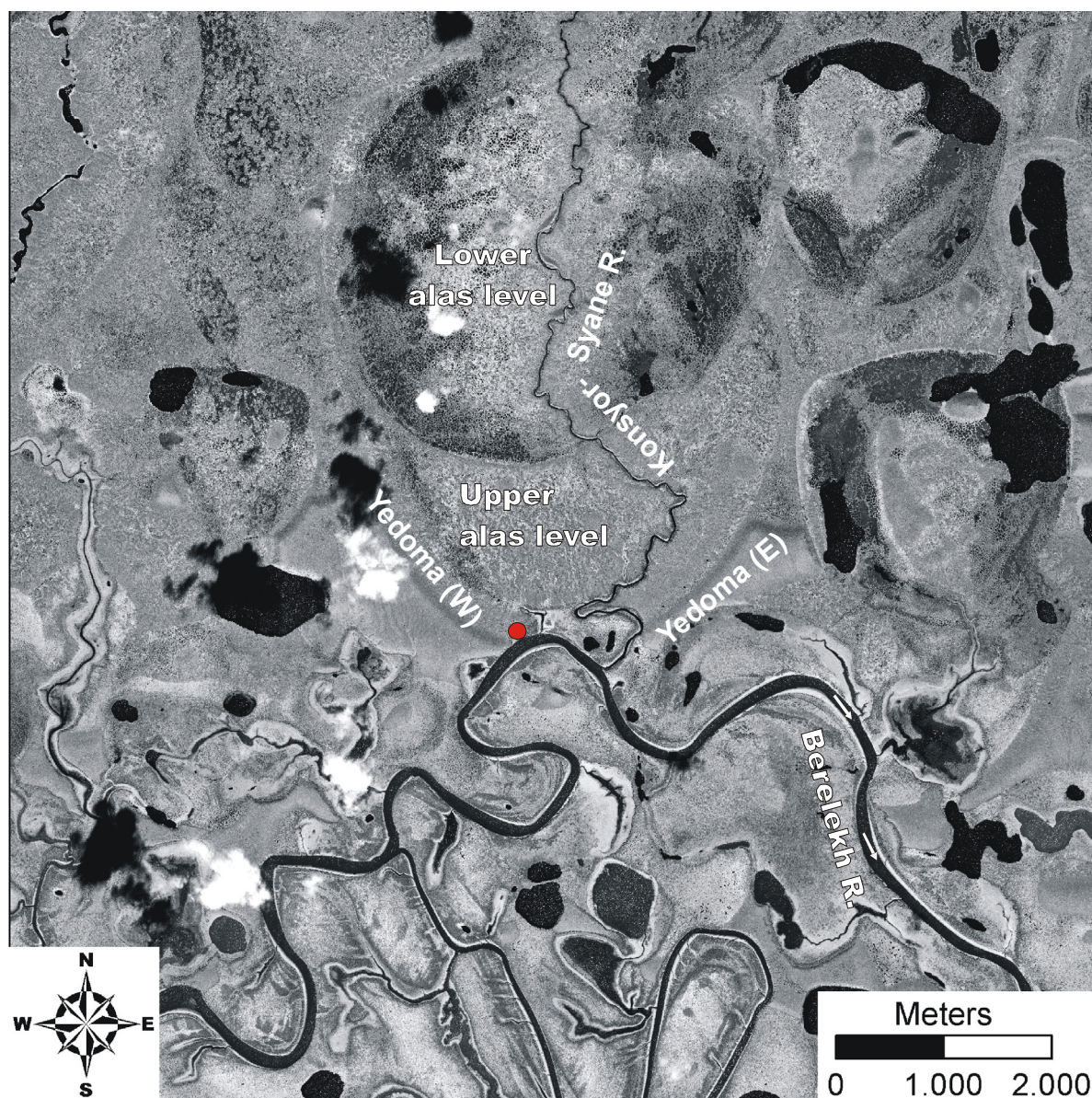
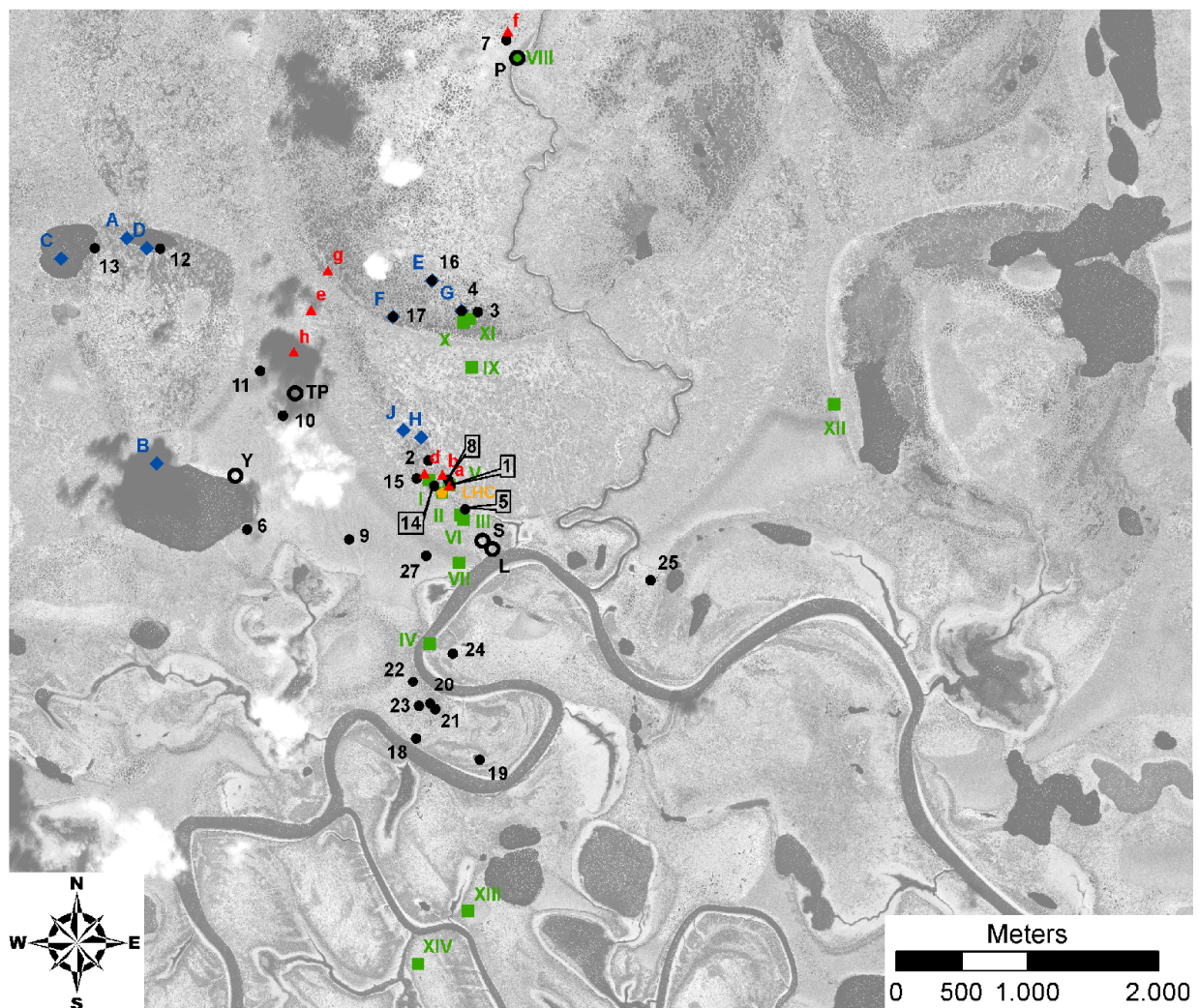


Fig. 2-2: The major study area around the Kytalyk station (red dot), (GeoEye image from 2010, 0.5 m resolution, by courtesy of Ko van Huissteden, Vrije Universiteit, Faculty of Earth and Life Sciences, Amsterdam) Map compiled by Mathias Ulrich.



- 1 to 27: Ecological study sites KYT-1 to Kyt 27 (Chapter 3)
- ◆ A to J: Limnological study sites (Chapter 5)
A: GPS 128/LBR; B: GPS 38/1; C: LBL; D: LBR; E: GPS 34; F: GPS 201; G: GPS 24/KYT-4; H: GPS 26; J: GPS 26
- ⬠ LHC: Model polygon (Chapter 6)
- ▲ a to h: Pedological study sites KYTF-1 to KYTF-7, YED1 (Chapter 7)
- Y, P, L: Permafrost exposures (Chapter 8)
Y: Yedoma exposure 11-KH-3007-1, P: pingo exposure 11-KH-2807-1, L: ice celar (lednik) exposure 11KH-2607
- S: Kytalyk Station, TP: Trigonometric Point
- I to XIV: Drill holes and pits (Chapter 9)
I: 11-KH-2707-1; II: 11-KH-2307-1/2/3/4; III: 11-KH-2107-1/2; IV: 11KH-2008-1; V: 11KH-1907-1; VI: 11KH-2107-1;
VII: 11KH-2407-1; VIII: 11KH-2807; IX: 11KH-2907-2; X: 11KH-2907-9 BUGOR, XI: 11KH-3007-1LOGGER,
XII: 11KH-2208-3; XIII: 11KH-2308-2-PINGO; XIV: 11KH-2308-7 POLY

Fig. 2-3: Overview of the study sites (Map compiled by Mathias Ulrich).

In this area (Fig. 2-3), the monitoring program on two low-centered polygons was carried out as well as the detailed botanical, active layer and surface survey of one model polygon and the comprehensive ecological and limnological survey of polygon ponds and thermokarst lakes. In addition, exemplary polygon sites were selected for pedological analyses and permafrost exposures, pits and short permafrost cores were studied here. The coordinates of each site are summarized in appendix 1.

3. MONITORING OF A POLYGON SITE (KYT-1)

Andrea Schneider & Lutz Schirrmeister

3.1 Site description and scheme

The monitoring site is located on the upper alar level where polygons occur as low-centered type (70°83'12.1'' N, 147°48'29.9'' E). We selected a site in a typical low-center polygon area to investigate present-day conditions of both a polygonal pond and a dry polygonal depression right next to it. Polygon walls and frost cracks enclose them directly. The entire area is vegetated with characteristic tundra plant communities as described in chapter 3.5.

The monitoring site covers an area of approx. 30 x 50 m. In the vicinity other polygonal depressions and ponds of different sizes exist recently. To reduce disturbances by walking, people we chose a place 500 m north of the research station.

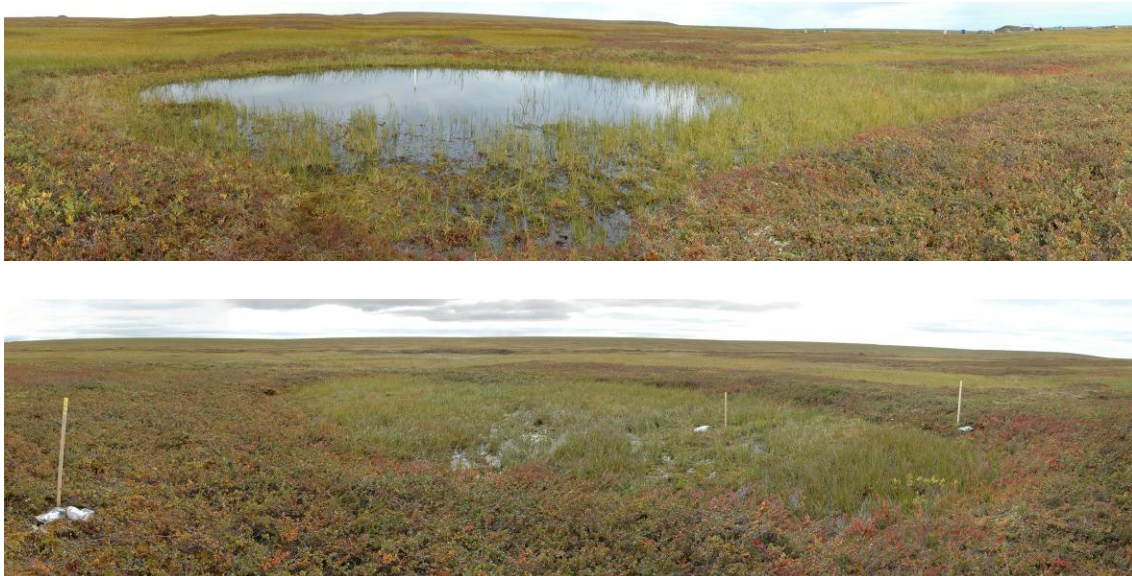


Fig. 3-1: Photographs of the pond and the depression with data logger markers.

We visited the monitoring site every four days to collect the following data and sample packages:

- Water and air temperature,
- Active layer depth,
- Water depth,
- Water samples for measurements of alkalinity, acidity, oxygen content, total hardness, electrical conductivity, pH, cations, anions, isotopic composition and nutrients,
- Ostracods (approx. 100 individuals per sample),

3. Monitoring site

- Macrozoobenthos,
- Phytoplankton and Zooplankton.

Testate amoebes and sediment samples were taken in the beginning (19.07.2011), midway (testate amoebes only, 05.08.2011) and at the end of field season (25.08.2011). Unfortunately, we could not obtain a short core from the pond sediment.

Since mosses and other plants are very sensitive to trampling damage, we moved carefully at the site and avoided to walk directly through the pond.

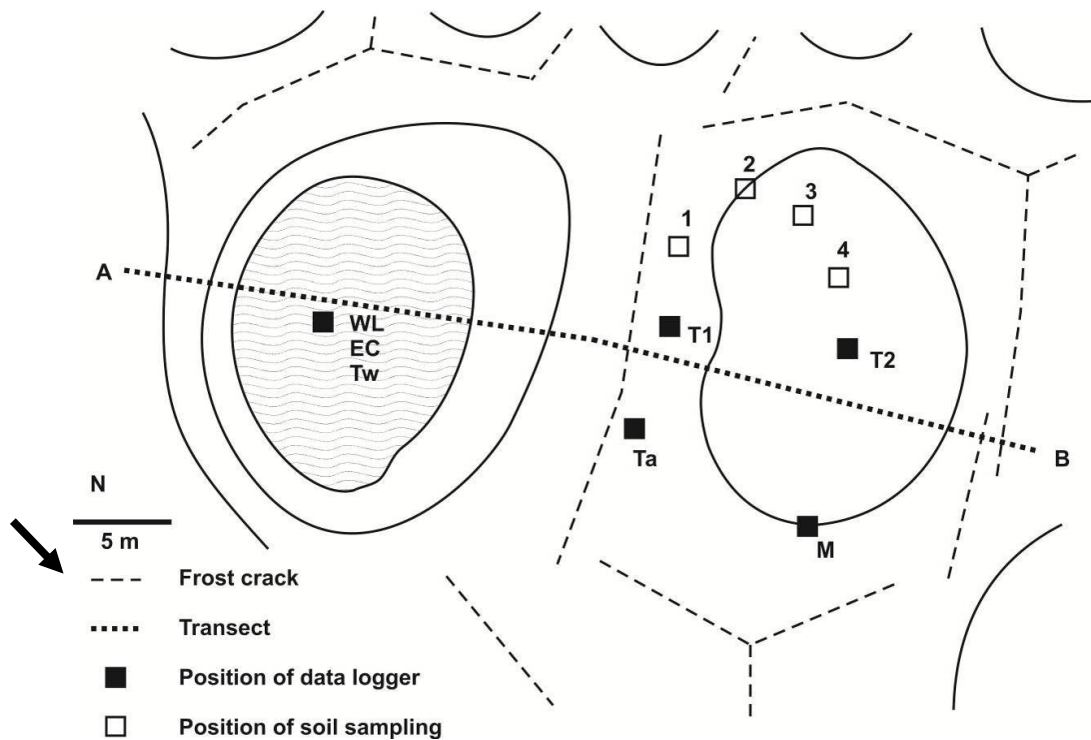


Fig. 3-2: Site scheme (top view) and location of all data loggers.

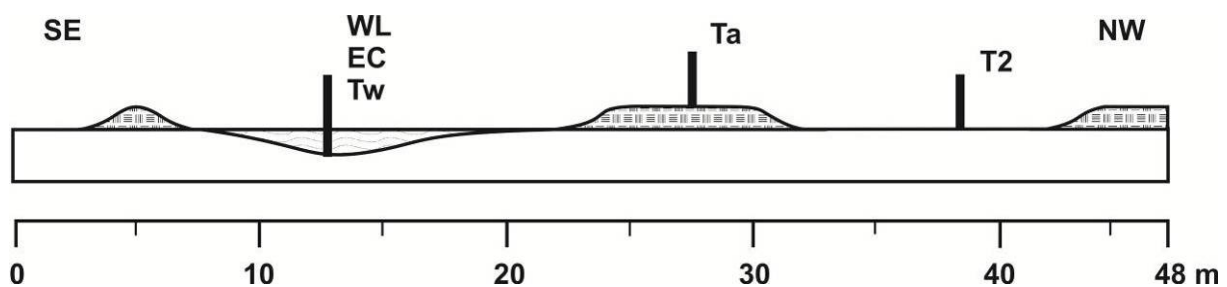


Fig. 3-3: Profile of the monitoring site with data logger markers.

Furthermore, we installed different data loggers at specific spots in the period from July 19th and 20th until August 26th in order to receive continuous data-sets (Tab. 3-1, Fig. 3-2 to 3-7). We installed ground temperature sensors at two sites (T1 and T2) and soil moisture conditions (M) at one site of the dry depression. In the pond water, electrical conductivity, water level and water temperature were logged. The air temperature (Ta) was measured in 2 m height on the wall between both polygons. All

data loggers measured their specific value every 30 minutes to provide a daily resolution. Hobo-temperature loggers have been calibrated at AWI Potsdam by putting them into icy water for 24 hours.

To reduce disturbing influences from the logger boxes lying directly on the ground surface we set them up in little distance depending on the length of the cables and closed the pit carefully. According to the manufacturer, the logger systems are said both waterproof and cold resistant from -30 to +50°C. But to prevent any kind of data loss due to technical problems both cables and connectors were wrapped in PE-bags and fixed with tape additionally. Finally we marked the data logger positions with a wooden stick.

At the end of the field work season in 2011 we read out the data from the temperature loggers T1 and T2 and prepared them to collect data until summer 2012. All other data loggers have been read out and depleted at the end of the season.

Tab. 3-1: Overview about location, logger type and time period of the installed data loggers.

Name	Location	Logger type	Measuring period
<i>Data loggers installed at the dry low-centered polygon:</i>			
Ground temperature (T1)	polygon wall, depth: 5; 10; 15; 20 cm	HOBO Micro Station; HOBO 12-Bit Temperature Smart Sensor	19.07. - 26.08. 2011, until summer 2012
Ground temperature (T2)	polygon centre, depth: 10; 15; 20; 30 cm	HOBO Micro Station, HOBO 12-Bit Temperature Smart Sensor	19.07. - 26.08. 2011, until summer 2012
Soil moisture (M)	inner polygon wall, depth: 12; 22; 27; 30 cm	HOBO Micro Station, Soil Moisture Smart Sensor	19.07. - 26.08. 2011
<i>Data loggers installed in the polygonal pond:</i>			
Electrical Conductivity (EC)	pond centre	HOBO U24 Conductivity Logger	20.07. - 26.08. 2011
Water level (WL)	pond centre	HOBO Water Level/ Temp (U20-001-04)	20.07. - 26.08. 2011
Water temperature (Tw)	pond centre	MinidanTemp 0.1, ESYS	20.07. - 26.08. 2011
<i>Data logger installed on a pole between the two polygons:</i>			
Air temperature (Ta)	2 m above ground	MinidanTemp 0.1, ESYS	20.07. - 26.08. 2011

3. Monitoring site

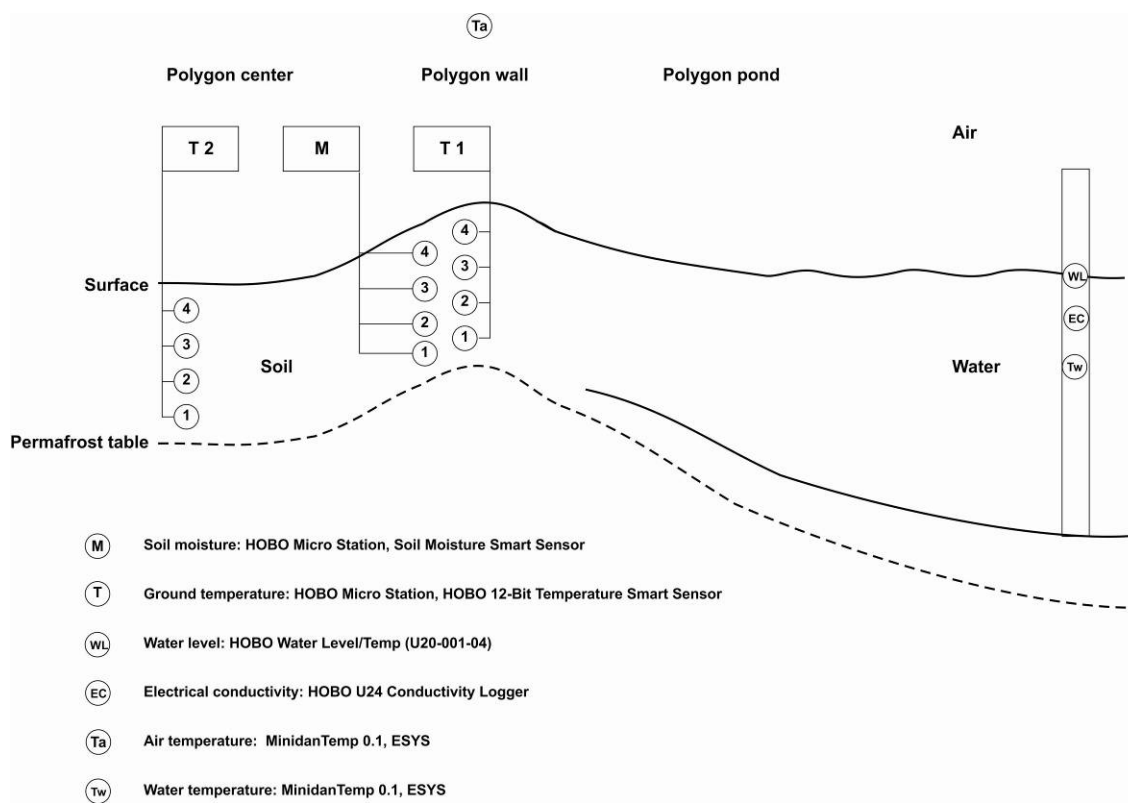


Fig. 3-4: Monitoring instrumentation with data logger positions.



Fig. 3-5: Air temperature data logger at the pole in 2 m height with a solar radiation shield.



Fig. 3-6: Installing soil moisture data loggers at the polygon wall. They were installed shifted against each other with approx. 5 cm height distance between each sensor. We installed the lowest one directly above the permafrost table on July 19th.



Fig. 3-7: Installing ground temperature data loggers in the polygonal wall. They were installed shifted against one other with approx. 5 cm height distance between each sensor. We installed the lowest one directly above the permafrost table on July 19th.

3.2 Logging results

The recorded air and water temperatures (Fig. 3-8) behave parallel and show similar daily patterns during the mentioned time period. A generally cooling trend towards the end of the season is obvious. Both air and water temperatures seem to be in relation with water level changes and variations in electrical conductivity of the shallow pond water body.

Ground temperature records appear to be in relation with the air temperature as well (Fig. 3-9). An apparent cooling trend towards the end of the season is visible. Furthermore, a thermal differentiation of the active layer is present (Figs. 3-8, 3-9). Main peaks and dips follow air temperature patterns, even in the lowest and coldest component of the active layer. Compared to the record from the enclosing wall the thermal differentiation in the polygonal depression is more distinct in the lower section and shows a wider temperature range.

The data derived from the soil moisture sensors shown in figure 3-9 do not feature a significant pattern. They represent a largely constant moisture differentiation in the active layer. The upper sensor indicates the driest conditions, interrupted by some short term events, which point to abruptly increasing surface moisture (rainfall). They were also registered as a weaker signal in the deeper sections. The lowest sensor, which was located close to the permafrost table, did not measure the highest soil water content. This was recorded by the second lowest sensor three centimeters higher and coincides with field observations. For upcoming monitoring purposes we will probably make some changes in the setting of the moisture data loggers.

3. Monitoring site

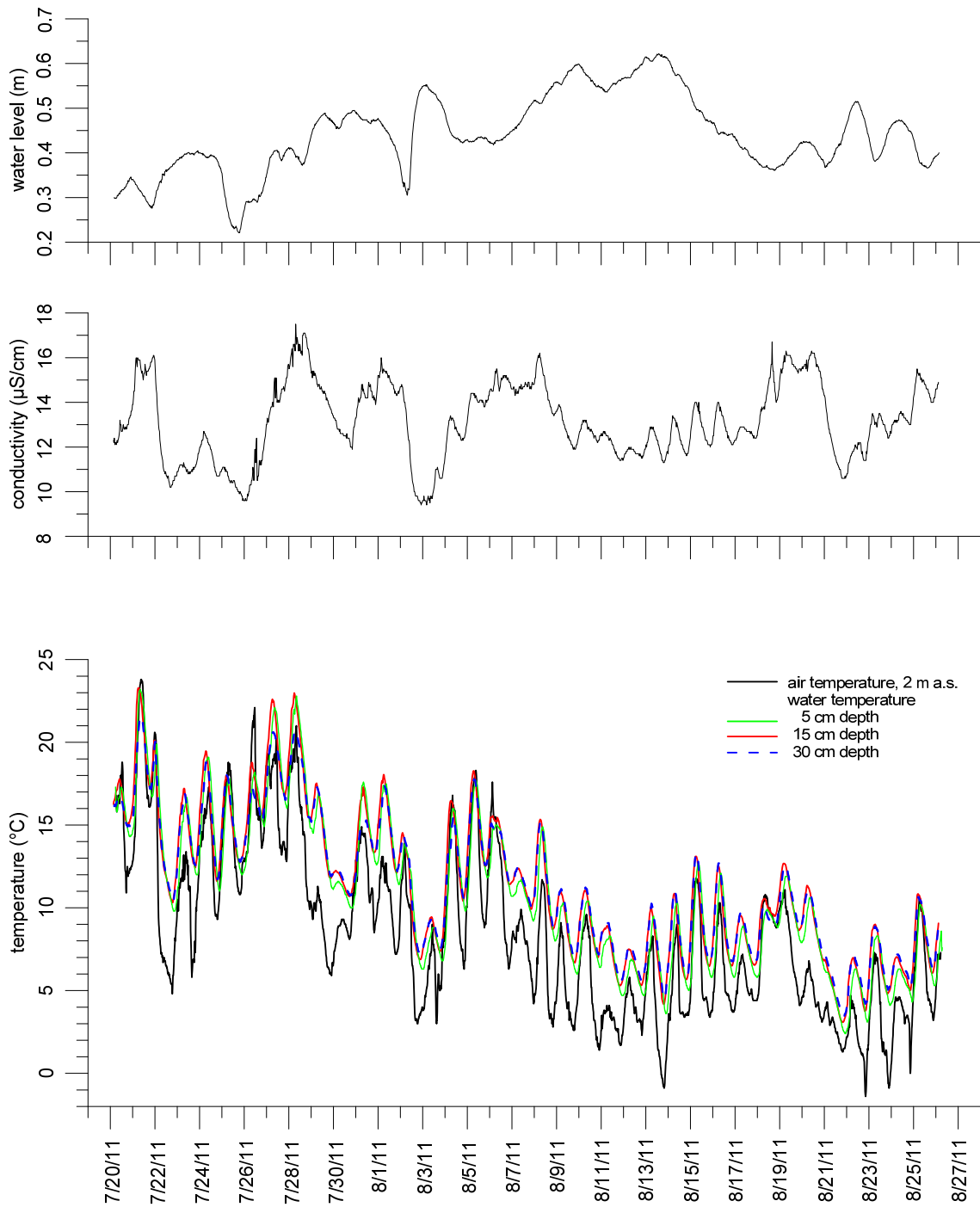


Fig. 3-8: Air and water temperatures and electrical conductivity at the monitoring site from July 20th until August 26th 2011.

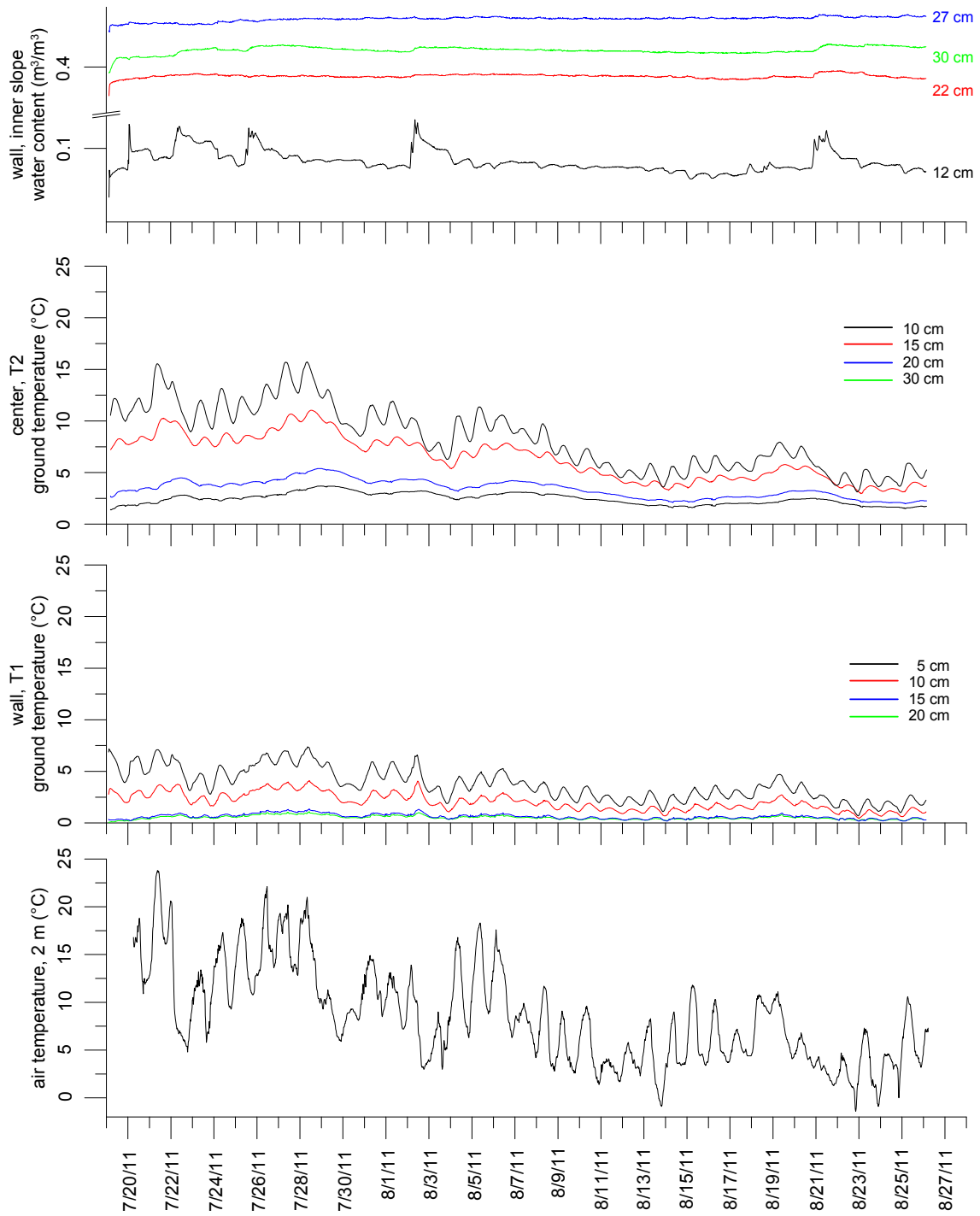


Fig. 3-9: Air and ground temperatures and soil moisture measured in the polygon wall and in the polygon centre from July 19th until August 26th 2011.

3.3 Hydrobiology

We caught living ostracods with plankton net and exhauster according to Viehberg (2002) at various zones in the pond: From the bottom, in the center and margin, from the water column, between plants and open water areas without vegetation. Since they are visible to the naked eye we picked approx. 100 animals and preserved them in alcohol. Further identification by soft body characteristics and isotopic analyses of the valve calcite will be undertaken.

We collected macro-zoobenthos from different places, mainly from the margin of the pond. Macro-zoobenthos are living in or on the upper layer of the sediment layer and between plants. Therefore, we took sample material for quantitative analyses with a net from the bottom of the pond at one place. From three to four points material was collected for qualitative analyses. We picked eye-visible animals and preserved them in Whirl Packs with water and formalin.

Zooplankton and phytoplankton was taken from the water body. We waved the net (Fig. 3-10) for 10 times through the water column and obtained 100ml sample volume. The samples were filled into Whirl Packs and preserved with water and formalin. Both macro-zoobenthos and plankton samples will be analyzed by colleagues from the Yakutsk Federal University. The samples and corresponding measuring data from KYT-1 are summarized in appendix 2 (Tab. A 2-1).



Fig. 3-10: Sampling with the plankton net (20 cm in diameter, mesh size of 65 μ l). The 100ml PE-bottle was used for plankton samples only, we caught ostracods and macrozoobenthos with a similar net without PE-bottle.

3.4 Hydrochemistry

We collected water samples for analyzing standard water parameters (alkalinity, acidity, electrical conductivity, pH, oxygen content, cations, anions, total hardness), isotopic composition and nutrients ~15 cm below water table. Samples and measuring data are summarized in appendix 2 (Tabs. A 2-1, A 2-2.).

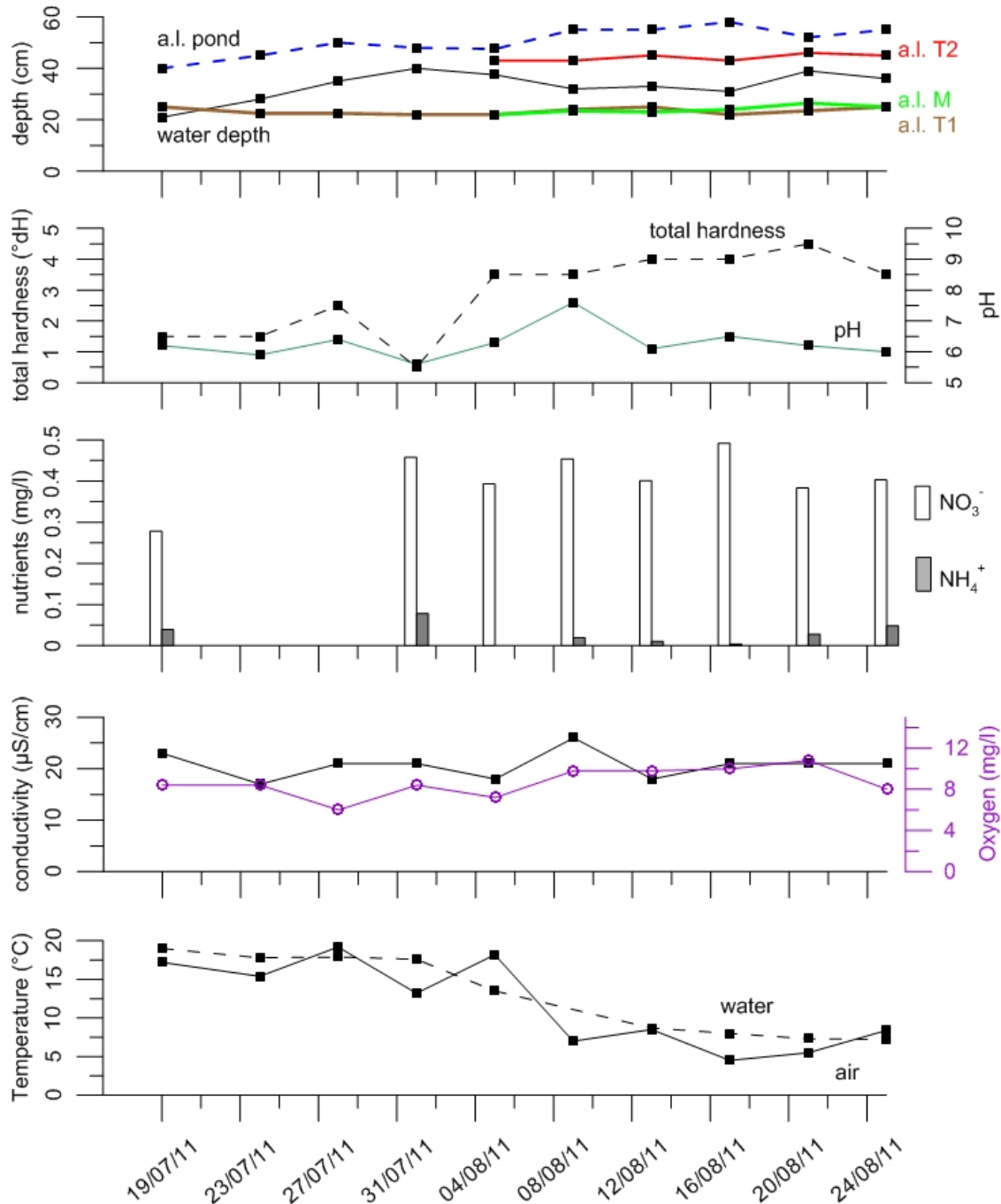


Fig. 3-11: Temperatures, chemical properties and water and thaw depth of the monitoring sites.

The water parameters were measured in the station after our return from the field. Acidity, alkalinity, oxygen content, and total hardness were analyzed with titrimetric test kits (Viscolor). Electrical conductivity and pH were quantified by a WTW pocket

meter additionally. We used a spectral photometer (Hach Lange DR 2800) for nutrient analyses (see chapter 7) such as NH_4^+ , NO_3^- and PO_4^{3-} .

Samples for cation (8ml), anion (15ml) and isotopic analyses (30ml) and residue samples were prepared in PE bottles or PE tubes for transport and stored in a cool place. Cation and anion samples were filtered by a cellulose-acetate filtration set (pore size 0.45 μm) prior to conservation. Cation samples were acidified with 200 μl HNO_3 . Samples for anion analysis, isotope analyses and residue samples were preserved without any conservation.

Obtained hydrochemical characteristics and physical properties are presented in figure 3-11. Both air and water temperature reflect a decreasing trend towards the end of the season and coalescent with the main trends measured by the temperature loggers (Fig. 3-8). The conductivity varies between 17 and 26 $\mu\text{S}/\text{cm}$ and deviates little from the dataset received from the conductivity logger. Values of NH_4^+ and NO_3^- are related to the molecular weight of N and P and seem to be generally low. PO_4^{3-} values have been below detection limit.

Total hardness of the pond water was quantified between 1.5 and 4.5 $^\circ\text{dH}$ and pH values were measured around 6. Oxygen content of the pond water varies between 6 and 10.8 mg/l. Interrupted by some dips the amount of dissolved oxygen in the water is generally increasing.

The water level lies between min. 21 and max. 40 cm. The thaw depth at T1; T2; M and the pond centre increases during the summer season.

3.5 Transect with active layer, ground surface and vegetation record

When we visited the monitoring site every four days we also undertook active layer measurements at the positions of the installed data loggers (Fig. 3-2, 3-3). The thaw depth was generally increasing during summer season and interrupted by short stable or slightly decreasing conditions (Fig. 3-11).

Along the transect we carried out active layer and ground surface measurements at the end of the summer season (August 26th). To obtain data about the surface microrelief we used the spirit level principle: A flexible tube with open ends was filled with water. Based on the position of the meniscus in the tube we could construct a horizontal line. A string fixed every three meters on a wood pole indicated the horizontal line (Fig. 3-12). From this string we undertook surface elevation and active layer measurements in one-meter intervals (see also the use of the water level tube in chapter 6).

We measured the ground surface elevation and the height of the water table with a wood stick. Active layer depth was measured by the help of a metal tube. We detected the permafrost table three times around the same spot since it is not completely flat. Finally, the average was calculated and plotted (Fig. 3-13).

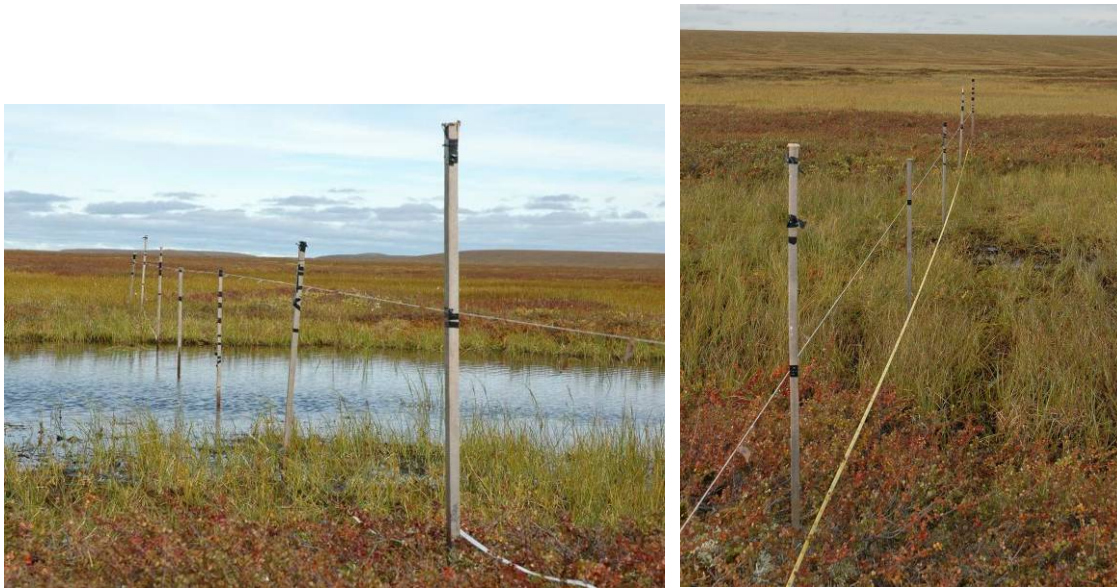


Fig. 3-12: Construction to obtain a horizontal line in order to obtain ground surface height and active layer thickness. To the right little flags indicate one meter intervals.

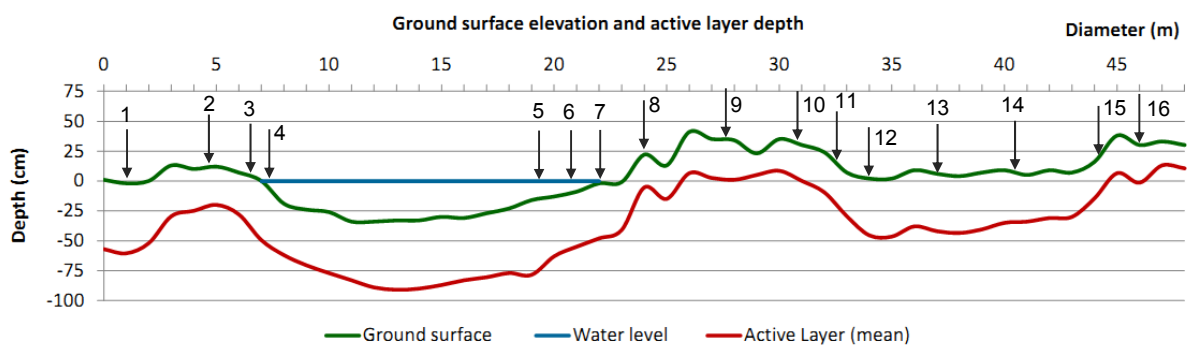


Fig. 3-13: Ground surface elevation and active layer depth of the monitoring site. Numbered arrows indicate the position of the vegetation record (see appendix 3, Tab. A 3-1).

In order to describe the plant communities at the monitoring site we undertook a detailed vegetation record along a 48 m long SE-NW transect (Tab. 3-2 and Fig. 3-2). It covers both the polygon pond and the dry polygon. We carried out 16 single records by using a 1x1m square. The square positions were chosen randomly with varying intervals but at a representative place (Fig. 3-13). The cover of each plant species in percent was estimated according to the decimal scale after Londo (1976). Compared to other usual techniques for vegetation records it was given preference to the decimal scale due to its ability to reflect small scale variations in plant assemblages on small sized study sites. A value of 0.1% represents the occurrence of only one individual of a species or its presence with similar small amounts outside of the square.

3. Monitoring site

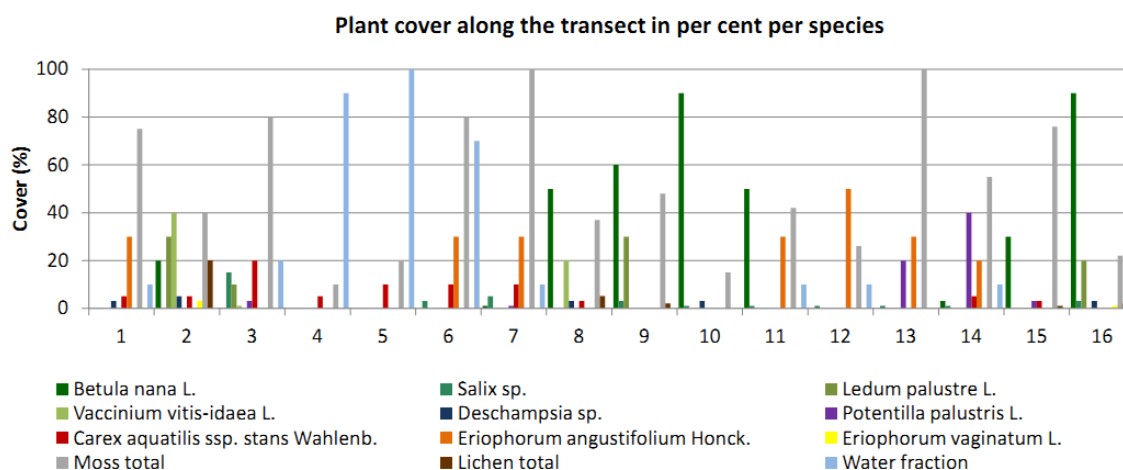


Fig. 3-14: Vegetation record along the SE-NW transect across the monitoring site. The plant cover is shown in per cent per species. The position of each record is indicated in fig. 3-16.

The total number of recorded plant species is 14. Both moss and lichen species are combined since it was not possible to identify them in the field. Further taxonomic work to identify them will be performed in the laboratory.

The vegetation differentiation at the monitoring site varies depending on the microrelief. Clearly visible differences between communities on polygonal walls, rims and depressions exist (Fig. 3-14): Shrubs such as *Betula nana*, *Salix* sp. and *Ledum palustre* form a predominating plant community on polygonal walls. *Deschampsia* sp., *Eriophorum vaginatum*, *Carex aquatilis* ssp. *stans* and some lichens are present in small values.

Carex aquatilis ssp. *stans*, *E. angustifolium* and several moss species (mainly *Sphagnum* sp.) seem to represent characteristic plant assemblages at pond margins and in shallow waters. The mosses do not disappear immediately in shallow waters – some species also grow submerged and were included in the record. *Potentilla palustris* appears in the dry polygon.

Water at positions 1; 11; 12 and 14 does not represent pond water. Small wet zones occurred after increased precipitation. Additionally, footsteps in mossy areas can cause small depressions that fill up with water which was released by the compressed plants.

Tab. 3-2: Vegetation record along the SE-NW transect across the monitoring site. The plant cover is shown in per cent. Records from positions on polygon wall locations are highlighted in light grey. The position of each record is indicated in fig. 3-16.

Plant species / cover in % at each site	1	2	3	4	5	6	7	8	9	10	11	12	13	14	15	16
<i>Betula nana</i> L.		20	0.1				1	50	60	90	50			3	30	90
<i>Carex aquatilis</i> ssp. <i>stans</i> Wahlenb.	5	5	20	5	10	10	10	3						5	3	
<i>Deschampsia</i> sp.	3	5						3		3						3
<i>Eriophorum angustifolium</i> Honck.	30					30	30				30	50	30	20		
<i>Eriophorum vaginatum</i> L.		3														1
<i>Ledum palustre</i> L.		30	10						30							20
<i>Potentilla palustris</i> L.	0.1		3	0.1		0.1	1						20	40	3	
<i>Salix</i> sp.			15			3	5		3	1	1	1	1	1		3
<i>Vaccinium vitis-idaea</i> L.	0.1	40	1					20								
*Others	0.1		1										0.2			1
Moss total	75	40	80	10	20	80	100	37	48	15	42	26	100	55	76	22
Lichen total		20.1						5.1	2			0,1			1	2
Water	10		20	90	100	70	10				10	10		10		

* *Caltha palustris* L. (0.1% in 1), *Carex chordorrhiza* Ehrh. ex. L. f. (1% in 3), *Hierochloe* sp. (0.1% in 13), *Luzula* sp. (0.1% in 13), *Pyrola rotundifolia* L. (1% in 16).

4. ECOLOGICAL STUDIES OF POLYGONAL PONDS

Andrea Schneider, Lyudmila Pestryakova & Lutz Schirrmeister

4.1 Polygonal ponds on different landscapes

In order to receive extensive datasets from different ponds, we sampled 26 randomly distributed waters (KYT-2 to KYT-27) from the three major landscape components Alas, Yedoma and floodplain area (Figs. 2-2, 2-3, 4-1). The selection criteria for the ponds to be sampled are listed below:

- Polygonal origin (except ponds on the Yedoma),
- Location clearly related to one of the major landscape components,
- Dominating open water surface,
- Presence of ostracods.

We sampled 14 ponds in the alas depression, nine in the floodplain and three from the Yedoma ridge in the west of the research station. Both, ponds in polygonal depressions (intrapolygonal ponds) and in collapsed polygonal walls (interpolygonal ponds) have been studied. The ponds on the floodplain are surrounded by approximately one meter high *Salix* sp. shrubs. Two study sites (KYT-12 and 13) are located at the shore of larger thermokarst lakes where we could observe flooded polygonal structures.

The data and sample packages were measured and collected as previously described in chapter 3 (see also appendix 2 Tabs. A 2-3, A 2-4). All ponds were documented in a photo collection.

In order to characterize the surrounding plant communities we recorded the main vegetation components for each study site. Here we concentrated on vascular plants because the mosses (chapter 10) were not identified in the field. Bottom sediment samples and samples for testate amoebae analyses were taken additionally.

Additionally short cores from ten ponds were taken in order to describe surface sediment parameters and diatom thanatocoenosis. For the coring process, plastic tubes were pushed into the sediment and closed with covers at both ends. The cores were described and sub-sampled in one-centimetre intervals (see chapter 5).



Fig. 4-1: Examples of sampled ponds from the Alas depression (KYT-4), top of the Yedoma ridge (KYT-27) and the floodplain area (KYT-20).

4.2 Hydrochemical characteristics of the studied waters

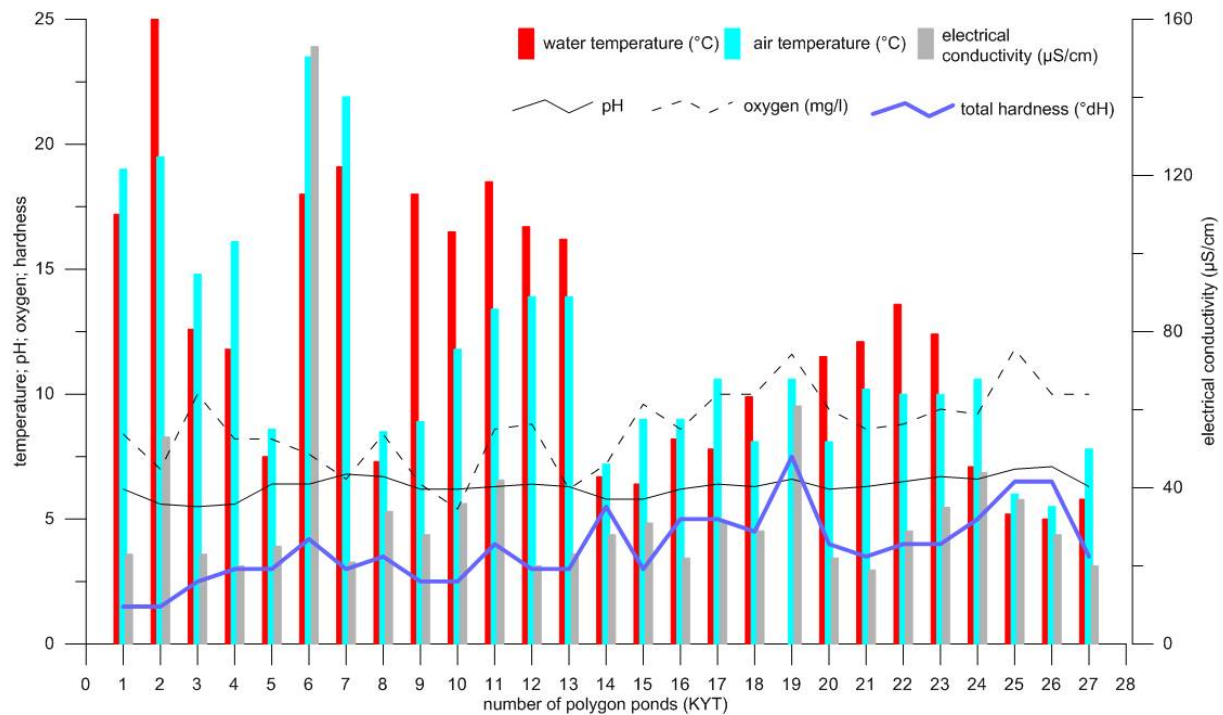


Fig. 4-2: Temperatures and hydrochemical properties in the studied ponds KYT-1 to KYT-27.

In Fig. 4-2 some of the measured hydrochemical parameters and temperatures are visualized. From the monitoring pond KYT-1 (chapter 3) the first sampling day (20/07/2011) is included in the diagram. Electrical conductivity varies between 20 and 44 $\mu\text{S}/\text{cm}$ except pond KYT-6 where 153 $\mu\text{S}/\text{cm}$ were measured. The obtained pH-values show generally stable and slightly acidic conditions in the waters. Acidity values are stable at 0.4 mmol/l with two exceptions up to 0.6 mmol/l. The alkalinity values vary between 0.2 and 1.6 mmol/l. Both oxygen content and water hardness vary in relatively broad ranges. The oxygen content is between 5.4 and 11.6 mg/l. Nutrients such as NH_4^+ , NO_3^- and PO_4^{3-} are present in low concentrations and which are partly below the detection limits of the used spectral photometer (Hach Lange DR 2800) (see also chapter 7).

4.3 Pond characteristics

KYT-2 **Area:** Alas
Date: 21.07.2011 **Type:** Intrapolygon pond
Coordinates: 70.83291°N 147.47839°E



Size of the water body: 20.5 x 12.7 m
Water depth: 70 cm

Substrate

Brown loose plant material, medium decomposed

Vegetation

Andromeda polifolia, *Betula nana*, *Caltha palustris*, *Carex aquatilis* ssp. *stans*, *Carex* sp., *Ledum palustre*, *Polygonum viviparum*, *Potentilla palustris*, *Salix* sp., *Sphagnum* spp.

Remarks

At least two coalescent polygonal ponds, steep margins

KYT-3 **Area:** Alas
Date: 23.07.2011 **Type:** Intrapolygon pond
Coordinates: 70.84306°N 47.48895°E
Short cores: 2x



Diameter of the water body: 20.9 m
Water depth: 50 cm

Substrate

Brown loose plant material, medium decomposed

Vegetation

Betula nana, *Carex aquatilis* ssp. *stans*, *Eriophorum angustifolium*, *Sphagnum* spp.

Remarks

Located in an area with other low-centred polygonal ponds

KYT-4 **Area:** Alas
Date: 23.07.2011 **Type:** Intrapolygon pond
Coordinates: 70.84312°N 147.48555°E
Short core: 1x



Diameter of the water body: 20,8 m
Water depth: 32 cm

Substrate

Brown loose plant material, medium decomposed

Vegetation

Betula nana, *Carex aquatilis* ssp. *stans*, *Eriophorum angustifolium*, *Salix* sp., *Sphagnum* spp.

Remarks

Located in an area with other low-centred polygonal ponds

KYT-5	Area: Alas	Size of the water body: 20.4 x 16.5
Date: 03.08.2011	Type: Intrapolygon pond	Water depth: > 1 m
Coordinates: 70.82958°N 147.48596°E		
Short cores: 2x		
		Substrate Medium decomposed plant material
		Vegetation <i>Betula nana</i> , <i>Carex aquatilis</i> ssp. <i>stans</i> , <i>Ledum palustre</i> , <i>Potentilla palustris</i> , <i>Rumex arcticus</i> , <i>Sparganium hyperboreum</i>
		Remarks At least two coalescent polygon ponds, steep margins

KYT-6	Area: Alas	Diameter of the water body: 18 m
Date: 27.07.2011	Type: Intrapolygon pond	Water depth: 15 cm
Coordinates: 70.82832°N 147.44064°E		
Short core: 1x		
		Substrate Medium decomposed fibrous peat ("Radzellentorf")
		Vegetation <i>Betula nana</i> , <i>Carex aquatilis</i> ssp. <i>stans</i> , <i>Eriophorum angustifolium</i> , <i>Lychnis</i> sp., <i>Polygonum viviparum</i> , <i>Rumex arcticus</i> , <i>Salix</i> sp., <i>Saxifraga hirculus</i> , <i>Utricularia ochroleuca</i>
		Remarks Occurrence of gas bubbles and rotten smell

KYT-7	Area: Alas	Size of the water body: 12.8 x 8.9 m
Date: 28.07.2011	Type: Intrapolygon pond	Water depth: 29 cm
Coordinates: 70.86152°N 147.49527°E		
Short core: 1x		
		Substrate Weakly decomposed plant detritus
		Vegetation <i>Betula nana</i> , <i>Eriophorum vaginatum</i> , <i>Ledum palustre</i> , <i>Sphagnum</i> spp., <i>Salix</i> sp., <i>Vaccinium vitis-idea</i>
		Remarks Located in an area with other low-centred polygonal ponds

KYT-11 **Area:** Alas
Date: 04.08.2011 **Type:** Intrapolygon pond
Coordinates: 70.83910°N 147.44356°E



Size of the water body: 10 x 25 m
Water depth: 20 – 30 cm

Substrate
 Slightly decomposed plant material

Vegetation
Andromeda polifolia, *Betula nana*,
Carex aquatilis ssp. *stans*, *Ledum palustre*,
Salix cf. *myrtiloides*

Remarks
 Location in a field of polygonal ponds closed to NNW foot area of the Yedoma ridge

KYT-12 **Area:** Alas
Date: 06.08.2011 **Type:** Thermokarst lake
Coordinates: 70.84752°N 147.42291°E
 Short core: 1x



Size of the water body: 7 x 10 m
Water depth: 40 cm

Substrate
 Slightly decomposed plant remains, branches and leafs from *Betula nana* visible

Vegetation
Carex aquatilis ssp. *stans*, *Eriophorum angustifolium*, *Potentilla palustris*,
Sphagnum spp., *Salix* sp.

Remarks
 Flooded polygon pond at the margin of a thermokarst lake

KYT-13 **Area:** Alas
Date: 06.08.2011 **Type:** Non-polygon pond
 (shallow rivulet)
Coordinates: 70.84760°N 147.40939°E
 Short core: 1x



Size of the water body: 5 - 10 x 25 m
Water depth: 45 cm

Substrate
 Slightly decomposed plant remains, branches and leafs from *Betula nana* visible

Vegetation
Betula nana, *Eriophorum angustifolium*,
Eriophorum vaginatum, *Ledum palustre*

Remarks
 Pond connected to a small stream towards the thermokarst, polygonal shape

4. Polygonal ponds

KYT-14 **Area:** Alas
Date: 12.08.2011 **Type:** Interpolygonal pond
Coordinates: 70.83120°N 147.47955°E



Size of the water body: 24.6 x 18.6 m
Water depth: 60 – 75 cm

Substrate
Fine brown plant detritus

Vegetation
Betula nana, *Carex aquatilis* ssp. *stans*,
Eriophorum angustifolium,
Eriophorum vaginatum, *Ledum palustre*,
Poaceae, *Rubus chamaemorus*,
Salix cf. *myrtoloides*, *Sphagnum* spp.,
Utricularia ochroleuca, *Vaccinium vitis-idea*

Remarks
Steep margins, flooded *Betula nana*, water-filled frost cracks

KYT-15 **Area:** Alas
Date: 12.08.2011 **Type:** Intrapolygon pond
Coordinates: 70.83173°N 147.47595°E



Size of the water body: 7.7 x 8.2 m
Water depth: 20 cm

Substrate
Fine brown plant detritus

Vegetation
Andromeda polifolia, *Betula nana*, *Carex aquatilis* ssp. *stans*, *C. chorrhizza*,
C. rotundata, *Pedicularis* cf. *lapponicus*,
Polygonum viviparum, *Utricularia ochroleuca*,
Salix sp., *Sphagnum squarrosum*,
Sphagnum spp., *Vaccinium vitis-idea*

Remarks
Collapsing polygon walls, comparatively dense vegetated pond water surface

KYT-16 **Area:** Alas
Date: 13.08.2011 **Type:** Intrapolygon pond
Coordinates: 70.84522°N 147.47943°E
Short core: 1x



Size of the water body: 14 x 19 m
Water depth: 35 cm

Substrate
Fine brown plant detritus

Vegetation
Caltha palustris, *Carex aquatilis* ssp. *stans*,
Carex chorrhizza, *Eriophorum angustifolium*, *Ledum palustre*, *Pedicularis* cf. *lapponicus*, *Poaceae*, *Potentilla palustris*,
Salix sp., *Sphagnum* spp.,
Vaccinium vitis-idea

Remarks
Located in a field of polygonal ponds

KYT-17 **Area:** Alas
Date: 13.08.2011 **Type:** Intrapolygon pond
Coordinates: 70.84276°N 147.47131°E
Short core: 1x



Size of the water body: 8 x 6.5 m
Water depth: 30 cm

Substrate
Fine brown plant detritus

Vegetation
Andromeda polifolia, *Betula nana*, *Carex aquatilis* ssp. *stans*, *Carex chordorrhizza*, *Eriophorum angustifolium*, *Pedicularis* cf. *lapponicus*, *Polygonum viviparum*, *Potentilla palustris*, *Ranunculus pallasii*, *Salix* sp.

Remarks
Located in a field of polygonal ponds

KYT-18 **Area:** Floodplain
Date: 15.08.2011 **Type:** Interpolygon pond
Coordinates: 70.81393°N 147.47542°E



Size of the water body: 15 x 7 m
Water depth: 55 cm

Substrate
Coarse brown plant detritus, plant and wood fragments visible, leafs from *Salix*

Vegetation
Caltha palustris, *Carex aquatilis* ssp. *stans*, *Hippuris vulgaris*, *Pedicularis* cf. *lapponicus*, *Potentilla palustris*, *Ranunculus* sp., *Salix* sp., *Sphagnum squarrosum*, *Sphagnum* spp., *Valeriana capitata*

Remarks
Near to recent Berelekh River course

KYT-19 **Area:** Floodplain
Date: 15.08.2011 **Type:** Non-polygon pond
(small thermokarst lake)
Coordinates: 70.81393°N 147.47542°E



Size of the water body: ca. 50 m
Water depth: 70 cm (margin)

Substrate
Coarse brown plant material, plant and wood fragments visible

Vegetation
Caltha palustris, *Carex aquatilis* ssp. *stans*, *Petasites frigidus*, *Potentilla palustris*, *Ranunculus pallasii*, *Rumex articus*, *Sparganium hyperboreum*, *Sphagnum squarrosum*, *Sphagnum* spp.

Remarks
Occurrence of gas bubbles, steep margins

4. Polygonal ponds

KYT-20 **Area:** Floodplain
Date: 16.08.2011 **Type:** Interpolygon pond
Coordinates: 70.81631°N 147.47833°E



Size of the water body: 10 x 4 m
Water depth: 55 cm

Substrate

Coarse brown plant material, plant and wood fragments visible, transparent roots

Vegetation

Carex aquatilis ssp. *stans*, *Hippuris vulgaris*,
Potentilla palustris, *Salix* sp.,
Sphagnum squarrosum, *Sphagnum* spp.,
Utricularia vulgaris

Remarks

Surrounded by approx. 1.5 m high *Salix* sp. shrubs, occurrence of gas bubbles

KYT-21 **Area:** Floodplain
Date: 16.08.2011 **Type:** Interpolygon pond
Coordinates: 70.81596°N 147.47942°E



Size of the water body: 7 x 5.5 m
Water depth: 50 cm

Substrate

Coarse brown plant material one side of the pond, fine brown and black plant detritus, plant and wood fragments, leafed branches from *Salix*

Vegetation

Carex aquatilis ssp. *stans*, *Hippuris vulgaris*,
Potentilla palustris, *Salix* sp.,
Sphagnum squarrosum, *Sphagnum* spp.,
Utricularia vulgaris

Remarks

Flooded *Salix* shrubs

KYT-22 **Area:** Floodplain
Date: 18.08.2011 **Type:** Interpolygon pond
Coordinates: 70.81786°N 147.47485°E



Size of the water body: 9.3 x 7.7 m
Water depth: 50 cm

Substrate

Medium decomposed brown plant material, leafes from *Salix*

Vegetation

Caltha palustris, *Carex aquatilis* ssp. *stans*,
Hippuris vulgaris, *Potentilla palustris*,
Salix sp., *Sphagnum squarrosum*,
Sphagnum spp., *Utricularia vulgaris*

Remarks

Densely vegetated water area with *Potentilla* and *Utricularia*, steep margins

KYT-23 **Area:** Floodplain
Date: 18.08.2011 **Type:** Intrapolygon pond
Coordinates: 70.81617°N 147.47600°E



Size of the water body: 10.3 x 8.5 m
Water depth: 50 cm

Substrate

Medium decomposed dark brown plant material, leaves from *Salix*, coarse undecomposed plant fragments

Vegetation

Carex aquatilis ssp. *stans*, *Hippuris vulgaris*, *Potentilla palustris*, *Sparganium hyperboreum*, *Sphagnum squarrosum*, *Sphagnum* spp., *Utricularia vulgaris*

Remarks

Located in a field of polygonal ponds

KYT-24 **Area:** Floodplain
Date: 20.08.2011 **Type:** Non-polygonal pond
Coordinates: 70.81973°N 147.48322°E



Size of the water body: 20 x 35 m
Water depth: 50 – 60 cm (2 m from margin)

Substrate

Black coloured dark brown plant detritus, fine decomposed, coarse slightly decomposed plant material

Vegetation

Caltha palustris, *Carex aquatilis* ssp. *stans*, *Hippuris vulgaris*, *Petasites frigidus*, *Ranunculus pallasii*, *Salix* sp., *Sphagnum squarrosum*, *Sphagnum* spp., *Utricularia vulgaris*

Remarks

Perhaps abandoned channel from the Berelekh River, steep margins

KYT-25 **Area:** Floodplain
Date: 22.08.2011 **Type:** Intrapolygon pond
Coordinates: 70.82465°N 147.52426°E



Size of the water body: 10 x 12 m
Water depth: 70 cm (2 m from margin)

Substrate

Fine brown plant detritus, little amount of silty material, undecomposed *Salix* leaves

Vegetation

Caltha palustris, *Carex aquatilis* ssp. *stans*, *Salix* sp., *Ranunculus* cf. *hyperboreus*, *Ranunculus triparitus*, *Rumex arcticus*, *Sparganium hyperboreum*, *Sphagnum* spp., *Utricularia ochroleuca*

Remarks

Located in a field of polygonal ponds

4.4 First result of diatom studies

4.4.1 Material and methods of diatom analyses

In order to get an initial overview about the diatom association and their differentiation, bottom sediments of some ponds were selected for first diatom analyses from the two alas levels.

As quantitative indicators the species number, the number of shells per gram of sample, the frequency, and the saprobity index were determined. The taxa were determined to the species level and if possible down to the subspecies and variety level. According to the frequency, the spectra were classified in single < 1%, common 1-2%, abundant >5%, subdominant 5-10%, and dominant >10%. The classification of diatom taxa was made with regard to their preferred habitat (planktonic, benthic, epiphytic), salinity (indifferent, halophytic, halophilous, meso-halophilous), pH (alkaliphilous, alkalibiontic, acidophilous, acidobiontic, indifferent), and biogeography (boreal, arctic-alpine, cosmopolitan).

The uppermost two centimeters of pond deposits were studied from the lower alas level (sites KYT7, GPS34, KYT17/GPS201, KYT17/GPS24) and from the upper alas level (sites KYT-2, KYT-5/1, GPS26, GPS25, see Fig. 2-3).

4.4.2 Analytical results and ecological classification

In the studied eight ponds 48 species of 14 genera and 9 families were classified. Most frequent is only the family Naviculaceae, which represents about 40% of the studied diatom flora (Tab. 4-1). The major genera are *Eunotia* (16 species), *Pinnularia*, *Neidium* (8 species), and *Gomphonema* (3). The genera *Eunotia* together with *Pinnularia* and *Tabellaria* are characterized as elements of a specialized flora, which is adapted to nutrient deficit, low temperatures, high contents of humic acid and low pH values.

The richness of diatom algae varies only between 7 and 17 taxa in different polygonal ponds. The mean number of taxa is a little bit higher in the lower alas level (16) than in the upper level (13). Eight taxa occurred with a high frequency in all the studied polygons (Fig. 4-4). That concerns the acidophilous diatoms *Tabellaria flocculosa* (100 %) and *Eunotia bilunaris* (90 %). Other taxa like *Pinnularia brevicostata* (90 %), *Gomphonema lagerheimii* and *Stauroneis anceps et f. gracilis* (up to 80 %) belong to the pH-indifferent (neutrophil) class, while the frequent species *Stauroneis phoenicenteron* (100 %) is considered as alkaliphilous. One additional frequent species that occurred in 80% of the studied ponds is characterized as weakly halophilous and alkaliphilous.

However, besides of the wide distribution of the above mentioned diatoms, the arcto-alpine *Tabellaria flocculosa* dominates the associations in all studied ponds. This species is characterized variously according to the habitat (epiphytic, epiphytic-planktonic, weakly planktonic, facultative benthic), as halophobous and acidophilous concerning salinity and pH, and by a wide tolerance (distotroph to mesotroph?) of the water quality. Because of the high oxygen requirement *Tabellaria flocculosa* is an indicator for very pure water (oligo-xenosaprobic). Their content decreases significantly by water pollution. In northern regions this species often occur in the phytoplankton, the periphyton and the epipelon of rivers and lake. In thermokarst lakes, this species is often dominant and also occur in peats of bogs (i.e. sphagnophil).

A large role in the composition of the diatom associations play also the species *Eunotia bilunaris*, *E. arcus*, *E. subarcuatoides*, *E. septentrionalis*, *E. intermedia*, *Pinnularia brevicostata*, *P. microstauron*, *P. gibba*, and *Sellaphora pupula*, which are indifferent concerning the salinity. In polygonal pond of the upper alas level the two rare taxon *Eunotia nymanniana* Grun. and *E. steineckii* Peterson were found frequently.

Ecologic-geographical analysis shows that the water in ponds of the lower alas level are more clear than those of the upper level, where epiphytic forms dominated. The mineralization conditions are rather stable. The saprobity index range from 0.66 to 1.22 for the lower alas level and from 0.26 to 0.82 for the upper level (Fig. 4-3). That means all the studied ponds are oligosaprobic with pure to very pure water.

Tab. 4-1: Taxonomic structure of the diatom flora from the studied ponds.

Family	Genus	Total Species	Lower alas level						Upper alas level				
			KYT-7	GPS34	KYT-17/GPS201	KYT-17/GPS201	KYT-4/GPS24	KYT-4/GPS24	KYT-2	KYT-5(1)	GPS26	GPS25	
<i>Fragilariaceae</i>	<i>Fragilaria</i>	1				1							
<i>Tabellariaceae</i>	<i>Tabellaria</i>	1	1	1	1	1	1	1	1	1	1	1	1
<i>Naviculaceae</i>	<i>Navicula</i>	1					1						
	<i>Caloneis</i>	1			1								
	<i>Stauroneis</i>	2	2	2	2	2	2	2	1	2	1	2	
	<i>Pinnularia</i>	8	3	4	4	2	4	3	2	1	1	3	
	<i>Neidium</i>	8	2	1	2	1	3	2	2	3		1	
<i>Achnantheaceae</i>	<i>Cocconeis</i>	1											
<i>Eunotiaceae</i>	<i>Eunotia</i>	16	4	6	3	5	1	4	4	5	3	6	
<i>Cymbellaceae</i>	<i>Cymbella</i>	2	1				1		1	1			
	<i>Anomoeoneis</i>	1							1				
<i>Gomphonemataceae</i>	<i>Gomphonema</i>	3	1	2	1	1	2	1		2	1	1	
<i>Rhopalodiaceae</i>	<i>Sellaphora</i>	2	1	1	1	2	1	1	1	1		1	
<i>Nitzschiaceae</i>	<i>Nitzschia</i>	1				1							
	Total species:	48	15	17	15	16	16	14	13	16	7	15	

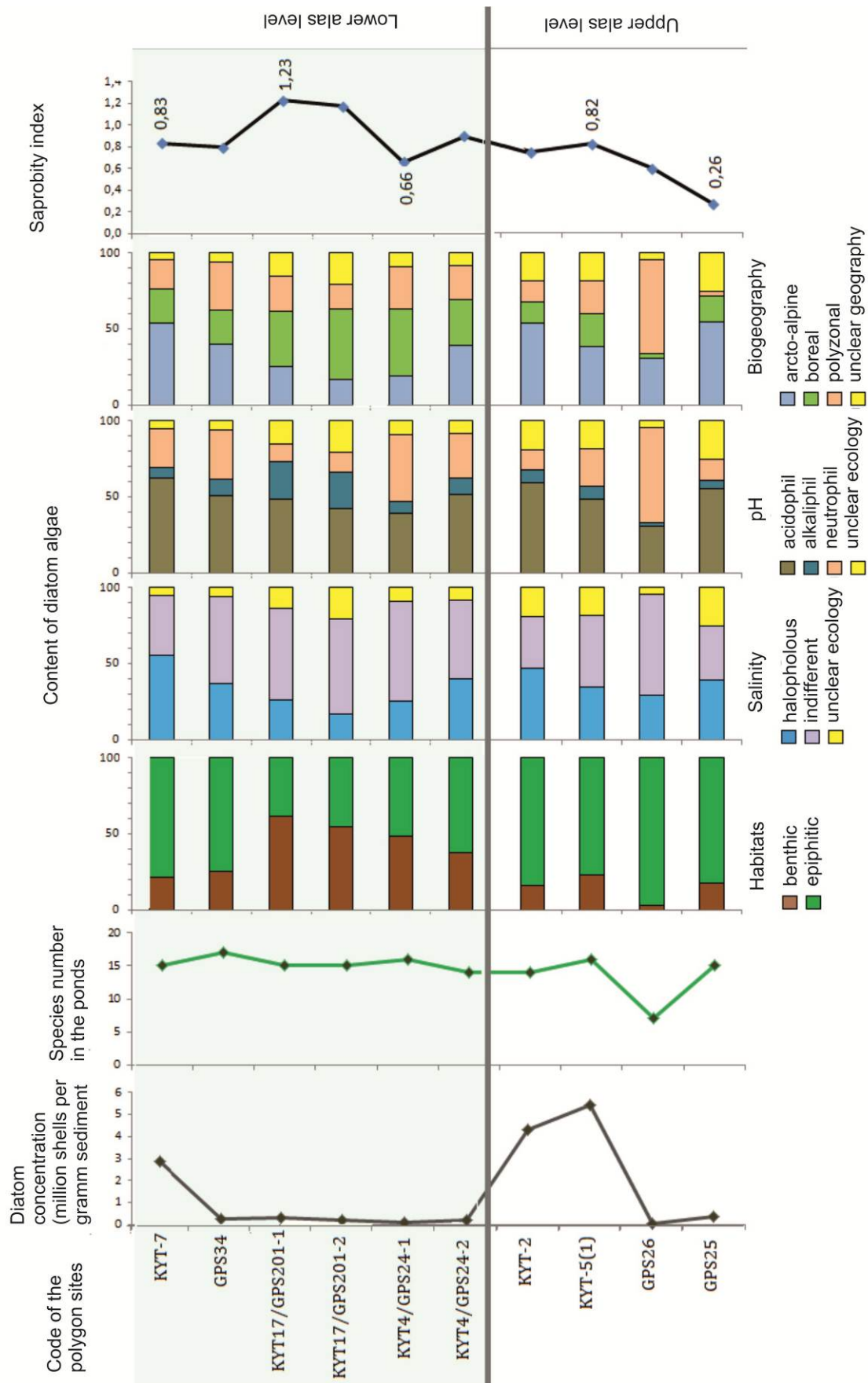


Fig. 4-3. Diagram of the ecological-geographic characteristics of the diatom association in polygonal pond of the Kytalyk study area.

4. Polygonal ponds

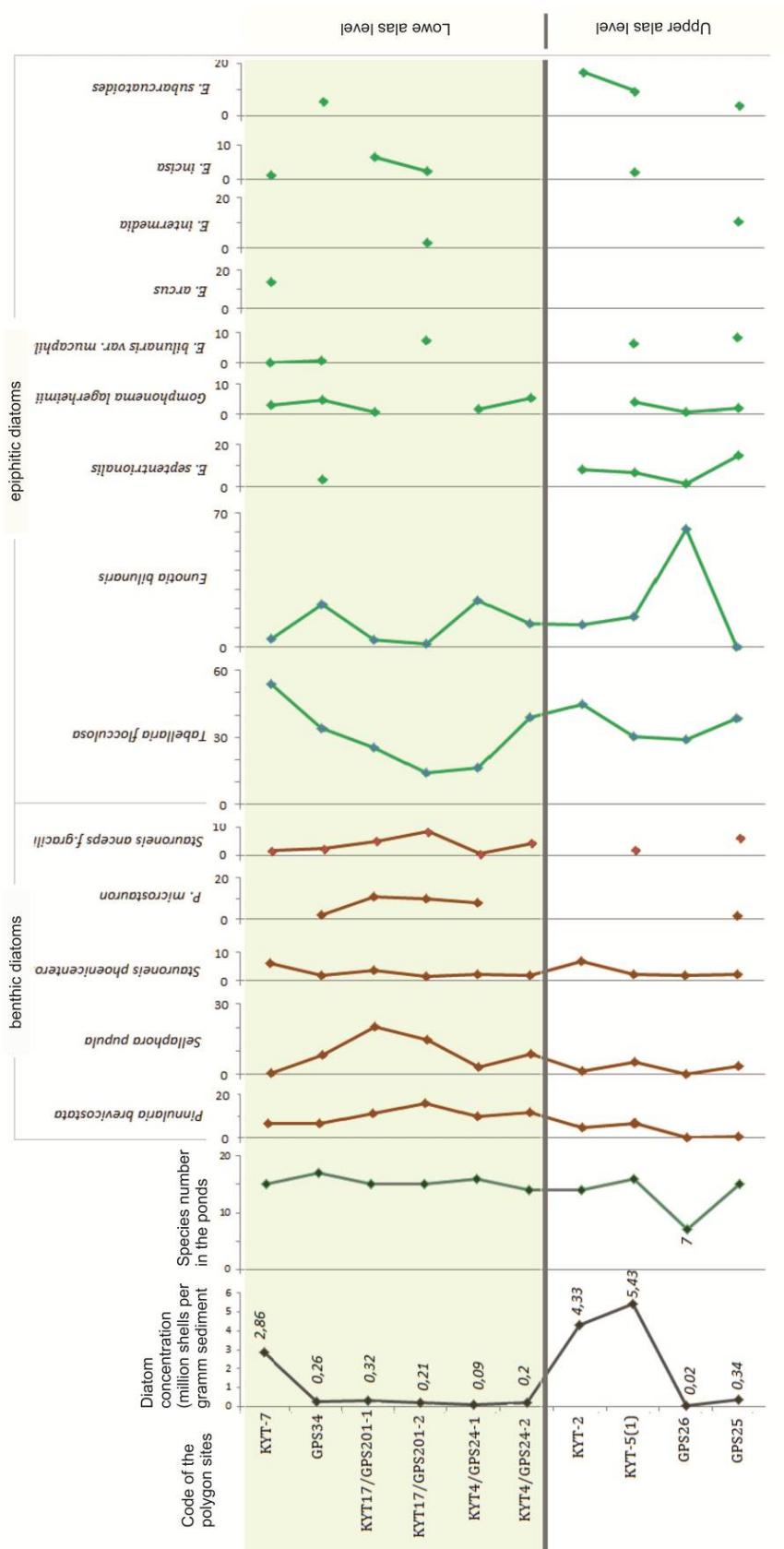


Fig. 4-4: Diagram of the frequent diatom algae found in polygonal pond of the Kytalyk study area.

Tab. 4-2: Species list off the diatom flora.

Taxon	Habitat	Salinity	pH relation	Biogeography	Saprobity ^b	Lower alas level						Upper alas level			
						KYT-7	GPS34	KYT-17/GPS201	KYT-17/GPS201	KYT-4/GPS24	KYT-4/GPS24	KYT-2	KYT-5(1)	GPS26	GPS25
<i>Anomoeoneis brachysira</i> (Breb. in Rabh.) Grun. In Cleve	Btn	Hb	Ac	AA								0,4			
<i>Caloneis</i> spp.	Ep							5,1							
<i>Cocconeis placentula</i> Ehr.	Ep	I	Ak	Bo	b					0,8					
<i>Cymbella cuspidata</i> Kutz.	Ep	I	N	Bo								1,1			
<i>Cymbella paucistriata</i> Cleve-Euler	Ep			Cos		0,6						0,8			
<i>Eunotia arcus</i> Ehr.	Ep	I	N	Cos	Os	13,8									
<i>Eunotia bilunaris</i> (Ehr.) Mills.	Ep	Hb	Ac	Cos	x	4,4	22,2	3,7	1,7	24,4	12,4	11,5	15,9	61,8	
<i>Eunotia bilunaris</i> var. <i>mucaphila</i>	Ep						0,6		7,4				6,5		8,4
<i>Eunotia exigua</i> (Breb.) Rabenh.	Ep	II	Acb	Cos	x		0,6								
<i>Eunotia faba</i> (Ehr.) Grun.	Ep	Hb	Ac	AA			2,5								
<i>Eunotia incisa</i> Gregory	Ep					1,3		6,5	2,5				2,2		
<i>Eunotia intermedia</i> (Krasske et Hust.) Norpel & L.-B.	Ep								2,1						10,5
<i>Eunotia nymanniana</i> Grun.	Ep											1,5			
<i>Eunotia parallela</i> Ehr.	Ep	I	N	AA	Os										1,4
<i>Eunotia praeupta</i> Ehr.	Ep	Hb	Ac	Cos	x						0,9				
<i>Eunotia pseudopectinalis</i> Hust.	Ep	Hb	Ac	AA					2,5						
<i>Eunotia septentrionalis</i> Oest.	Ep	I	Ac	AA			3,7					8,4	7,0	1,8	14,7
<i>Eunotia</i> spp.	Ep					1,9		2,3		8,1	2,7			3,6	
<i>Eunotia steineckii</i> Peterson	Ep														2,1
<i>Eunotia subarcuatoides</i> Alles, Norpel & L.-B.	Ep						5,6					16,9	9,7		4,2
<i>Eunotia subatomoides</i> (Hust.)L.-B.	Ep										1,8				
<i>Fragilaria</i> spp.	Ep								7,4						
<i>Gomphonema angustum</i> Ag.	Ep	I	Ak	Bo	Os				7,4						
<i>Gomphonema lagerheimii</i> A. Cleve	Ep	I	H	Bo		3,1	4,9	0,9		1,6	5,3		4,0	0,9	2,1
<i>Gomphonema truncatum</i> Ehr.	Ep	I	Ak	Bo	b		0,6						0,8		
<i>Navicula</i> spp.	Btn									0,8					
<i>Neidium amphliatum</i> (Ehr.)Krammer	Btn	Hb	N	Bo						5,7		0,8	1,6		0,7
<i>Neidium apiculatum</i> Reimer	Btn										3,1				

4. Polygonal ponds

Taxon	Habitat	Salinity	pH relation	Biogeography	Saprobity ^ь	Lower alas level						Upper alas level					
						KYT-7	GPS34	KYT-17/GPS201	KYT-17/GPS201	KYT-4/GPS24	KYT-4/GPS24	KYT-2	KYT-5(1)	GPS26	GPS25		
<i>Neidium dilatatum</i> (Ehr.)Cl.	Btn	I	Ак	Bo			1,4										
<i>Neidium hitchcockii</i> (Ehr.)Cl.	Btn	I	Ac	AA					1,6								
<i>Neidium iridis</i> f. <i>vernales</i> Reich.	Btn	Hb	Ac	Bo					3,3			3,0					
<i>Neidium iridis</i> (Ehr.) Cl.	Btn	Hb	Ac	Bo		1,9	0,6	0,9				0,8					
<i>Neidium</i> spp.	Btn					1,3			0,4		0,9						
<i>Nitzschia</i> spp.	Btn								0,8								
<i>Pinnularia borealis</i> Ehr.	Btn	I	Ак	AA	x				1,6								
<i>Pinnularia brevicostata</i> Cl.	Btn	I	Ac	Bo		6,9	6,5	11,2	16,1	9,8	11,6	5,0	6,5			0,7	
<i>Pinnularia</i> spp.	Btn														0,9		
<i>Pinnularia gibba</i> Ehr.	Btn	I	N	Bo	x	1,9	2,8		11,4	2,7		0,8				3,2	
<i>Pinnularia incognita</i> G.Krasske	Btn	I						0,9									
<i>Pinnularia interrupta</i> W.Sm.	Btn	I	Ac	Bo			0,6										
<i>Pinnularia microstauron</i> (Ehr.) Cl.	Btn	I	Ac	Bo	Os		2,2	10,7	9,9	8,1							1,4
<i>Pinnularia viridis</i> (Nitzsch.) Ehr.	Btn	I	N	Bo	b	0,6		1,9			4,4						
<i>Sellaphora bacillum</i> (Ehr.) Mann	Btn	I	N	Bo					2,5								
<i>Sellaphora pupula</i> Kutz.	Btn	HI	Ак	Cos	b	0,6	8,3	20,1	14,9	3,3	8,9	1,5	5,4			3,5	
<i>Stauroneis anceps</i> et f. <i>gracilis</i> Rabh.	Btn	I	N	Bo		1,9	2,5	5,1	8,7	0,8	4,4		2,2			6,3	
<i>Stauroneis phoenicenteron</i> (Nitzsch.)Ehr.	Btn	I	Ак	Bo	b	6,3	1,9	3,7	1,7	2,4	1,8	6,9	2,4	1,8	2,1		
<i>Tabellaria flocculosa</i> (Roth.) Kutz.	Ep	Hb	Ac	AA	Os	53,8	34,0	25,2	14,0	16,3	39,1	44,8	30,2	29,1	38,6		

Ep – epiphytic, Btn – benthic

Hb – halophilous, HI – halophytic, I – indifferent

Ac – acidophilous, Acb – acidobiontic, N – indifferent, Ak – alkaliphilous

AA – arcto-alpine, Bo – boreal, Cos – cosmopolitan

Os – oligosaprobic, b - beta-mesosaprobic, x - saproxenous

5. LIMNOLOGICAL AND SEDIMENTOLOGICAL STUDIES

Viktor Sitalo, Dmitry Subetto & Lutz Schirrmeister

5.1 Introduction

The objective of the limnological part of the expedition was the retrieval of surface sediment samples and short sediment cores for later multiproxy palaeolimnological analyses in connection with a survey of lake-hydrology and bathymetry. The study is designed to contribute to a better understanding of the sedimentary environment in polygonal ponds and of regional late Quaternary palaeoenvironmental changes. During the field campaign the limnological and sedimentological studies were carried out near the Kytalyk station (Fig. 2-2). These studies included morphological description, measurement of water properties (water temperature, pH, electrical conductivity), sediment sampling, and the description and subsampling of the cores. An UWITEC gravity corer (Fig. 5-3), equipped with a 6 cm wide and 60 cm long PVC liner, was used for the undisturbed retrieval of the uppermost water-rich lake sediments. In small polygon ponds only the plastic liner were pushed into the soft sediment.

The choice of studied objects – polygonal ponds (Fig. 5-1) and thermokarst lakes (Figs. 5-4, 5-5) were made on the basis of their stage of development: (1) typical ponds in well-developed polygonal structures; (2) water basins formed due to merge of two and more polygonal ponds; (3) polygonal ponds in a stage of overgrowing.



Fig. 5-1: View of polygon ponds KYT-2 (left) and KYT-5 (right) near the Kytalyk field camp.

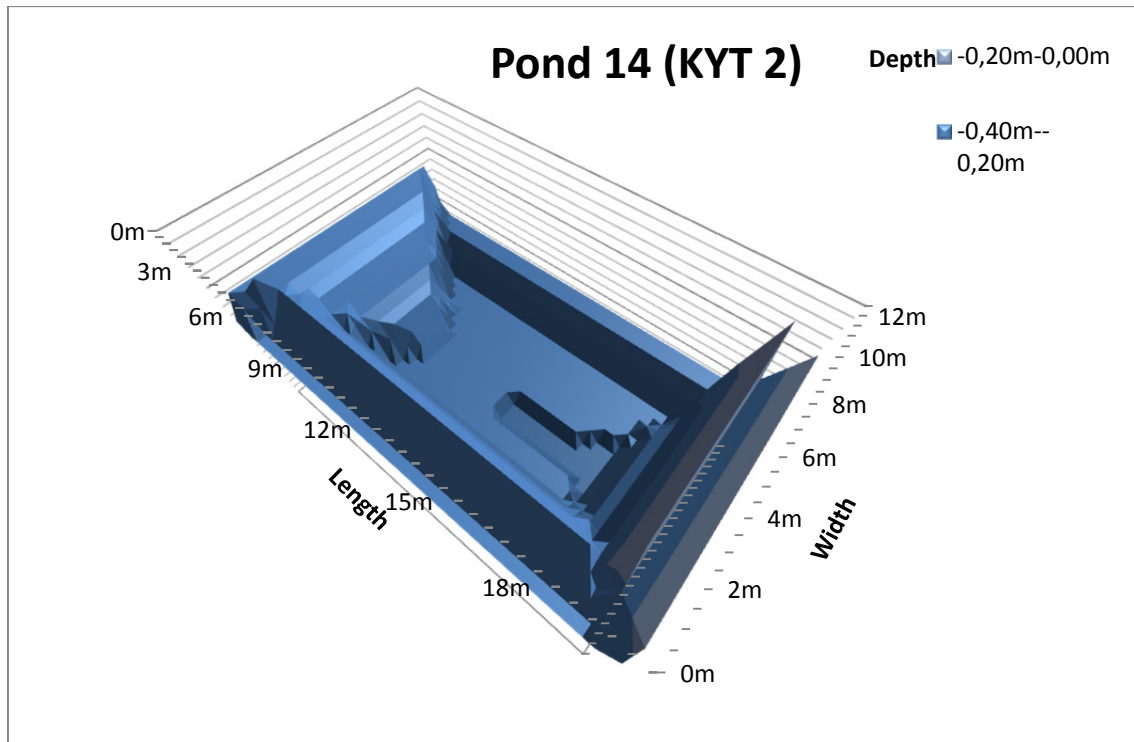


Fig. 5-2: Bathymetric model of the polygonal pond Kyt-2



Fig. 5-3: UWITEC gravity corer

Subsampling of each centimeter was made in the field laboratory of the Kytalyk station. Totally, 17 sediment cores were taken from 14 polygonal ponds and thermokarst lakes with length from 5 to 22 cm. The total number of sediment samples taken in the studied lakes and polygonal ponds is 223. Some duplicated cores as well as the upper centimeter of several cores was shared with colleagues of the Northeast Federal University Yakutsk for diatom analysis.

The results of the hydrological measurements from studied polygon ponds and thermokarst lakes are shown in Tab. 5-1. Values of water temperature varied in slightly from 16.1°C to 14.2°C in the surface waters. The conductivity varied around 20 to 53 $\mu\text{S}/\text{cm}$ and indicates extreme fresh-water conditions. The pH values between 5.5 and 6.4 pointed to slightly acidic conditions in water of studied basins.

Tab. 5-1: Water properties of studied water basins.

Site code	Water temperature (°C)	pH value	NH ₄ ⁺ (mmol/l)	NO ₂ ⁻ (mmol/l)	Conductivity, (µS/cm)	Date of sampling
14	14.2	5.6	0.003	0.402	53	20.07.2011
16	14.6	6.4	0.048	0.523	25	21.07.2011
20	14.8	5.5	0.024	0.188	23	21.07.2011
24	15.1	5.6	0.045	0.245	20	23.07.2011
124	16.1	6.8	0.028	0.730	40	26.07.2011
201	16.3	6.1	-	-	38	07.08.2011
25	14.5	6.2	-	-	32	10.08.2011
26	14.2	6.5	-	-	34	10.08.2011

5.2 Sediment description

5.2.1 Cores in polygon ponds



Sample Code	WP 14 / KYT-2
Date	21.7.2011
Type	polygonal pond
Location	upper alas level
Coordinates	70.83291°N 147.47839°E
Sampling interval	1 cm
Subsamples	11
Surface sample	x
Water depth	60 cm
Description	1-4cm brown organic material, medium decomposed, 4-8cm grey-brown organic material, little silty-sand content 8-11cm grey, compact organic material, compact, silty-sand



Sample Code	WP 20 / KYT-3 (1)
Date	23.7.2011
Type	polygonal pond
Location	lower alas level
Coordinates	70.84306°N 147.48895°E
Sampling interval	1 cm
Subsamples	8
Surface sample	x
Water depth	50 cm
Description	1 cm coarse-decomposed plant detritus, brown, roots visible 2 cm fine-decomposed, brown 3-8 cm coarse-decomposed plant detritus with silt

5. Limnological studies



Sample Code	KYT-7
Date	28.7.2011
Type	polygonal pond
Location	lower alas level (near the pingo site)
Coordinates	70.86152°N 147.49527°E
Sampling interval	2 cm
Subsamples	7
Surface sample	x
Water depth	29 cm
Description	medium decomposed peat, brown, roots and wood fragments visible



Sample Code	KYT-5 (2)
Date	4.8.2011
Type	polygonal pond
Location	upper alas level
Coordinates	70.82958°N 147.48596°E
Sampling interval	1 cm
Subsamples	16
Surface sample	x
Water depth	34 cm
Description	1-8 cm medium-decomposed plant detritus, brown 9-11 cm plant detritus, greyish-brown with small amounts of silty sand 12-16 cm silty sand, grey, compact, small amounts of plant detritus



Sample Code	KYT-8 (2)
Date	5.8.2011
Type	polygonal pond
Location	upper alas level
Coordinates	70.83157°N 147.48248°E
Sampling interval	1 cm
Subsamples	11
Surface samples	x
Description	collapsed polygon wall 1-4 cm undecomposed twigss and leafs of Betula, dark-brown/black 5 cm undecomposed with roots 6-7 cm weakly decomposed plant material, dark, roots, some silty sand 8-10 cm increasing amount of sandy silt, no roots



Sample Code	GPS 34
Date	9.8.2011
Type	polygonal pond
Location	lower alas level
Coordinates	70.84522°N 147.47943
Sampling interval	1 cm
Subsamples	12
Surface sample	x
Water depth	40 cm
Description	1 cm fine, decomposed plant detritus, dark-brown 2 cm fine, decomposed plant detritus, dark-brown, small roots 3-6 cm decomposed plant detritus, dark-brown, small roots, grey sandy silt 7 cm increasing amount of sandy silt 8-12 cm sandy silt, grey, compact, few roots



Sample Code	GPS 201 / KYT-17
Date	9.8.2011
Type	polygonal pond
Location	lower alas level
Coordinates	70.84276°N 147.47131°E
Sampling interval	1 cm
Subsamples	22
Surface samples	x
Water depth	31 cm
Description	1-3 cm fine plant detritus, decomposed, brown 4 cm fine plant detritus, decomposed, brown, some roots 5-10 cm medium decomposed plant detritus, many roots 11-16 cm medium decomposed plant detritus, many roots, more compact 17 cm medium decomposed plant detritus, many roots small amount of sandy silt 18 cm sandy silt, grey with small amount of plant detritus 19-22 cm sandy silt, grey, compact,

5. Limnological studies



Sample Code	GPS 25
Date	10.8.2011
Type	interpolygonal pond
Location	upper alas level
Coordinates	70.83495°N 147.47324°E
Sampling interval	1 cm
Subsamples	22
Surface sample	x
Water depth	59 cm
Description	0-2 cm fine decomposed plant detritus, brown, some leaves visible 3 cm medium decomposed plant detritus, brown 4-5 cm medium decomposed plant detritus, with sandy silt, grey 7-19 cm sandy silt, grey 20 cm sandy silt, grey, some medium decomposed brown plant detritus 21-22 cm sandy silt, grey



Sample Code	GPS 26
Date	10.8.2011
Type	polygonal pond
Location	upper alas level
Coordinates	70.83447°N 147.47691°E
Sampling interval	1 cm
Subsamples	17
Surface sample	x
Water depth	42 cm
Description	1-3 cm organic material, fine, brownish-greenish, single leaves and branches visible 4 cm moss (polytrchum ?) 5-7 cm moss and leaves 8-9 cm weakly-decomposed plant material, brown 10 cm medium decomposed plant material, sharp transition to grey sandy silt 11-12 cm sandy silt, grey, small amount of medium-decomposed plant material 13-16 cm sandy silt, grey, compact 17 cm sandy silt, grey, compact, very small amount of plant material

Sample Code	KYT-4/GPS 24
Date	9.8.2011
Type	polygonal pond
Location	lower alas level
Coordinates	70.84312°N, 147.48555°E
Sampling interval	1 cm
Subsamples	12
Surface samples	x
Water depth	32 cm
Description	1-2 cm fine, decomposed plant detritus, brown 3 cm fine, decomposed plant detritus, brown, small roots 4 cm slightly-decomposed plant detritus, dark-brown, small roots 5-8 cm slightly-decomposed plant detritus, dark-brown, small roots. small amount of sandy silt 9 cm sharp transition to sandy silt, grey 10-12 cm sandy silt, grey, compact

5.2.2 Cores in thermokarst lakes



Fig. 5-4: Thermokarst lake beneath the Yedoma Ridge (cores 128 and 38 (1; 2))



Fig. 5-5: Thermokarst lake behind the Yedoma ridge (core LBL)



Sample Code	WP 128/LBR
Date	31.7.2011
Type	Thermokarst lake
Location	70.84826°N 147.4741611°E
Coordinates	70.84826°N 147.41611°E
Sampling interval	1 cm
Subsamples	13
Surface sample	no
Water depth	286cm
Description	1-2 cm highly decomposed "organomudde", dark brown, some small roots visible 3 cm grey-brown, silty, smells rotten 6-8 cm grey, silty, more compact, less wet, no organics visible, smells rotten 9-10 cm grey, silty-sandy, organic free 11-15 cm grey, fine-sandy silty, brown organic detritus, intense rotten smell



Sample Code	WP 38/2
Date	1.8.2011
Type	thermokarst lake
Location	beneath the Yedoma ridge
Coordinates	70.83282°N 147.42198°E
Sampling interval	1 cm
Subsamples	19
Surface sample	no, second core (see Tab. 5-2)
Water depth	230 cm
Description	1 cm brownish organo-mud, 2-4 cm grey-brownish sandy silt 5-20 cm grey sandy silt, organic free



Sample Code	LBL
Date	6.8.2011
Type	Thermokarst lake
Location	Behind Yedoma
Coordinates	70.84688°N 147.40230°E
Sampling interval	1 cm
Subsamples	14
Surface samples	---
Water depth	221 cm
Description	1-4 cm fine plant detritus, brown, decomposed 5-14 cm fine plant detritus, brown, decomposed, more compact, rotten smell



Sample Code	LBR
Date	6.8.2011
Type	Thermokarst lake
Location	Behind Yedoma
Coordinates	70.83157°N 147.48248°E
Sampling interval	1 cm
Subsamples	15
Surface samples	--
Water depth	cm
Description	fine decomposed organic material, brown, rotten smell

5.3 Conclusions and outlook

The expedition was very successful, as it was possible to obtain short sediment records from the different types of water basins (polygonal ponds and thermokarst lakes). The recovered sediment cores will be studied by a multi-proxy approach. Pollen analyses are used for the reconstruction of regional vegetation history and climate. Chironomids will provide information on palaeo July temperatures and palaeoecological changes. Diatoms will be determined for the reconstruction of palaeoecological conditions and lake history. A major issue will be the characterization and provenance analysis of the detrital sediment fraction to infer changes in lake-level fluctuations. High-resolution geochemical and grain size data help to gain insights into short-term environmental changes at millennial to centennial time scales.

Tab 5-2: Additional cores. Taken for bioindicator studies

Sample Code	WP 38/1	KYT-5 (1)	KYT-8 (1)
Date	1.8.2011	17.7.2011	5.8.2011
Type	thermokarst lake	polygonal pond	Polygonal pond
Location	beneath the Yedoma ridge	upper alas level	upper alas level
Coordinates	70.83282°N 147.42198°E	70.82958°N 147.48596°E	70.83157°N 147.48248°E
Sampling interval	1 cm	--	1 cm
Subsamples	14	--	5
Water depth	80 cm	34 cm	286 cm
Description	1-4 cm brownish mud 5-14 cm sandy silt, grey		undecomposed plant material, branches and leafs of Betula, dark-brown/black

6. RECORDS FROM THE MODEL POLYGON LHC-11 FOR MODERN AND PALAEOECOLOGICAL STUDIES

Annette Teltewskoi, Juliane Seyfert & Hans Joosten

6.1 Introduction

Polygon mires are typical mires of the (sub)arctic zone. They show typical short-distance diversity in vegetation and site-conditions. As far as known, ice wedge polygons are quite complex and highly dynamic ecosystems with a complex interplay of water, ice, vegetation and peat. Over a period of a few decades a polygon may change from wet to dry vegetation (de Klerk et al., 2011).

Climate change has been particularly intense in the Arctic (McGuire et al., 2007, Serreze et al., 2000). But how large is the influence of external climate change on the polygon mires actually and how is the impact of internal polygon dynamics? Does a trend exist?



Fig. 6-1: The model polygon LHC-11. a) LHC-11 from the south east. b) Vegetation pattern with *Betula exilis*, *Vaccinium vitis-idea* and *Sphagnum* sp. c) LHC-11 from the south.

To answer these questions modern ice wedge polygons must be understood and compared with sub-recent and fossil ice-wedge polygons in correlation with weather and climate data. This requires high resolution temporal and spatial studies.

High resolution temporal studies are possible with a new instrument called DAMOCLES. This was developed and applied in Greifswald and allows high-

resolution palynological analyses, reaching with sample distances as small as 0.05 cm a resolution of one year (Joosten & de Klerk, 2007a/b, De Klerk et al., 2011).

During the fieldwork our working group chose one representative polygon as a model polygon called LHC-11 (Fig. 6-1), which was analyzed in detail (Tab. 6-1).

Our hypothesis is, that the polygon LHC-11 is developing from a low center polygon to a high center polygon. At the moment it has a Low center but looks more like a High Center polygon (2011) because of its wide ridges and relatively small central depression. According to our hypothesis the former ice wedge ridge of the low center polygon collapsed and “moves and grows” into the center of the polygon.

To describe the modern polygon LHC-11 we did detailed vegetation sampling, measured surface ground, water level and active layer depth (Tab. 6-1). In addition, surface samples were taken. To describe a) palaeoecology of sub-recent and fossil ice-wedge polygons and b) the dynamic of LHC-11 seven peat profiles were taken. These seven peat profiles from one polygon will allow the three-dimensional reconstruction of polygon development.

The development of polygon LHC-11 seems to be quite complex. Because unexpectedly deep peat layer and polymorphology of the modern landscape with large height differences reveal a relatively old system. In addition, loamy peat layers show that a further influence operates. It might be flooding.

Tab. 6-1: Methods and sample amounts for studying the model polygon.

No	Methods	Amount	Chapter
1	vegetation relevés	546	6.3
2	herbarium	30 species	6.3
3	mosses for determination	about 200	6.3
4	height measurements of ground surface height, permafrost table height and water level	2 x 546	6.4
5	surface samples for pollen, macrofossil and rhizopod analyses	546	6.5
6	peat profiles for pollen, macrofossil and rhizopod analyses, C/N, LOI...	7	6.6
7	reference material for macrofossil analysis	16	6.6

6.2 Study site

The study site, including the polygon LHC-11 (70,83069° N, 147,48115° E) is located in an alas, about 300 m from a Yedoma ridge and about 600 m from the Berelekh River bank (Fig. 2-3). It is a regular grid within an area of 21 x 26 m with coordinates 0 to 25 (x-axis) and A to U (y-axis) (Fig. 6-3). The study site was divided into 546 plots, each square and 1 m². The grid was built with the help of wooden sticks and strings. A stable frame could be constructed with the help of four wooden sticks fixed in permafrost in each corner of the study site.

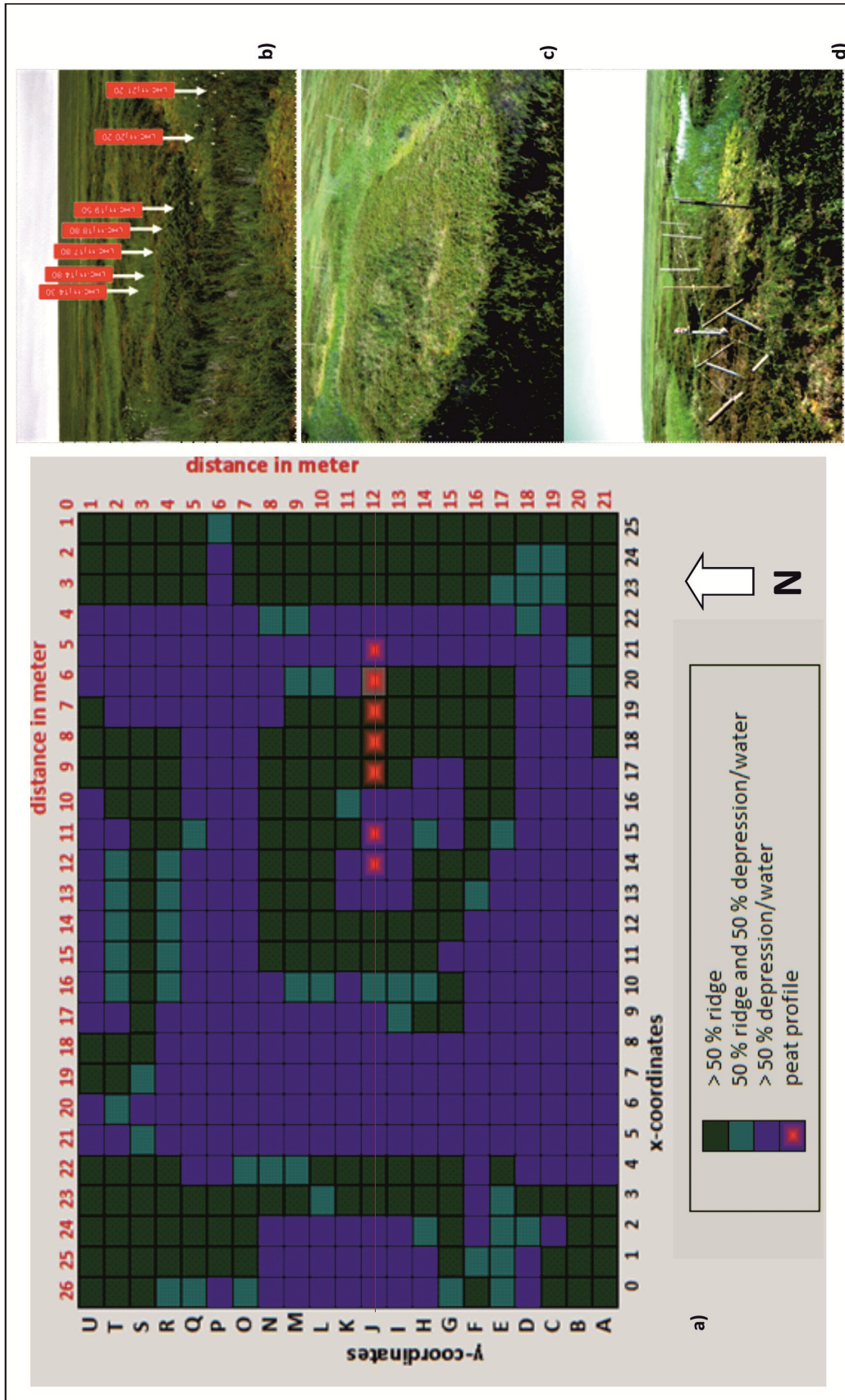


Fig. 6-2: Study site of LHC-11. a) Grid with ridge-depression distribution and position of the seven peat profiles. The red line marks the cross section. b) Picture from south-east with position of the peat profiles. c) Picture from south and above. d) Grid construction.

The morphology of the polygon LHC-11 can be described as follow:

- It is quite regular.
- It consists of a rectangular ridge system.
- The ridges are dry and differ in height.
- The center is a shallow pool.
- Behind the ridges deep pools follow that border to further ridges/degraded ridges of adjacent polygons.
- The southern ridge of LHC-11 forms a “hydrological window”, a hydrological connection between the central depression and the outer pools. Deeply thawed areas in polygon ridges form “hydrological windows” (Minke et al., 2007a, 2007b, 2009; Donner et al., 2009).

6.3 Vegetation

The vegetation cover of all 546 plots of LHC-11 was assessed using a modified scale according to Londo (1976) (Tab. 6.2). The total cover of shrubs, dwarf shrubs, herbs, mosses, lichens, litter and water was estimated in percent. Nomenclature of vascular plants follows Czerepanov (1995).



Fig. 6-3: Vegetation sampling. a) Impression of the fieldwork. b) Plot A24 with 1 x 1 m model square, dry ridge vegetation. c) Plot B13 with model square and wet depression vegetation.

The vegetation sampling was carried out with the help of a 1 x 1 m model square, containing 25 subplots (Figs. 6-3, 6-4). Almost all higher plants were determined during the fieldwork. Mosses and lichens were collected in paper bags. They will be determined at University of Greifswald with the help of experts and special literature. All higher plants, found in the study site were collected in a herbarium (Appendix 5, Tab. A 5-1).

Tab. 6-2: Scale, modified according to Londo (1976), used for assessing vegetation cover.

Cover	Class/mean
one plant and <1%	0.01%
<0.5%	0.1%
0.5-2%	1%
2-4%	3%
4-7%	5%
7-15%	10%
15-25%	20%
25-35%	30%
35-45%	40%
45-55%	50%
55-65%	60%
65-75%	70%
75-85%	80%
85-95%	90%
95-100%	100%



a)



b)

Fig. 6-4: Vegetation pattern. a) Typical dry ridge vegetation with mosses, lichens and *Vaccinium vitis-idaea*. b) Typical wet depression vegetation with *Carex concolor* (*Carex aquatilis* ssp. *stans*) *Eriophorum angustifolium* and *Sphagnum* spp..

In all 546 vegetation relevés 25 vascular plant taxa were found (Appendix 5, Tab. A 5-1). 44 moss types, including 21 *Sphagnum* types, and seven lichen types were distinguished during the fieldwork. The mosses contain probably doublets. The lichens are supposedly seven different species.

6.4 Ground surface height, permafrost table height, water level and active layer thickness

Height measurements from the central spot of each plot of the study site included

- ground surface height (referring to the surface of the living moss or litter),
- permafrost table height (determined mechanically with a 304 g heavy wooden rod), and
- water level.

The active layer thickness can be calculated as the difference between ground surface height and permafrost table depth. All measurements were related to a horizontal reference plane above the ground surface, established by horizontally stretched strings with the help of a water level tube (see below). During the fieldwork the measurements were carried out under various weather conditions, as a consequence the water level changed (range 11 cm).

To get an idea of the dynamic of the active layer thickness of a whole polygon all measurements were carried out twice: 1st period in the middle of the summer season (24th July to 4th August) and the 2nd period at the end of the summer season (19th to 22th August). The measurements of the 2nd period show approximately the maximal active layer thickness at the end of the summer. The data of the height

measurements allow the 3-dimensional reconstruction of the study site, which is visible in figure 6-5. The 3D-graphics were generated with the mac-software Grapher 2.1. Further results, based on the data taken in the 1st period are visible in the cross section of the study site (Fig. 6-6).

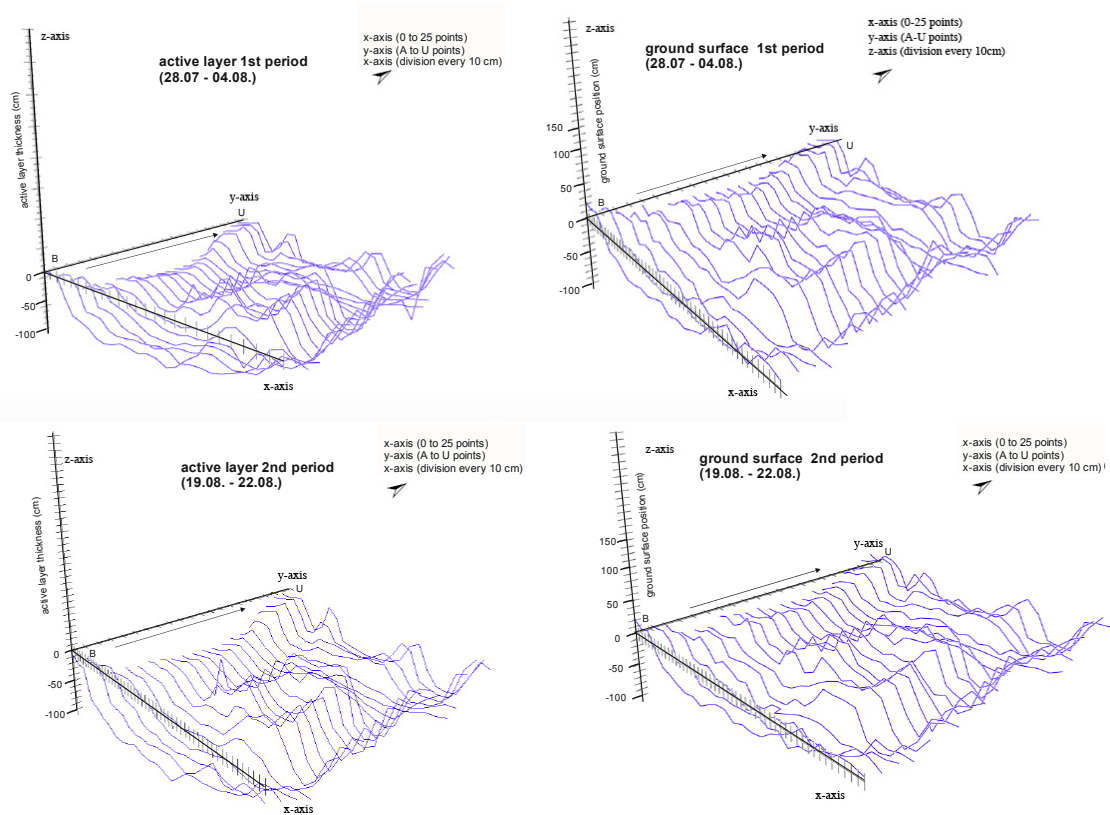


Fig. 6-5: 3D graphics of permafrost table height and ground surface level measurements of the model polygon LHC-11 in the beginning and at the end of the field studies.

The range of the ground surface height is 110 cm. The maximal active layer thickness is 114 cm in the 1st period, however in the 2nd period 117 cm. The difference between the arithmetic means of the active layer thicknesses of 1st and 2nd period is 11 cm.

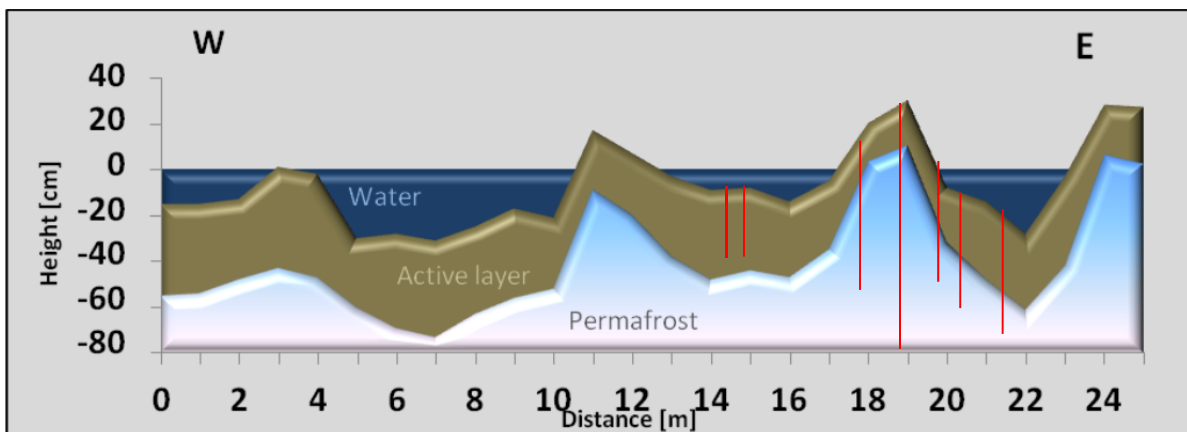


Fig. 6-6: Cross section of the study site. The red lines mark the position of the seven peat profiles.

For the establishment of a uniform horizontal reference plane above our study site, we used a so-called water level tube (Fig. 6-7). This is a simple but quite accurate device, which consists of a water filled tube. With the help of a water level tube two optional points can be scaled at the same height. The same height levels can be transferred over large distances, depending on the length of the used tube. The functionality of a water level tube is based on the physical principle of communicating vessels: in connected vessels, a homogeneous fluid balances out to the same level in all vessels (regardless of their shape and volume) because gravity and pressure are constant in each vessel. As a consequence both water levels of the tube ends have always the same height.

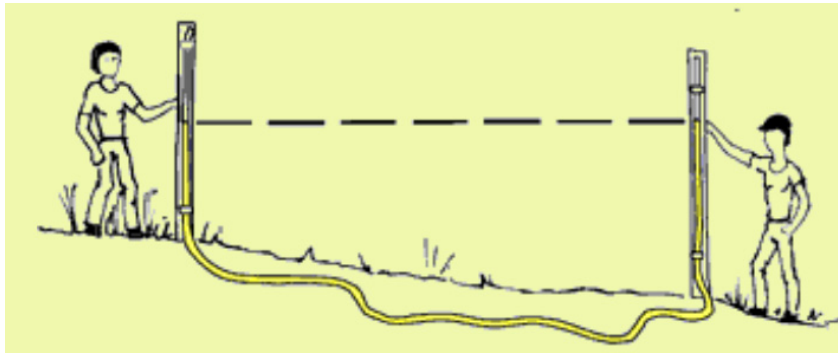


Fig. 6-7: Usage of a water level tube.
(<http://www.boeingconsult.com/tafe/ss&so/survey1/Module4/equipment-s1.htm>)

6.5 Surface samples

Surface samples were taken from the central spot of each plot (546). The surface sample consists of the surface of the moss-cover or, where water, of the first soil layer under water. One surface sample contains about 50 cm³. The surface samples are stored in plastic bags. They will be used for pollen, macrofossil and rhizopod analyses.

6.6 Peat profiles for palaeoecological research

For palaeoecological analyses (e.g. pollen, macrofossil, rhizopodes, C/N, LOI), seven peat profiles were taken along a transect from the eastern margin to the center of the polygon: through the outer depression, the ridge and reaching into the central depression (Fig. 6-3, 6-9).



Fig. 6-8: Collection of the peat profiles. a) Getting out the peat profile LHC-11 j20,20 with the tube corer. b) Ditch to get the three ridge peat profiles. In the middle of the ditch is the covered peat profile LHC-11 j18,80 visible. c) Ice wedge under the profile LHC-11 j14,30 in the central depression.

The peat layer was unexpectedly deep. Because of permafrost and ice (wedges), the cores could not be taken by a “normal peat corer”, but:

- 1.) The ridge profiles were dig and sawed out. The deepest core LHC-11 j18,80 is about 120 cm long. The mineral soil has not been reached.
- 2.) The profiles in the central depressions were dug out after drainage of the central depression.
- 3.) The profiles of the deeper outer depression were cored with a tube corer (Fig. 6-8). The metal tube corer has a radius of 20 cm and a length of 80 cm.

For transportation all cores were cut in 15 cm x 10 cm x individual length and stored in a stable wooden box. For macrofossil analysis reference material was collected (Appendix 5, Tab. A 5-1). Therefore, potential peat building plants were collected, in total 17 species. The entire plants are stored in ethanol.

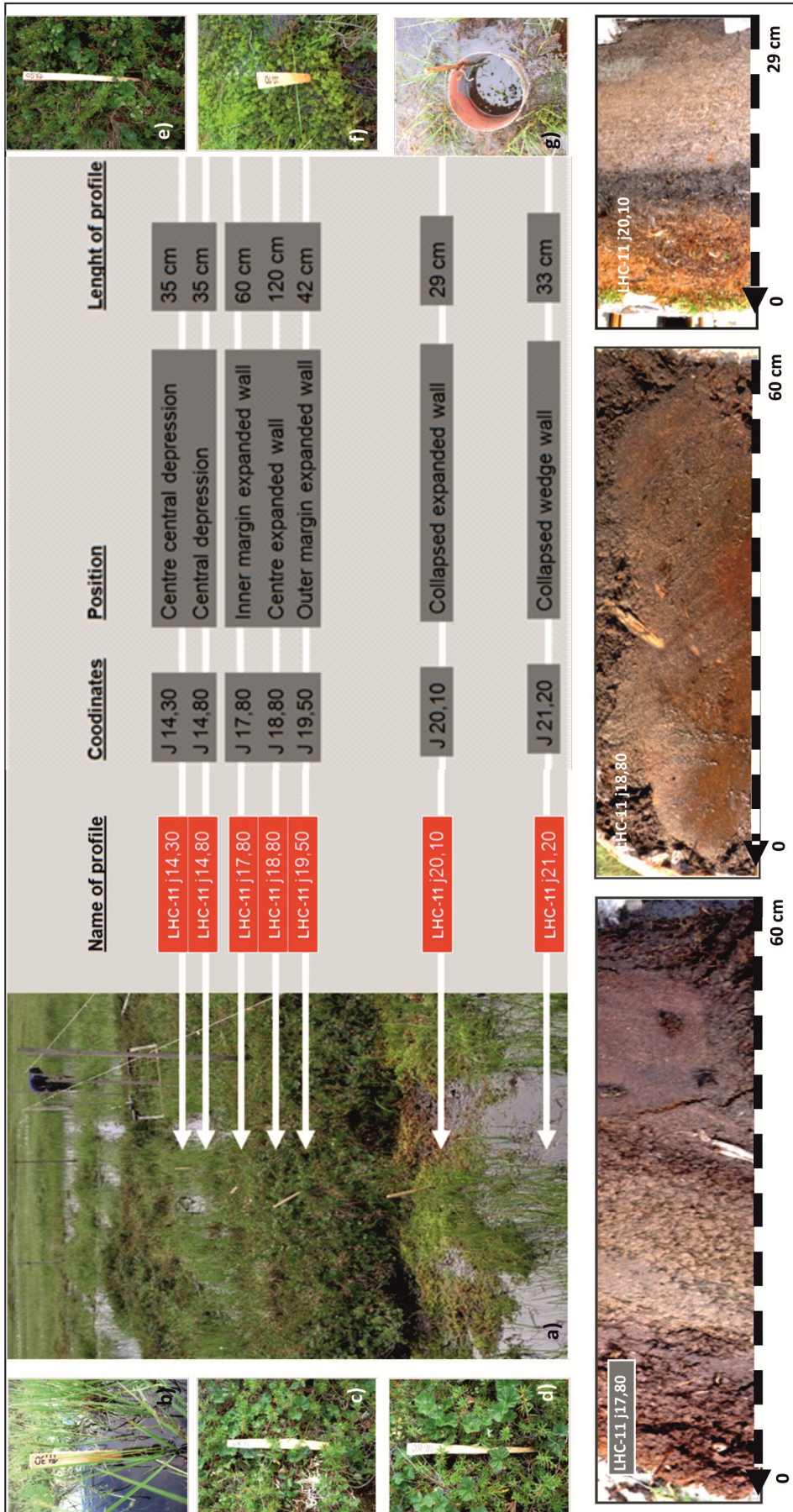


Fig. 6-9: Peat profiles. a) Polygon LHC-11 with marked position of the peat profiles. Location of peat profiles b) LHC-11 j14.30, c) LHC-11 j17.80, d) LHC-11 j18.80, e) LHC-11 j19.50, f) LHC-11 j20.10, g) LHC-11 j21.20. The profile LHC-11 j18.80 was divided into two parts, each 60 cm long.



Fig. 6-10: Sample preparation for high resolution palaeoecological studies. a) DAMOCLES instrument for peat slice cutting. b) Frozen peat core. c) Peat slice of 0.5 cm. d) Puncher with subsamples.

First sample preparation was carried out in Greifswald with the frozen core LHC-11 j18,80 (Fig. 6-10). This peat profile was cut into contiguous slices of 0.5 cm thickness with the DAMOCLES device (Joosten & de Klerk, 2007a). Afterwards, each slice was punched into the following subsamples:

- 1.) Pollen samples 2 cm³
- 2.) Rhizopod samples 2 cm²
- 3.) LOI samples 3 cm²
- 4.) Macrofossil samples 3 cm²
- 5.) C/N samples margin

The entire sample preparation was carried out in a freezer. Currently the pollen samples are being analyzed.

7. PEDOLOGICAL STUDIES OF VARIOUS POLYGON SITES

Fabian Beermann & Lyubov' Kokhanova

7.1 Introduction

The polygonal tundra is characteristic for poorly-drained arctic lowlands. This very heterogeneous ecosystem type has been found to be today a carbon sink (Wille et al., 2008). Changes in the nutrient availability of the soils can lead to changes in the ecosystem's primary production (Biasi et al., 2008). Plants will assimilate more carbon which could offset higher CO₂-emissions due to ecosystem respiration (Schuur et al., 2008). Hence, changes of nutrient availability will substantially affect changes of the carbon balance of arctic ecosystems (Weintraub & Schimel, 2005).

However, further progressions of arctic ecosystems depend on complex interactions between hydrology regime, plant-species composition and nutrient supply, which are currently not sufficiently understood. On the other hand, changes in the carbon budget of arctic ecosystems are likely to have global implications (Sturm et al., 2005). Hence, a comprehensive understanding of the nutrient dynamics in arctic soils is important to predict further responses of arctic ecosystems to climate change.

Testate amoebae (Rhizopoda, Testacea) are a group of free-living protozoans that have an organic shell (testa). Their well-defined ecological preferences and the relatively good preservation of fossil shells in peat deposits, lake sediments, and buried soils form the basis for the development of rhizopod analysis as a method for reconstruction of climate and environmental changes (Mattheeussen et al., 2005).

Testate amoebae, being inherently aquatic organisms, respond by restructuring their coenoses to environmental changes such as ground water table, moisture, pH, content of biophilic elements (N, P, K, Ca, Mg), and organic matter. They can be classified into ecological groups according to their moisture (hygrophiles, hydrophiles) and pH requirements (acidophiles, calciophiles), and habitat preferences (sphagnophiles, soil-living, xerophiles) (Charman, 1997). The significance of rhizopod analysis for palaeoecological studies and environmental changes are based on the fact that testate amoebae are permanently attached to the substrate. Their shells are normally destroyed if the sediments are redeposited. Therefore, they are often the only organisms that can directly indicate the palaeoenvironmental conditions during sediment formation, unlike many other biological remains (Bobrov et al., 2004).

7.2 Goals and Questions

The main objective of this study is to gain insight into nutrient dynamics and the complex of rhizopod communities of polygonal tundra ecosystems. By estimating bioavailability (especially availability of nutrients) of the organic material in the context of potential impacts of arctic climate warming on the polygonal tundra, this

study contributes to the discussion whether arctic polygonal tundra will turn into a carbon source or not.

Based on the main intend of this study, the following questions are planned to be answered:

A. Nutrient Distribution:

- How are nitrogen and phosphorus distributed on the micro-scale (10^0 to 10^2 m²) within the polygonal tundra ecosystems concerning all organic and inorganic pools?
- What are the differences on the ecosystem scale (10^4 to 10^6 m²) between different polygonal tundra sites?

B. Nutrient Transformation:

- Which effects do cryogenic processes have on the bioavailability of the organic material and on nutrient transformation?
- Which effects may (global) warming have on the bioavailability of the organic material and on nutrient transformation?

C. Rhizopod Analyses

- Which species can be found in the dominant rhizopod complexes?
- What are the differences of the complex of rhizopods between different polygonal tundra sites?

D. Synthesis

- How can increased understanding of the organic matter and nutrient dynamics within the polygonal tundra help to predict future changes in the ecosystem?
- Which changes in carbon emissions from polygonal tundra ecosystems can we expect in the future due to changes in the nutrient supply of the soils?

7.3 Fieldwork

Soil sampling in the field has been conducted in three steps: First, eight different polygons (KYTF1 to KYTF7, YED1, Fig. 2-3) were studied by establishing, describing and sampling four soil profiles within the active layer at each of these sites. Characterization of the soil types were conducted following US Soil taxonomy (Soil Survey Staff, 2010) as well as the Russian soil classification (Shishov et al., 2004). At each profile, one vegetation sample and on average three soil samples over the soil depth were taken. The polygons have been selected regarding differences in water level, extension of the elevated rim and state of degradation. This has been done to get an overview on the spatial variability of the nutrient availability on the ecosystem scale, as well as on the diversity of the soils in the investigation area.

In a second step, the polygon LHC11 on which also palaeoecological analyses have been done (chapter 6) has been investigated by 24 soil samples to get knowledge about the micro-scale differences in nutrient availability within one distinct polygon. At this site, also five soil-cores up to 120 cm long have been taken and investigated. The soil cores have been split into sub-samples from each 5 cm.

In a third step, the first three polygons that have been investigated at the start of the campaign have been reinvestigated at the end of the campaign to get first ideas about temporal dynamics of the nutrient availability in the polygonal tundra.



Fig. 7-1: Sampling of undisturbed soil samples.

Additionally, undisturbed soil samples were taken from three sites for incubation experiments in the laboratory. For this reason, metal rings have been pushed into the soil (Fig. 7-1). For each horizon, 12 replicates have been taken.

All soil samples have been investigated in the field laboratory for their gravitational water contents, for pH and electrical conductivity and for the extractable amounts of ammonium (NH_4^+), nitrate (NO_3^-) and phosphate (PO_4^{3-}) (see appendix 6). The water content of the fresh soil sample has

been measured gravimetrically after drying on a furnace. Due to challenging working conditions, these field laboratory measurements of the water contents are not very good: Many of the samples have been partly burnt during the drying process. Only the water contents that were measured in the later period of the expedition are reliable. Hence, all sample water contents will be reanalyzed in the laboratory to recalculate the dry-weights of the amounts of nutrients, and so not all field data can be used yet to produce preliminary results.

Electrical conductivity (EC) and pH have been measured by a portable measuring device (WTW pH/Cond 340i). Both investigated nitrogen compounds have been extracted by 0.0125-M CaCl_2 Solution (VDLUF, 1991). This extraction addresses only plant available molecules. Phosphate was measured by extraction with 0.5-M NaHCO_3 solution (Ivanoff et al., 1998). By this method, the pool of phosphorus which can be mobilized during one vegetation period is estimated (Bowman & Cole, 1978). Within these extracts, the amounts of nutrients have been photometrically measured with a portable photometer (Hach LANGE DR 2800) and rapid chemical analysis tests (Hach LANGE: LCK 304 (Ammonium), LCK 339 (Nitrate), LCK 349 (Phosphate)). In total, 260 soil samples have been taken, which have already been investigated during the expedition for their extractable amounts of nutrients and water as well as for pH and EC.

Furthermore, 60 vegetation descriptions were conducted and vegetation samples were taken and dried for later analyses of their elemental composition.

7.4 Preliminary Results

7.4.1 Site description

The location of each pedological study site is shown in figure 2-3.

KYTF1: This site is with the same as the monitoring site KYT-1. For detailed description see chapter 3.

KYTF 2: The center of this low-centered polygon had a diameter of about 2 0m in diameter and was wet but not flooded. The polygon rim had an extension of 6

m. The eastern part of the rim was collapsed and only fragments, covered by *Andromeda polifolia* were remaining.

KYTF3: This low-centered polygon was characterized by a very small center of 2 m in diameter and in contrast a very broad rim of 10 m width. The center was fallen dry but the ice-cracks were water filled. The rim was completely covered by *Betula nana* shrubs.

KYTF4: This polygon had a diameter of 15 m. The eastern part of the polygon rim was up to 50 cm high. In diameter, the rim was up to 10 m wide but the top of the ice-wedge was completely thawed and replaced by a water filled trench. The western part of the rim was again collapsed and only fragments, covered by *Andromeda polifolia* were remaining.

KYTF5: This low-centered polygon was located near the transition between the two alas-levels. The eastern part of the rim had a diameter of 5 m. In north-south direction, the center had an extension of 20 m. Between rim and center there was a small area covered by Sphagnum-mosses. The eastern part of the polygon was completely degraded and the water-filled center was connected with a flooded area which could be formed by thermokarst-processes.

KYTF6: This low-centered polygon was located in the second alas-level, near the river which flows through it. The rim had an extension of 6 m. The water-filled center had a diameter of 14 m. Between rim and center, there was again a moss-covered transition zone.

KYTF7: This polygon was also located in the second alas-level. It was characterized by a higher water level of 25 cm. The rim had an extension of 6 m. The center had a diameter of 10 m. The north-western part of the rim was completely degraded.

KYTF8: This polygon of the second alas-level was characterized by a low rim and little differences in height between rim and the water filled center. The rim was 3 m wide. The center had a diameter of 10 m and was connected with a flooded area.

7.4.2 Pedological Investigations

The greatest number of the investigated soil profiles belonged, after US Soil Taxonomy, to the subgroups of the Histels (“Histic Gelisols”) – permafrost soils with high contents of organic matter. Further differentiation into the great groups was carried out after criteria of different decomposition states of the organic material and the occurrence of underlying layers of ice: Only on the polygon rims, above recent ice-wedges, Glacistels were found (Fig. 7-2 A). Soils of the different peat decomposition states (Fibristels, Hemistels & Saprastels – (Fig. 7-2 B) have been found in the whole investigation area. In contrast, mineral soils with only thin peat layers and cryoturbation properties have been found only in the second alas level.

After the Russian classification (Shishov et al., 2004), the biggest part of the investigated soils has been classified as Gleyzems in the order of Gley Soils. The soils in the investigation area were further characterized by horizons which are primarily made up by slightly decomposed and moderately decomposed peat, respectively. These Peaty Gley Soils correspond to the Histels of the US Soil Taxonomy.



Fig. 7-2: Two soil profiles of the study site KYTF1. Horizon symbols after the US Soil Taxonomy in red, after the Russian classification in yellow **(A)**: Soil profile KYTF1.1. (polygon rim) – Typic Glacistel and Peaty Gley Soil, respectively. Two layers of peat in different decomposition states (Oi,Oe – T0, T1) and a mineral horizon (Bg - G) directly above the ice-wedge. **(B)**: Soil Profile KYTF1.4. (polygon center) – Typic Sapristel and Humic Peaty Gley Soil, respectively. Two layers of peat in different states of decomposition (Oi, Oa – T0, Th). Soil profile is dominated by highly decomposed peat (Oa - Th).

As a result of the microtopography in the polygonal tundra, the polygon rims have nearly always been dryer than the polygon centers. This had also implications for the thickness of the peat layers: In the polygon centers, the peat layers were much thicker than in the polygon rims. In addition, the peat layers of the polygon rims have been thicker in the first alas level than in the second. The peat layers of the polygon centers showed no strong difference between the two alas-levels (Tab. 7-1).

Tab. Fehler! Kein Text mit angegebener Formatvorlage im Dokument.-1: Thickness of peat layers in the investigation area

1 st alas Level		2 nd alas level	
Polygon rims	Polygon centers	Polygon rims	Polygon centers
14.6±1.7 cm	28±9.3 cm	10.5±2.6 cm	26.5±3.7 cm

7.4.3 Chemical Analyses

In the soil core taken from the intensively investigated polygon (LHC-11, chapter 6) there has been a coinciding maximum of water content and concentration of extractable ammonium at a depth of 75 cm. In this soil core, the amount of extractable nitrogen was decreasing over the first 20 cm. In contrast, the amount of extractable phosphate was slightly increasing in the depth with decreasing water content (Fig. 7-3, appendix 6, Tab. A 6-1).

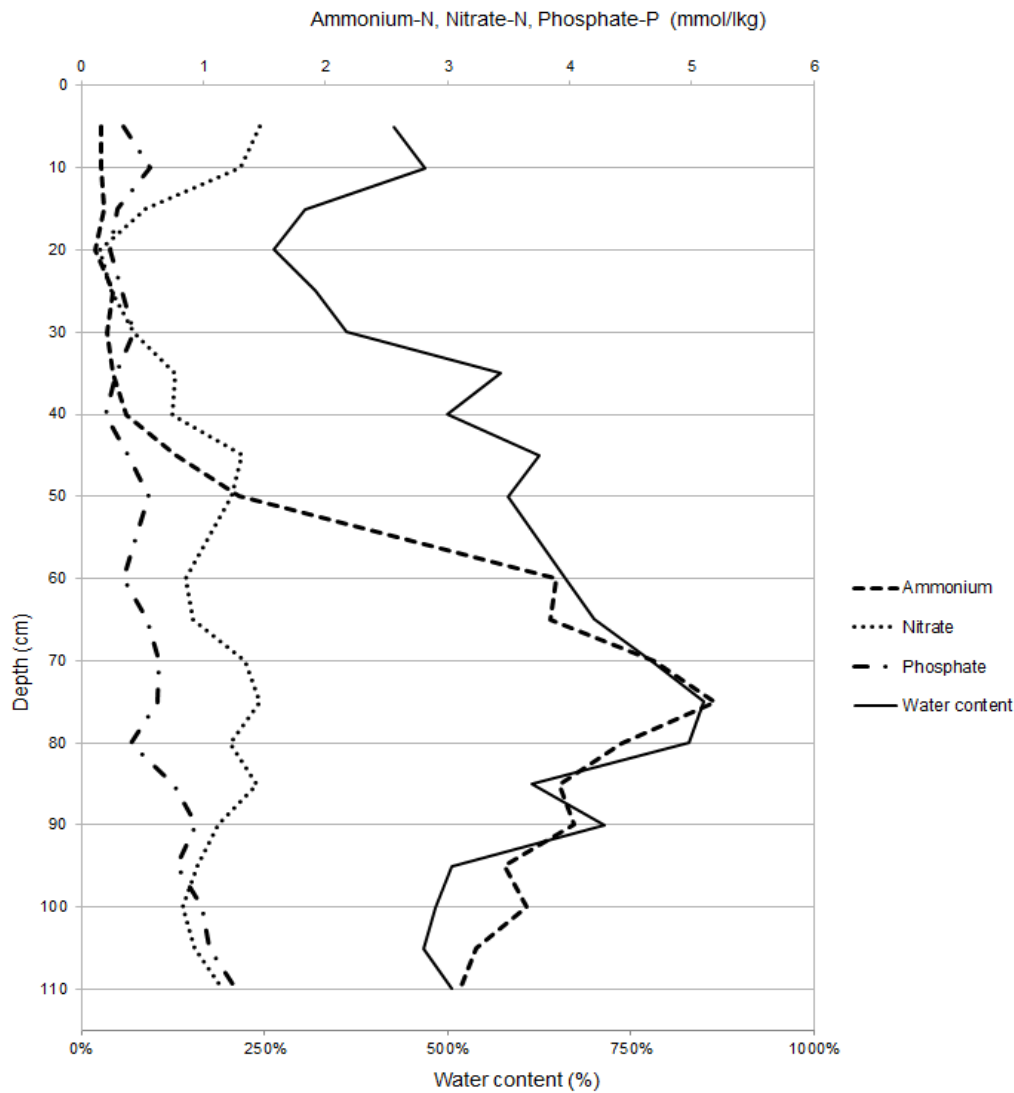


Fig. 7-3: Amounts of extractable nutrients and gravimetrical water content in the core J18,80 , taken out of a polygon wall from the polygon LHC11. Amounts of nutrients are shown in quantity (mol) of N and P, respectively, per dry mass of the soil. There is a coinciding maximum of water content and ammonium concentration at a depth of 75 cm. Concentration of extractable phosphate is increasing in the depth with decreasing water content

As there are no reliable water content data for most of the investigated polygons only field data for one investigated polygon is shown (Fig. 7-4). The concentrations of extractable phosphorus and nitrogen in relation to the dry weight of the soils are decreasing with depth while the concentration of extractable ammonium is increasing in the depth.

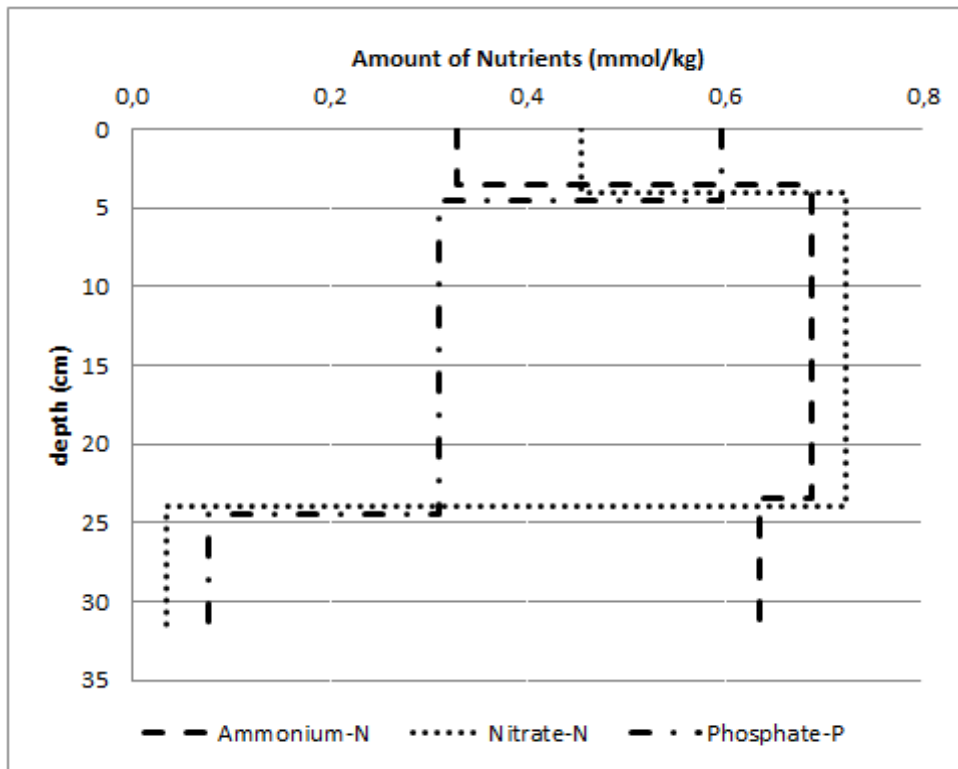


Fig. 7-4: Distribution of extractable nutrients in the soil profile KYTF3.4. (polygon center). Amounts of nutrients are shown in quantity (mol) of N and P, respectively, per dry mass of the soil. Concentration of ammonium is increasing with depth while concentration of nitrate as well as phosphate is decreasing with depth.

Although only in the later period of the expedition measurement of the water contents produced reliable results as was mentioned in chapter 7.3, figure 7-5 shows a comparison of the amounts of nutrients between the beginning and the end of field work. Data of the top soils along a transect from the polygon rim (KYT1.1.) to the polygon center (KYTF1.4.) are presented related to the molecular mass of Nitrogen and Phosphorus, respectively. First, it is apparent that the amounts of the phosphate are higher than the amounts of extractable ammonium and nitrogen, respectively. Furthermore, the ammonium values tend to decline during the period (Fig. 7-5A) while nitrate tends to increase (Fig. 7-5B). In contrast, the amount of extractable phosphate appears to increase in one soil profile while decreasing in the other soil profiles and also remains at the same level in a third soil (Fig. 7-5C). These patterns are also visible in other data set not presented here.

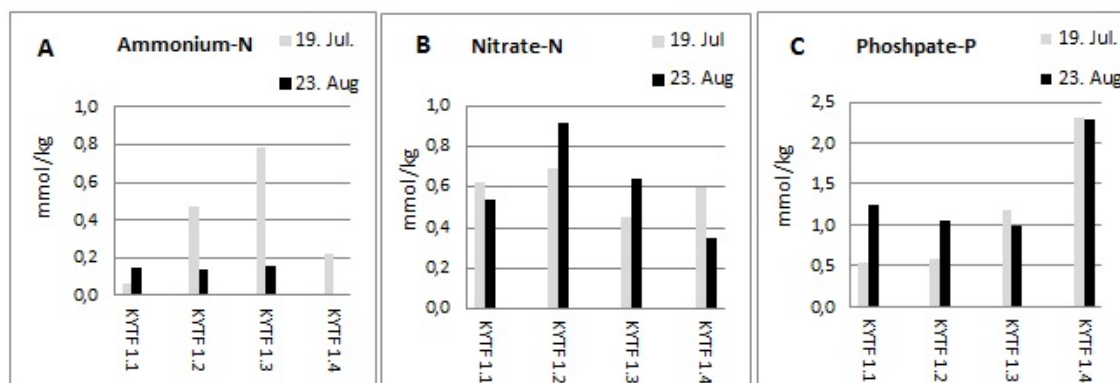


Fig. 7-5: Amounts of nutrients in extracts of CaCl_2 (A, B) and Na_2HCO_3 (C), respectively. Amounts of nutrients are shown in quantity (mol) of N and P, respectively, per dry mass of the soil. Comparison of four soils of one site between 19th of July and 23rd of August is made. Extractable ammonium appeared to decrease in all four soils while extractable nitrate remained mostly at the same level. Extractable phosphate decreased in two soils and increased in one other soil.

7.5. Field data interpretation

Although almost all soils were classified as Histels (histic Gelisols) and Peaty Gley Soils, respectively; there was still a great variability between the different soils. This variability depended for example on the type of the peat as well as on its state of its decomposition. Other characterizing properties have been the occurrence of ice-wedges, the hydrology and the chemical composition. In addition, some of the characterizing properties – as the amount of organic carbon – will only be measured in the laboratory. Also the composition of the testate amoebae communities will be investigated in the laboratory. This group of organisms is very sensitive to such ecological differences and therefore very likely to differ between these soils (Warner & Charman, 1994).

7.5.1 Chemical Analyses

The intensively investigated polygon LHC-11 (see chapter 6, Fig. 7-3) appeared to be in an advanced stage of degradation: It had a very broad and high rim. Probably, the development of segregation ice in the rim of this polygon led to its extension and to heaving of the ground, respectively. Furthermore, the tops of the ice wedges were all replaced by large water-filled trenches.

As ammonium gets oxidized under aerobic conditions (Scheffer & Schachtschabel, 2002), it is explainable that the amount of ammonium is correlating with the water content. But its maximum in depth could also indicate the zone where the polygon rim was less extended and where it was wetter in the past. As it is known that microorganisms can still be active at temperatures below 0 °C (Schuur et al., 2009; Wagner et al., 2007) it is also possible that there is recent decomposition of organic material. Due to high impermeability of the frozen ground, the produced ammonium could not be further oxidized to nitrate.

As there is more ventilation in the topsoil, the maximum of nitrate in the first centimeters can also be due to oxidizing conditions. Why the phosphate is increasing in the depth can only be answered by the planned analyses of total amount of phosphorus in the soil by x-ray fluorescence spectroscopy.

The distribution of the nutrients in the profile KYTF 3.4 (Fig. 7-4) can also be explained by oxidizing properties: In the topsoil, ammonium gets oxidized to nitrate while under the reducing conditions in the lower soil the produced ammonium does not get oxidized further (Scheffer & Schachtschabel, 2002).

The distribution of the amounts of extractable phosphate is hard to explain by the current data in both profiles: By the applied extraction method the pool of mobilizable phosphate, including the plant-available phosphate, was measured (chapter 7.3). But phosphate in the soil is stored in different more or less available pools (Chapin et al., 1978). Hence, detailed knowledge about all phosphorus pools in the soil is important for a correct interpretation of these results.

The results from the profiles that were investigated at the start and the end of the season can indicate, that ammonium tend to get consumed or oxidized during the season, while nitrate tends to increase, possibly due to oxidization from the ammonium. In contrast, the amount of mobilizable phosphate shows no such clear pattern. This can be explained by the fact that the pool of mobilizable phosphate depends on dynamics of the microbial communities. If these communities develop, they consume phosphate out of this pool. On the other hand, periodically crashes of these communities fill up this pool again (Chapin et al., 1978).

7.5.2 Rhizopod Analyses

The largest testacean population density and variety will possibly be present in the uppermost horizons of the profiles (Vincke et al., 2006).

It is possible to assume that the testacean community structure in the dry polygon rims will be mainly presented by the genera *Valkanovia* and *Corythion*. Species of these genera are common in coarse-humus litters and characterize rather xerophilous conditions (Trappeniers et al., 2002). Also dry moss habitats are characterized by *Assulina muscorum* assemblage (Beyens et al., 1992).

The transition from the polygon rims to the polygon centers was often covered by different species of *Sphagnum* mosses. Hence, the sphagnophilic species from the genera *Nebela* and *Euglypha* can possibly be found there (Beyens et al., 1986b). The populations in the wet polygon centers can contain hygro- and hydrophilic species from the genera *Diffugia* and *Centropyxis* (Beyens et al., 1986a; Vincke et al., 2004). The possibility to find the indicator calceophilic species *Cyclopyxis plagiostroma* is not very big because mainly of investigated soils are acidic (Bobrov et al., 2004).

Most likely, the dominant complex of rhizopods will comprise different eurybiotic species. Especially *Centropyxis aerophila*, which is dominant in the majority of high-latitude habitats and *Trinema lineare* may be found there. The former is characteristic for acid-oligotrophic waters while the latter prefers an intermediate type of water (Beyens et al., 1986b).

7.6. Conclusions

Our preliminary results suggest that there is a great variability concerning the nutrient availability within the polygonal tundra. The distribution of extractable nitrate and ammonium is apparently mostly driven by the hydrology regime in the soils. A

comprehensive understanding of the amounts of extractable phosphate can only derive by complete analyses of all phosphorus fractions in the soil. Despite the many samples that were analyzed we have no reliable overview on these data so far due to incorrect water content data. Hence, for complete examination of these data the water contents have to be reanalyzed in the laboratory. When the water contents will have been accurately determined, the field data of the contents of nutrients will be a very powerful basis for further investigations on nutrient availability in the investigated polygonal tundra.

8. PERMAFROST EXPOSURES

Lutz Schirrmeister & Vladimir Tumskoy

8.1 Scientific background and objectives

In addition to the monitoring, measurement and observation of modern conditions of the polygonal tundra, selected permafrost exposures were studied and sampled that preserve paleoenvironmental records of the Quaternary past. In this context, the composition and structure of frozen ground and of the source material for the recent thermokarst landscape will be characterized. In addition, the Kytalyk site will serve as a new point in the Beringia-wide net of paleoenvironmental records. Three composite profiles were studied on the slope of the western Yedomia ridge (11-KH-3007-1), in the ice cellar of the Kytalyk station (11-KH-2607-1) and on a pingo slope that was cut by the Konsor-Syane, River running through the large thermokarst depression (11-KH-2807-1).

8.2 Material and methods

The sampling design, field measurement and observation approaches are similar to previous expeditions already described in numerous field reports (e.g. Wetterich et al., 2011). The frozen sediments were dug with spades and cleaned by hacks. Sediment and ice structures were described, sketched and photographed. Frozen deposits of exemplary profiles were sampled for further multidisciplinary studies (sedimentology, hydrochemistry, paleoecology, geochronology, organic geochemistry) using hammers and small axes (appendix 7). The thawed sediment samples were stored in plastic bags. Already during expedition gravimetric ice contents were measured according to van Everdingen (1998). Therefore, frozen samples were taken in aluminium boxes, weighted, dried, and weighted again. In addition, ice wedges were described and sampled for hydrochemistry and stable isotope studies (appendix 8). Detritic plant and mineral remains were stored exemplarily for geochronological and palynological analysis. Thawed samples of ice wedges and segregation ice were measured for electrical conductivity (EC) and pH using the WTW pocket meter in the field lab. Similar to pond water samples the exemplary melt water samples were prepared for cation and anion analyses by filtering through a cellulose-acetate filtration set (pore size 0.45 μm). Melt water samples for cation analyses (15 ml) were acidified with 200 μl HNO_3 , whereas samples for anion analyses and residue samples were only cool stored. The samples for $\delta^{18}\text{O}$ and δD isotope analyses (30 ml) were preserved without any conservation.

8.3 The Yedoma exposure 11-KH-3007-1 (70° 50.478' N; 147° 26.305' E)

Several small thaw slumps on top of the western slope of the Yedoma ridge (Fig. 8-1) framing the studied thermokarst depression, expose the upper part of the ice-rich permafrost deposits. Such exposures are quite rare in the study region. One of the outcrops was selected for detailed studies to have an example of a Yedoma sequence here. The studied exposure was located about 20 m above the level of a thermokarst lake. The major part of the thaw slump was covered by debris. Only the upper about five meters were exposed.



Fig. 8-1: Thaw slumps on top of a yedoma ridge along a thermokarst lake.

According to previous approaches already used during pervious expeditions, subprofiles from the exposed wall of the thaw slump and from thermokarst mounds were studied to get a composed profile. Besides of frozen deposits, an ice-wedge transect was sampled at the exposed wall (Fig. 8-2)

The studied profile starts at the wall of the thaw slump at 19.5 m above lake level with a 0.3 m thick unfrozen active layer that consists of patchy, partly banded grey-brown to light grey clayish silt. In about 0.6 to 1.2 m depth below surface (b.s.) a small depression filled with cryoturbation structures was exposed. The silty deposits are dark-brown to reddish-brown as well as grey-brown coloured and ice-rich. The cryostructure was horizontally oriented lens-like to coarse lens-like. Large parts of the top wall are composed by a diagonal cut large ice wedge (visible wide ~5 m). This ice wedge was sampled in about 20 cm intervals by a 2 m long horizontal transect (11-KH-3007-2-7 to 2-20). The ice was milky-opaque and contained numerous small, non-oriented bubbles. The large ice wedge is penetrated by a thin younger ice wedge from below. This ice wedge was sampled by a short vertical transect (11-KH-3007-2-1 to 2-6).

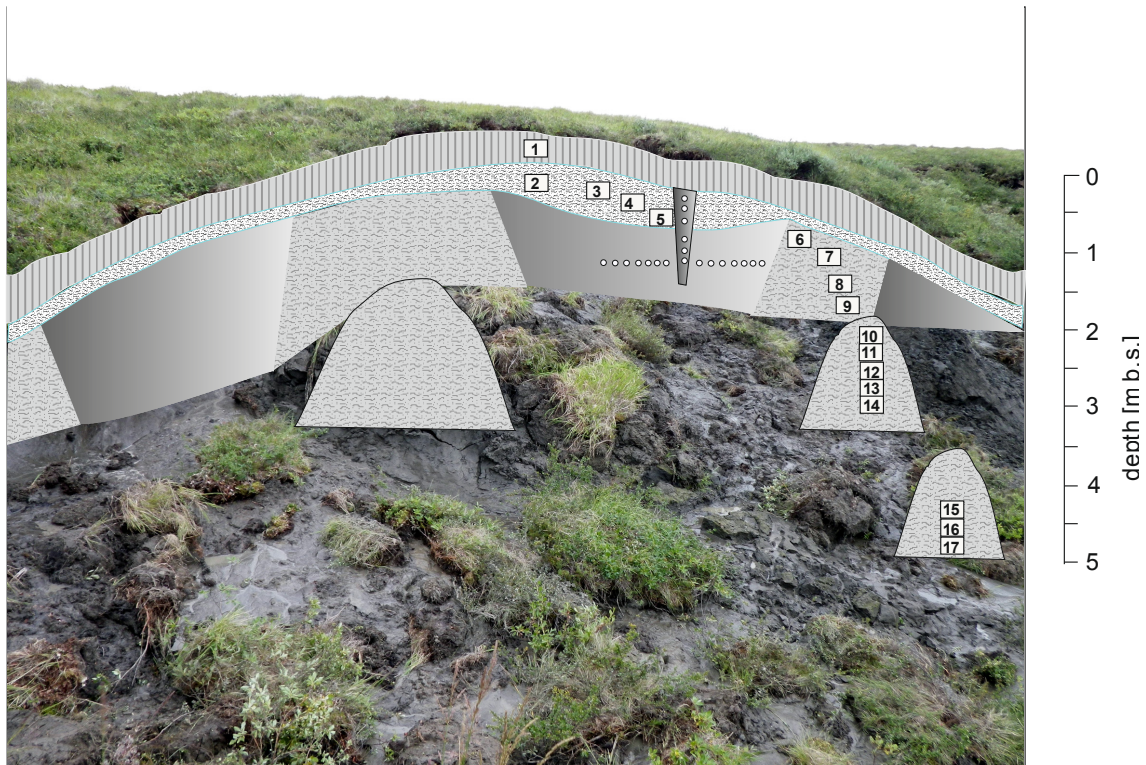


Fig. 8-2: Scheme of the Yedoma exposure 11-KH-3007 with sample sites for deposits and ice wedges.

The exposed sediment was sampled between two ice wedges down to 2 m b.s. The deposits consist of grey-brown, ice-rich deposits without visible organic fragments. The fine lens-like to coarse lens-like cryostructure (ice lenses 1 to 3 mm thick, 1 to 4 mm long) are horizontally oriented. Further down, two thermokarst mounds (baydzherakh) were studied and sampled (Fig. 8-2), consisting of light-brown to greyish deposits with fine-distributed plant detritus and numerous thin vertical roots. Black spots mark roots tracks. Micro-lenses (<1mm thick, 3 to 10 mm long) are parallel and horizontally oriented. The gravimetric ice content varied between 160 and 50 wt% (Fig. 8-3). Exemplary measured texture ice has pH values of 6.5 to 7.6 and EC values of 588 to 998 $\mu\text{S}/\text{cm}$.

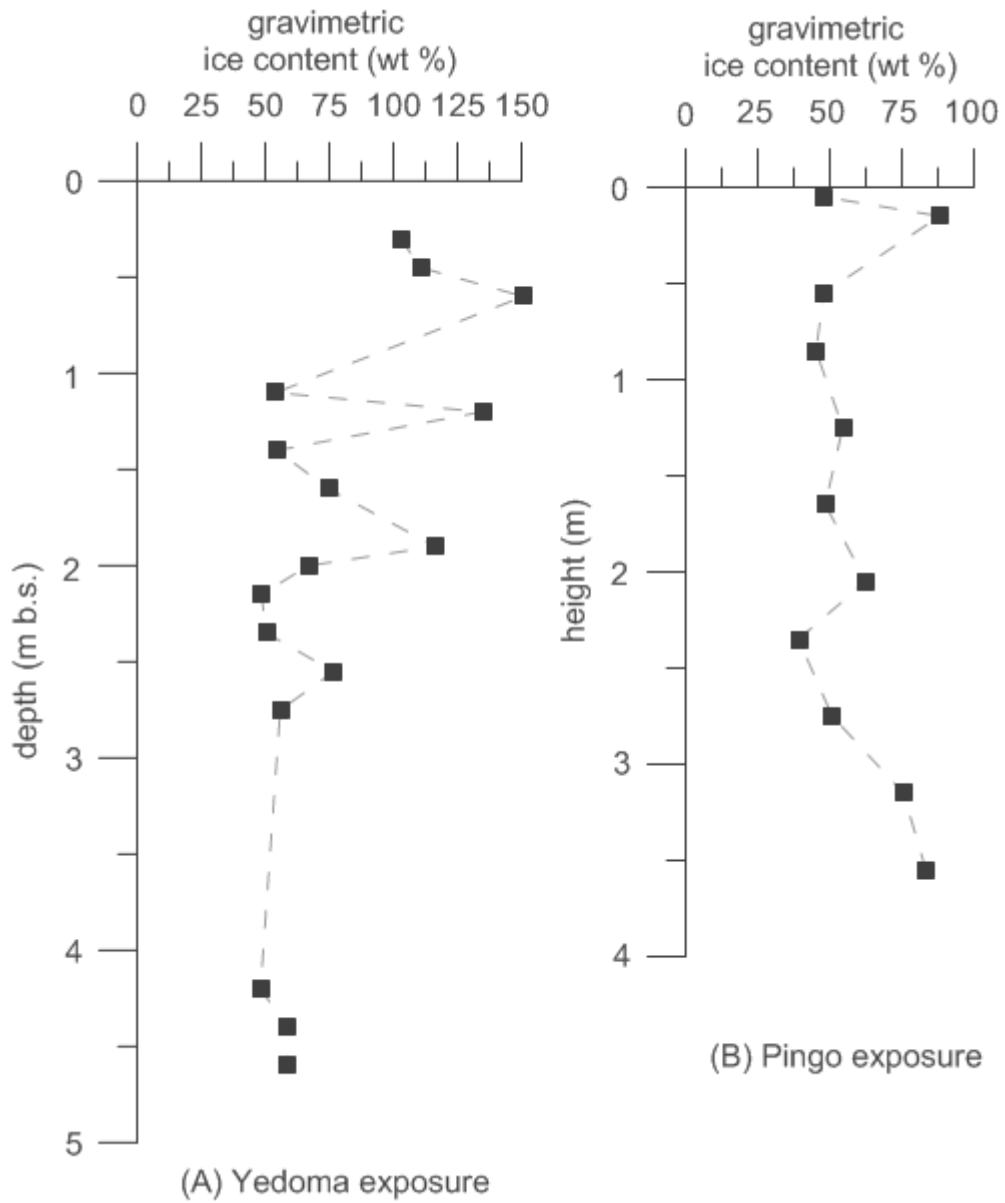


Fig. 8-3: Ice contents of the Yedoma exposure 11-KH-3007-1 (A) and the pingo exposure 11-KH-2807-1 (B).

8.3 The pingo exposure 11-KH-2807-1 (70.86152°N 147.49527°E)

The hill slope of a pingo cut by the small Konsor-Syane River (Fig. 8-4 right) exposed sediments that form the alas bottom. This study site is located in the central part of the alas depression on the second level (Fig.2-3). The pingo exposure allowed the study and sampling of deposits underlain thermokarst depressions that were heaven near the surface during the pingo formation. The hill is 10 to 12 m high and has an oval shape. At the exposure site the terrain surface at 5.6 m height is covered by moos, dwarf birches and grass. The dug profile was exposed between 2 to 4.6 m above the river level (a.r.l.).



Fig. 8-4: Exposure situation of the site 11-KH-2807-1. Left: Pingo hill cut by the Konsor-Syane River. Right: Sampled subprofiles.

The profile is composed of greyish-brown layered clayish to fine-silty lake deposits. Plant-detritus layers of 1-3 mm thickness formed non-regular ripple structures (Fig. 8-5 right). The cryostructure is dominantly lattice-like (Fig. 8-5 left). Single ice veins were 1 to 3 mm wide and 50 to 100 mm long. The distance between ice veins and the size of sediment block in between increased downward. The gravimetric ice content varied between 40 and 88 wt% (Fig. 8-3). In the lower part at 0.15 to 1 m a.r.l. the cryostructure was dominantly horizontal lens-like.

In the sample with the highest ice-content (11-KH-2807-1-12) a pH value of 5.7 and an EC value of 442 $\mu\text{S}/\text{cm}$ were measured. The permafrost table was observed at 3.65 m a.r.l.. The uppermost metre consists of unfrozen crumbly lake deposits. A small layer between 4.05 to 4.1 m a.r.l. was still frozen. The active layer contains numerous roots and was composed of greyish-brown loamy lake deposits that were influence by soil formation.

In total, 13 sediment samples were taken in 0.2 to 0.3 m distance (Fig. 8-6).



Fig. 8-5: Structures of the pingo exposure 11-KH-2807-1. Left: Lattice-like cryostructures. Right: Plant-detritus layers of the lake deposits.

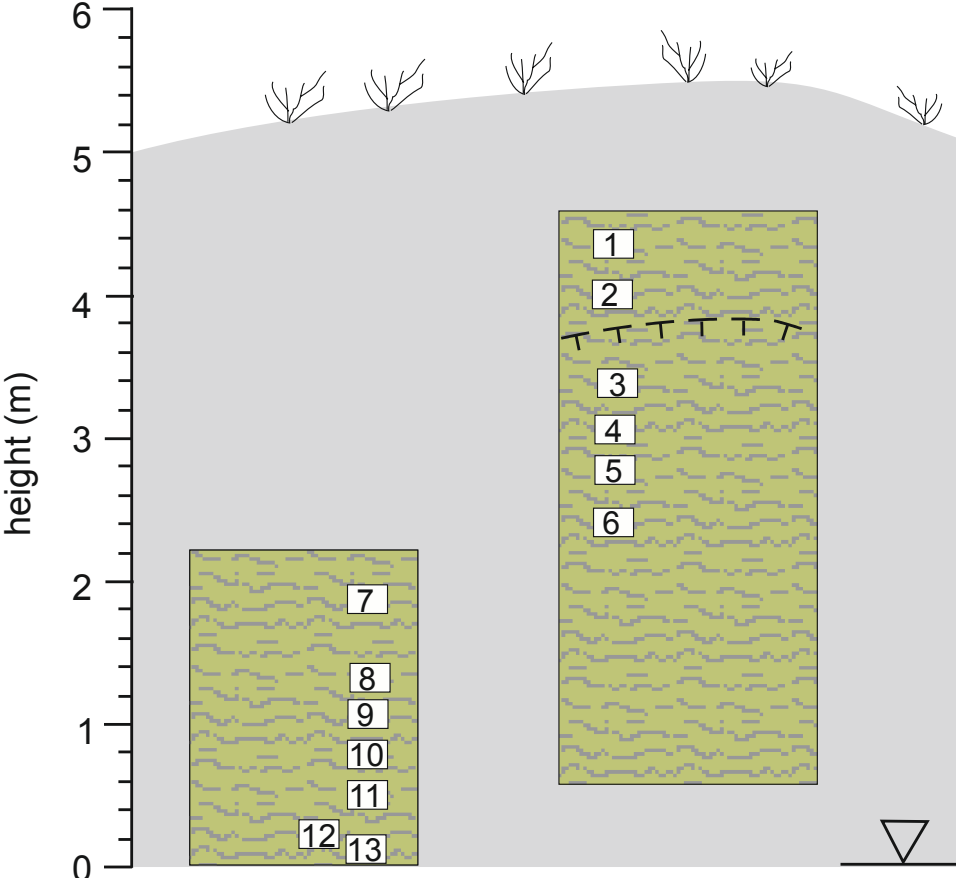


Fig. 8-6: Schematic profile of the exposure 11-KH-2807-1 with sample positions.

8.3 The ice cellar exposure 11-KH-2607-1 (70° 50.253' N; 147° 27.051' E)

The ice cellar is commonly used to store fresh fish and food for the station. We took the advantage of an additional subsurface exposure to study the frozen ground at the other end of the Yedoma ridge. The cellar is 4.5 m deep and has a bottom area of 4 x 3 m. A temperature of -6.2 °C was measured July 24th. The ice cellar was totally built within a large buried ice wedge system. Only in one place several cm above the bottom frozen sediment was exposed and could be sampled (11-KH-2607-1-1). The texture ice of this sample show a pH of 6.1 and an EC of 995 $\mu\text{S}/\text{cm}$.

The studied ice wedge was about 3 m wide and contains several mm-thick vertical sediment stripes, which were very-well visible due to ice sublimation (Fig. 8-7). A transect of 2.8 m length (Fig. 8-8) was sampled by chain saw in 10 cm intervals. In total 26 ice wedge samples were taken from this profile (11-KH-2607-1-2 to 1-26). At the opposite wall clear ice was visible that could originate from previous flooding of the cellar. Three samples in different height (11-KH-2607-1-27 to 1-29) were collected from this side. The wall of the entrance shaft (Fig. 8-7) was covered by ice crystals that were also sampled for isotope analyses (11-KH-2607-1-30).



Fig. 8-7: The entrance of the ice cellar (left) and the structure of the ice wedge (right) with vertical sediment laminae.

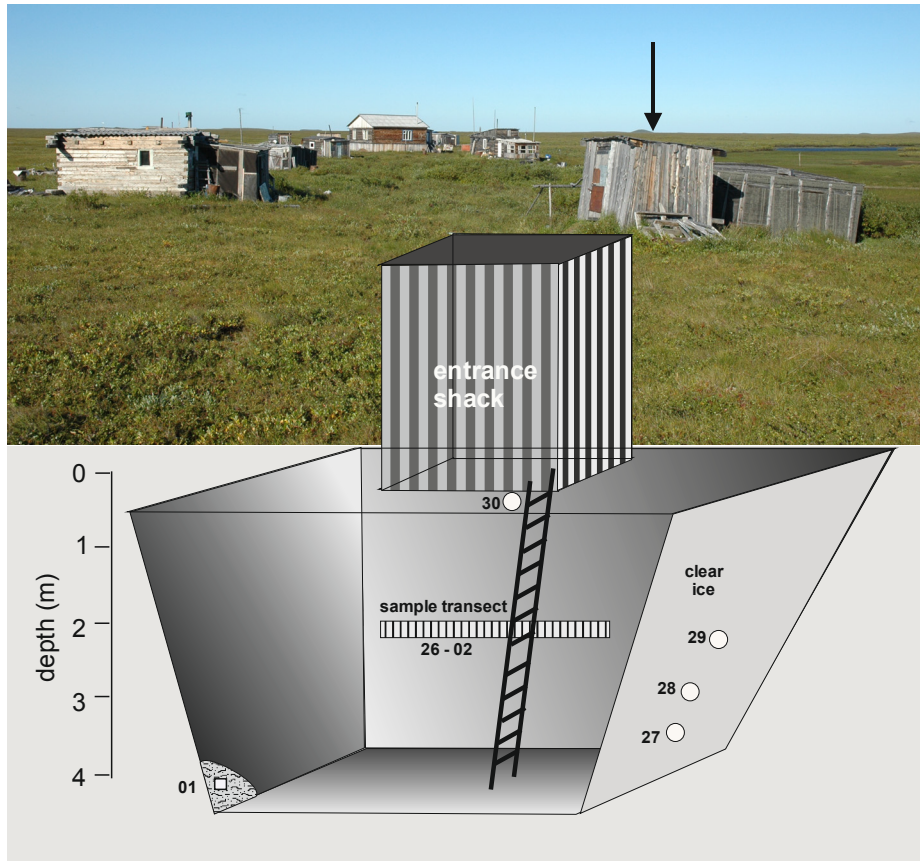


Fig. 8-8: Scheme of the ice cellar facility 11-KH-2607-1 in a buried ice wedge system with sample sites.

The pH values of the ice sample vary between 6.3 and 7.4 while the EC of the ice wedge transect is between 27 and 73 $\mu\text{S}/\text{cm}$ and of clear ice and ice crystals only 7 to 16 $\mu\text{S}/\text{cm}$ (Fig. 8-9).

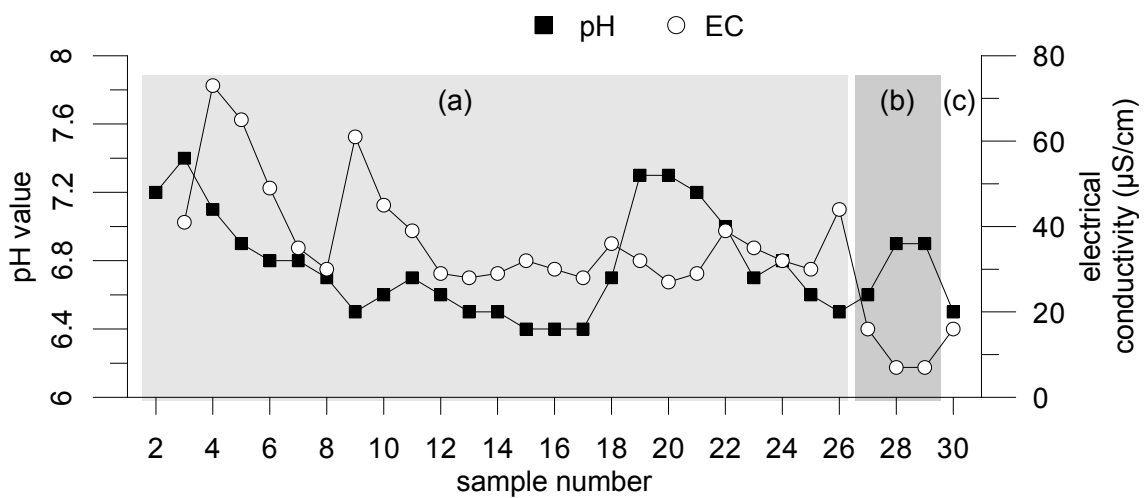


Fig. 8-9: Hydrochemical field data of the ice wedge transect (a), the clear ice (b), and the ice crystals (c).

9. DRILL HOLES AND PITS AROUND KYTALYK

Vladimir Tumskoy & Evgeniya Zhukova

9.1 Introduction

Studies of the geological and cryolithological composition of the upper horizon of alas and Yedoma deposits are used to understand the relationship between peculiarities of the polygonal micro-relief dynamics and the formation of ice wedges. According to Romanovsky (1977), the formation of a polygonal micro-relief is connected with cryogenic processes of frost cracking and the development of ice wedges (or wedge-like structures). Depending on stages of ice wedge formation (e.g. growth, stabilization, degradation), the polygonal micro-relief is shaped as low-centered polygons (polygonal walls with intra-polygonal ponds), flat-centered polygons, and high-centered polygons with convex centers and trenches above the ice wedges. Different formation stages could occur in different parts of the same landscape with polygonal micro-relief that determines a specific mosaic structure.

The uppermost horizon of frozen ground where polygonal micro-relief is formed was studied in different landscapes (e.g. flood plain terraces, alas bottom levels) and in different stages. It was assumed that the study depth would amount 3 to 5 m. It was planned to study frozen layers with ice wedges in natural exposures as well as by digging and drilling.

However, the real conditions at the key site Kytalyk were more complicated as expected. The long-term high-water until mid of august and the slow decline of the water level did not allow to study the structure of the upper horizon of frozen ground in the flood plain area. In addition, the widely distributed shallow lakes (russ. *layda*) on the flood plain of the lower reaches of the Berelekh River complicated the differentiation between the flood plain level, the level of flooded layda-lakes and of lower alasses. Therefore, the major attention was focused in the Kytalyk study area on the polygonal micro-relief of the upper and the lower alas level as well as of the western Yedoma ridge (Fig. 2-3). Similar studies were carried out during field trips in the middle reaches of the Berelekh River at the sites Dzhardakh and Nyuchcha-Kyuele (chapter 11). Natural exposures of alas deposits were not found in the Kytalyk study area. The river bank nearby is formed by fragments of the shallow layda-lakes, covered by shrubs and still flooded after the water-level decline.



Fig. 9-1: Drilling of the borehole 11KH-1907-1 in the upper alas level.

In order to study the upper horizon of frozen ground a hand drill (Fig. 9-1) was used to drill several holes and a chain saw to prepare pits.

Complete polygonal nets occurred only in separate parts of the upper alas level and in the lower level only along the boundary line between both levels. Because the surface of the lower level was totally boggy, the polygon structure was only visible by changes in the vegetation cover and height above the water level. Although the upper alas level was dryer, the water of the active layer filled each hole and pit during several minutes. Therefore, drilling of boreholes and the digging of pits were not very effective.

The drilling equipment Caiman (KAAZ) AG500-TB50 was used together with the engine Mitsubishi 1.8 h.p. Despite the lightweight engine, the drill head could not penetrate very well into the frozen ground and it was complicate to get a sediment core. Therefore, no holes were drilled deeper than one meter. However, the usage of a chain saw to get pits in frozen ground seemed to be more successful. The chain saw cut very-well silty and peaty frozen deposits, but the saw blunt quickly if such deposits contained sand. For future studies the motor drill equipment should be modified by a core catcher. It would be also very helpful to drill already in spring before active layer thawing. By using the chain saw, more additional bars are necessary.

During fieldwork five boreholes and six pits were made and an alluvial exposure was described at a sand bank of the Berelekh River.

9.2 Field data

9.2.1 Site 11KH-1907-1 (N 70.83127°; E 147.48263°)

This site located in the upper alas level is characterized by a wide flat wall between two low-centered polygons. The polygon southeast of the wall contains a small pond, while the northwestern polygon is boggy and almost total covered by vegetation (Fig. 9-2). The active layer depth ranged between 15 and 30 cm depending on the micro relief and the plant cover. The about 50 cm high polygon wall is covered by moss, lichens and dwarf birches of 10 to 15 cm height. *Sphagnum* mosses occur around the pond, while sparse sedge vegetation prevails in the water. Trenches over frost cracks of 10 to 15 cm wide and depth on the wall are covered by grass and shrubs. This site corresponds to the monitoring site KYT-1 (chapter 3).



Fig. 9-2: Landscape view near borehole 11KH-1907-1 and pit 11KH-1907-2. This location is marked by the left shovel. This site corresponds to the monitoring site Kyt-1.



Fig. 9-3: Structure of the upper horizon of alas deposits in the pit 11KH-1907-2 with two ice wedges (see also Fig. 9-4).

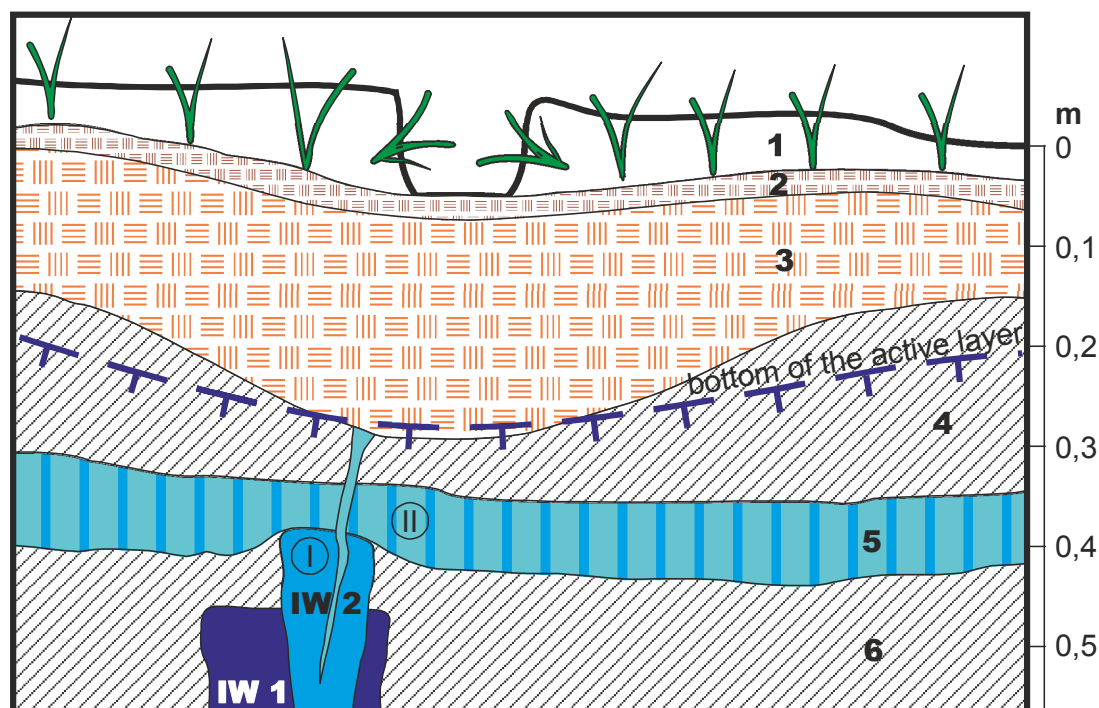


Fig. 9-4: Schematic structure of the upper horizon of alas deposits in the pit 11KH-1907-2. Bold numbers are numbers of layers, which are described in text. Latin number I and II in circles indicate ice samples (I – Kyt-1-IC-1, II – Kyt-1-IC-2). IW1 and IW2 are different ice wedges.

At first, the holes 11KH-1907-1 was drilled up to 65 cm depth, which was later extended for detailed studies of cryogenic structures to an about 1 m wide pit that showed the following stratigraphy (Figs. 9-3, 9-4):

- Layer 1: 3 to 10 cm thick; modern active layer moss, lichens, shrubs.
- Layers 2, 3: 10 to 20 cm thick; peat. In the upper part (layer 2, 3 to 5 cm thick) dark-brown peat less decomposed than layer 3, which is lighter colored and more decomposed.
- Layer 4: 5 to 20 cm, loam, weakly peaty, grey-brown, lens-like cryostructure, ice lenses about 1 mm thick, sediment blocks between ice lenses 2 x 3 cm.
- Layer 5: 2.5 to 6 cm thick, transparent pure ice layer with numerous vertical needle-like air bubbles penetrating the entire ice layer. The ice layer thinned out to 2.5 cm above the ice wedge IW 2.
- Layer 6: visible thick about 10 cm, loam similar to layer 4, lens-like reticulated cryostructure with 2 to 3 mm thick ice lenses and sediment blocks of 0.5 x 1.5 cm size.

Below the trench, two generations of small ice wedges are exposed that are connected with frost crack formation (Figs. 9-3, 9-4). Their central axis is shifted about 5 cm from the center of the trench. The older and lower ice wedge IW 1 is 10 to 15 cm wide on top and composed of vertical dark and clear ice stripes. The curved younger epigenetic ice wedge IW 2 is 2 cm wide and composed of white ice bands. In addition, a modern 2 to 3 mm wide ice vein was visible, which starts at the base of the active layer and penetrates through the frozen sediment layer 4 and as the ice layer 5 into the ice wedge IW 2. Samples for stable isotope analyses were taken from the ice wedge IW 2 (Kyt-1-IC-1) and from the ice layer 5 (Kyt-1-IC-II).

9.2.2 Site 11KH-2107-1 (N 70.82920°; E 147.48498°)

This site is also located on the upper alas level (Fig. 2-3). The surface is similar characterized as described in chapter 9.2.1. A distinct polygonal net system was not visible. The pit exposes the upper part of a profile below a frost crack that runs along the top of the polygon wall (Fig. 9-5). The active layer is 25 to 27 cm deep and the modern vegetation cover of moss, lichens, and shrubs is about 8 cm high.

- Layer 1: ~ 10 cm thick, brown peat, weakly decomposed.
- Layer 2: 6 to 7 cm thick, grey loam with numerous filamentous roots in chaotic orientation. The upper part was already thawed while the lower part was still frozen. Layer 2 is interrupted directly above the ice wedge and thermokarst-cave ice within the peat. The cryostructure of the frozen part is characterized by several vertical and diagonal 1 to 2 mm thick ice lenses in 10 cm distance. The cryostructure between the ice lenses is massive. The gravimetric ice content amounts to 27 wt%.
- Layer 3: 1.5 to 2 cm, lens of clear segregation ice with some silt inclusions.
- Layer 4: 5 cm thick, brownish-grey partly ochre loam, horizontal net-like cryostructure. The horizontal 1 to 3 mm thick ice lenses are weakly bent downward penetrated by subvertical 2 mm thick ice lenses in 4 to 5 cm distance.
- Layer 5: Visible thickness 7 to 8 cm; icy ground with numerous inclusions of loam of about one millimeter size. Its number increase downward; some peat inclusions occur near the ice wedge; clear ice without bubbles; near the ice wedge and the lens of thermokarst-cave ice this layer is lifted about 4 cm.

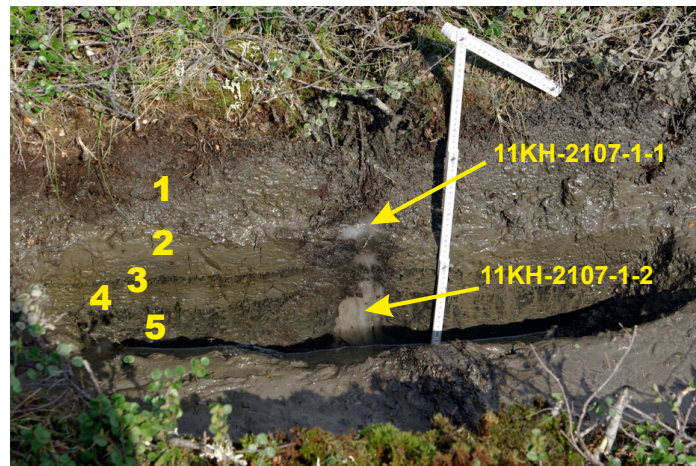


Fig. 9-5: Structure of the upper horizon of alas deposits in the pit 11KH-2107-1 with sample sites. Bold numbers are numbers of layers, which described in text. Arrows showed samples locations.

The upper part of a 7 to 8 cm wide ice wedge was visible in the center of the pit (Fig. 9-5). This ice was light-grey and white vertical striped but separate ice veins were not visible. The head of the ice wedge was located about 30 cm below the grass cover and 15 cm below the trench of the frost crack. Three lenses of thermokarst-cave ice (size: 1.5 x 3 cm, 3 x 5-6 cm, 4.5 x 7-8 cm) were observed directly above the head of the ice wedge, which are separated each other as well as from the ice wedge by several mm-thick horizontal peat lenses. The two upper lenses consist of pure clear ice with needle-like bubbles in about 40 % of the entire lens thickness. In its uppermost part, a large number of bubbles results in a white color of the lens. All

bubbles were radial oriented to the center of the lens. The lower lens consists only of white ice. Modern elementary ice veins were not visible but a 2 mm wide ice vein went from the middle lens to the ice wedge. Ice samples were taken from the upper ice lens (11KH-2107-1-1) and from head of the ice wedge (11KH-2107-1-2).

9.2.3 Site 11KH-2107-2, (N 70.82887°; E 147.48557°)

This site is also located on the upper alas level (Fig. 2-3). The surface is similar characterized as described in chapter 9.2.1. This pit 11KH-2107-2 is located on a wall with the larger trench above the frost crack compared to the site 11KH-2107-1. The thickness of the active layer amounts 20 to 30 cm. The exposed ice wedge consisted of three different segments (Fig. 9-6).

The lower ice wedge (LIW) is exposed at bottom of the pit and consists of whitish striped ice. The visible wide is about 15 cm. The upper rim of this ice wedge is regular, partly thawed and covered by the loam of layer 3 (see below). In the head of lower ice wedge penetrated the middle ice wedge (MIW), which is 12 cm long and 6 to 9 cm wide. The ice is whitish and well-striped. An open 1 cm wide and 10 to 11 cm long vertical crack occurred in the center, which did not continued upward. Water flow horizontally trough the crack. The upper ice wedge (UIW) of 5 cm length penetrated the head of the middle ice wedge 2 cm right of the crack. It consisted of dark transparent ice without bubbles and contained some sediment inclusions.

Description of the deposits exposed in the pit 11KH-2107-2:

Layer 1: 10 cm thick, modern moss-lichen cover with shrubs.

Layer 2: 10 cm thick, brown peat, less decomposed.

Layer 3: Visible thickness 35 cm, grey loam, weakly colored by iron-oxide. The uppermost part (about 3 to 5 cm) was thawed.

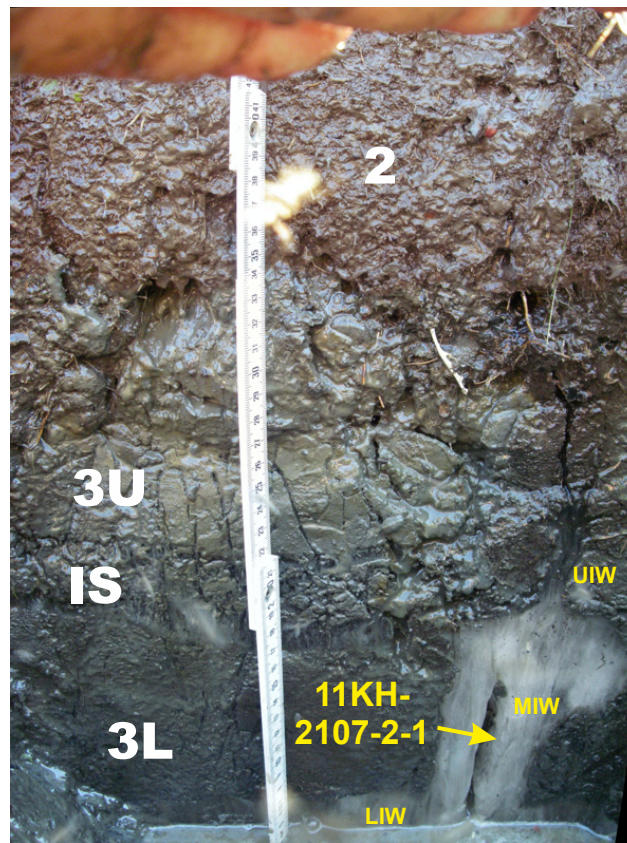


Fig. 9-6: Structure of the upper horizon of alas deposits in the pit 11Kh-2107-2. Bold numbers and other symbols are explained in text.

According to the cryostructure, two different sub-layers were classified in the frozen part (Fig. 9-6) – the upper layer (3U) and the lower layer (3L). The sub-layer 3U contains vertical and diagonal 1-1.5 mm thick ice lenses in 1.5-3 cm distances. Both sub-layers were separated by a 2 cm thick ice band (IS) that is merged into the upper rim of the middle ice wedge. Above this ice band occurred 3 cm of loamy deposits with net-like cryostructure mostly situated above the ice wedge. The ice lenses were 2 to 4 mm thick and the size of horizontal oriented sediment blocks ranged from 5x6 mm to 5x20 mm. Direct right of the middle ice wedge and left of the upper ice wedge a peat of dark-brown color appeared along the lateral contact to the ice wedges. From the left edge of the upper ice wedge a 2 mm wide open crack stretched in peat 4 cm upwards to the thawed covering peat. Between the roof of the lower ice wedge (LIW) and the ice band (IS) existed the lower sub-layer 3L. This horizon consisted of more peaty brownish loam with a net-like cryostructure. The net-structure is composed of 1 to 1.5 mm wide ice lenses and sediment blocks of 5x10 mm size. Clear visible vertical 2 mm wide ice veins in a distance of 4 to 5 cm penetrated the layer 3 from top to bottom. Samples for stable isotope analysis were taken from the middle ice wedge (11KH-2107-2-1).

9.2.4 Site 11KH-2407-1 (N 70.82595°; E 14748454 °C)

This site was located on slope of the western yedoma ridge framing the Kytalyk alas depression. The site surface is weakly inclined ($\sim 5^\circ$) to the northwest. The real yedoma top area is 1-2 m higher. The surface is characterized by a hummocky microrelief with slightly inclined flat hillocks of about 1 m in diameter and 10 to 15 cm height above trenches that are usually masked by vegetation. The 1.5 m long and 0.5 m wide pit is situated in SW-NE direction and exposed a crack between two hummocks. The plant cover is composed of moss, lichens and alder shrubs and Labrador tea (*Ledum palustre*). Shrubs were less than 8 to 15 cm and sometimes up to 30 cm high.

Description of the pit 11KH-2407-1 (Fig. 9-7):

Layer 1: 10 to 15 cm thick, modern plant cover.

Layer 2: 35 to 40 cm thick, sandy loam with numerous root of grass vegetation; brownish-grey colored with ochre patterns. At the base of the active layer in the central part of the trench, lenses of clear ice and ice with fibers and fragments of peat are visible that are spatial related to depressions between the hummocks at the yedoma surface (Fig. 9-7). The 15 to 20 cm long lenses form a heave of the active layer base and the surrounding peaty loam.

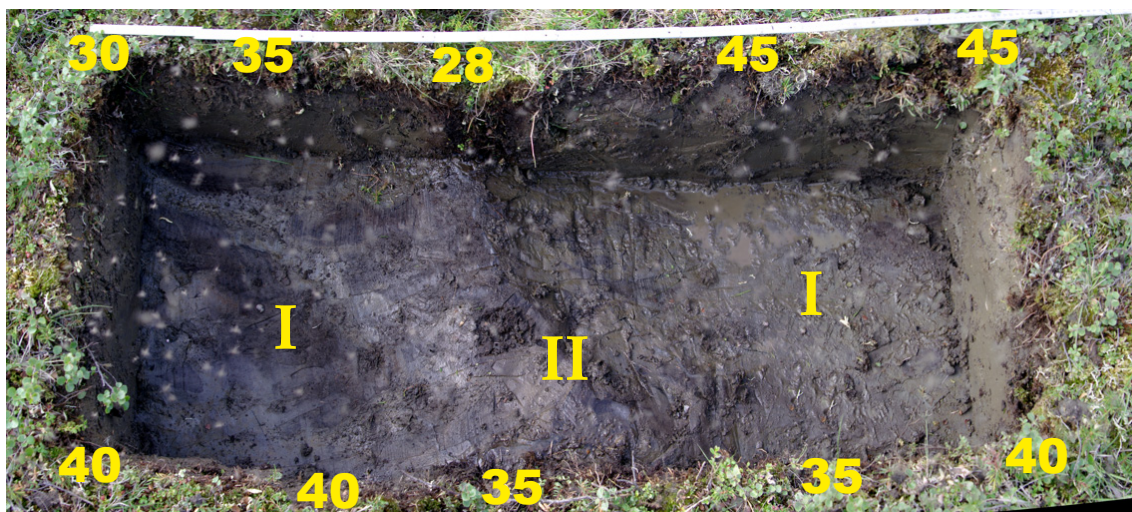


Fig. 9-7: Overview of pit 11KH-2407-1. Arabic figures show the active layer depth (in centimeters). I – depressions of active layer bottom under small hills on the surface, II – heave of active layer bottom under small ditches on the surface.

Between 30 and 50 cm depth frozen loam occurred with irregular net-like cryostructure composed of 2 to 4 mm thick ice lenses and 1x2 to 2x4 cm large sediment blocks (number 1 in Fig. 9-8). The number of lenses decreased higher in the profile, while in the uppermost part of the layer only vertical lenses existed.

An ice-rich layer of about 5 cm thickness is located at about 50 cm depth (number 2 in Fig. 9-8) with ataxitic cryostructure and a sharp upper but a gradual lower contact. About 2 cm deeper the ataxitic cryostructure transferred in net-like cryostructure with 2 to 6 mm thick ice lenses and sediment blocks of 1x1 to 1x2 cm size.

The laminar horizontal lens-like cryostructure in 55 cm depth (number 3 in Fig. 9-8) is composed of lenses 1 mm thick and sediment blocks of about 1x5 mm size. In the

visible part of the pit the ice lenses in the 6 mm thick transition zone contain vertical bubbles.



Fig. 9-8: Cryogenic structure of frozen loam in pit 11KH-2407-1.

9.2.5 Site 11KH-2707-1 (N 70.83162°; E147.47849°)

This site is located in the upper alas level about 100 to 150 m north of the model polygon LHC-11 (chapter 6) and represents a well expressed half polygon wall of 2 to 3 m width and 40 to 50 cm height above the pond level. Between both wall halves above an ice wedge a partly grass-covered trench stretches that was 0.2-0.3 m to 2-2.5 m wide. The size of the polygonal system ranges from 10x15 to 15x20 m. On several walls hillocks of up to 1 m height exist. The vegetation cover on the wall consists of Labrador tea (*Ledum palustre*), cloudberry, moss, lichens, and of rare sedge near the water level. *Sphagnum* and sedge occurred in the water.

The concerning 40 cm wide pit 11KH-2707-1 located on a 2 m broad wall was continued by a drill down to 1.1 m depth. The thickness of the active layer varied between 22-25 cm (wall, rare *Ledum palustre*) and 30-32 cm (wall, rich *Ledum palustre*, wall seldom rosemary). Down to 92 cm depth the profile consisted of brownish, frozen peat with massive cryostructure. From 92 to 105 cm depth ice inclusions of 1 to 1.5 cm size with thin vertical air bubbles occurred within the peat. A horizontal striated ice layer of about 5 cm thickness was visible in 105 to 110 cm depth (Fig. 9-9).

Samples for radiocarbon AMS dating were taken from the core in 92-96 cm depth (11KH-2707-1-1), in 96-101 cm depth (11KH-2707-1-2), and in 101-105 cm depth (11KH-2707-1-3)

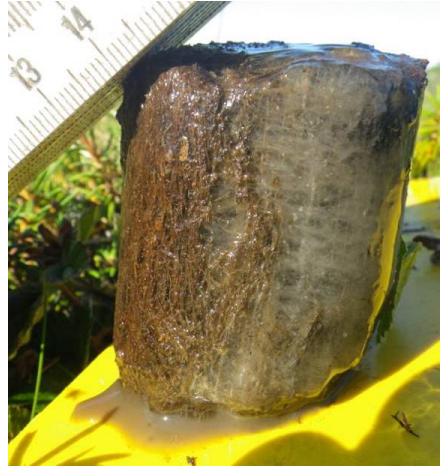


Fig. 9-9: Drill core of site 11KH-2707-1 with ice inclusion in peat (depth 105-110 cm).

9.2.6 Site 11KH-2907-9BUGOR (N 70.84235°; E147.48587°)

The pit is located in the lower alas level, where the polygonal microrelief is well-developed but highly flooded (Fig. 9-10). Many walls are located below water level but grass grows at the surface. The polygonal ponds are up to 1 m deep, in average 0.5 to 0.7 m.



Fig. 9-10: Polygonal landscape on the lower alas level.

The studies of wall structures were carried out at a fragment of a wall system framing polygonal ponds (Fig. 9-11). The wall is about 0.5 to 0.6 m high above the water level.

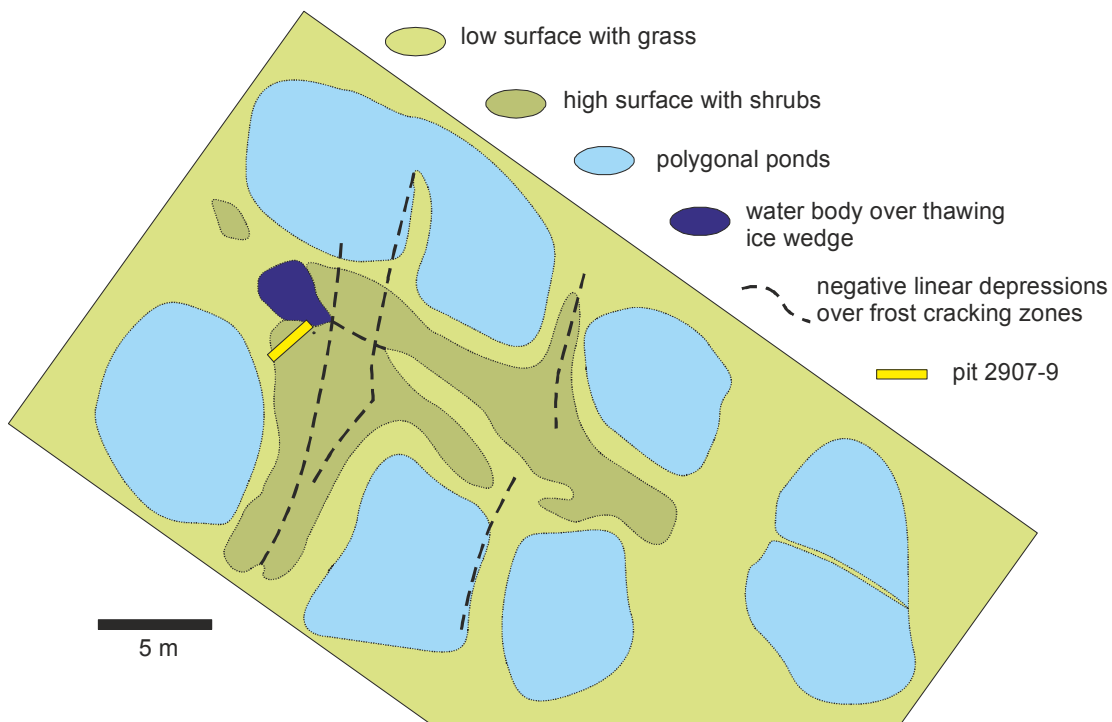


Fig. 9-11: Polygonal net around the pit 11KH-2907-9.

On top of the wall a water-filled trench occurred. The pit was dug in the higher side of the wall (Fig. 9-12). After removing the thawed layer the pit was deepened with a chain saw down to 0.7 m depth. The pit was 2.4 m long. The thickness of the active layer is shown in figure 9-13.

The description of the thawed layer was done in the interval of 210 to 220 cm at the SE-side of the pit:

- 0 to 6 cm: Modern vegetation cover with grass and dwarf birches with roots of 5 to 8 mm in diameter and the highest root concentration in the profile.
- 6 to 17 cm: Dark-brown to black middle to strong decomposed peat with grey-brown patches. Black layers occurred in the intervals of 160 to 170 cm and of 200 to 240 cm. Many grass roots were visible.
- 17 to 30 cm: Greyish-ochre sandy loam with a large number of brownish and reddish peaty patches
- 30 to 58 cm: Dark-brown weakly mineralized peat. The top of the peat is irregular with small (2 cm diameter) loam inclusions. Grass roots occurred.



Fig. 9-12: Overview of pit 2907-9.

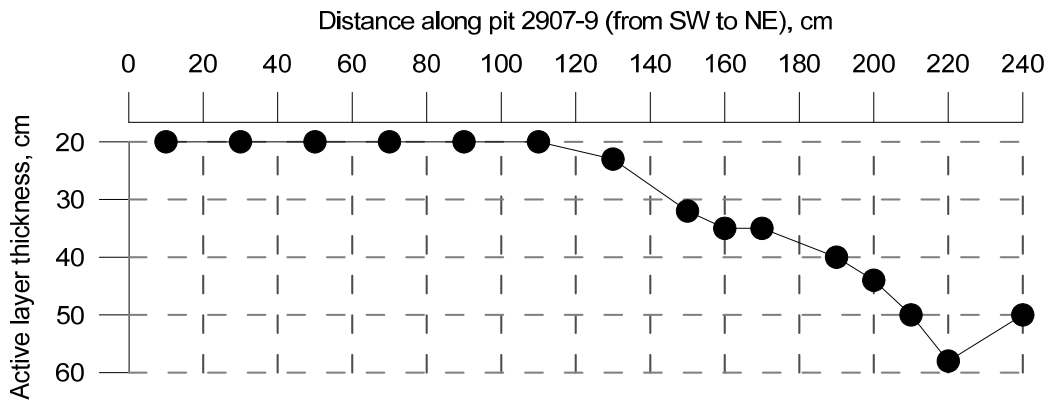


Fig. 9-13: Distribution of the active layer thickness along the pit 11K-2907-9.

The frozen part was opened by chain saw of 30 to 170 cm length and 45 cm further down from the base of the active layer. The description was done upwards in the lateral interval of 30 to 70 cm at the SW-wall. Several lenses of different cryostructure were visible in the entire frozen part. Homogenous grey loam composed the lowermost part of the profile (I in Fig. 9-14) containing a 6 cm thick clear ice lens with small circular bubbles. This ice was striped visible reflected by the variable dense distribution of bubbles. Four ice bands of 1 cm thick penetrated the ice lens II at the right rim of pit. The second, the third and the fourth lenses (II, III, and IV in Fig. 9-14) represent alternating grey and brown peaty loam and peaty layers. These lenses were specifically formed and cut each other. Lens II contained a folded deformed peaty loam layer that base cut the structure of lens I. Lens III is characterized by

parallel ice bands of 0.5 to 1.5 cm thickness, which were separated by a 1 cm thick extended parallel to the base. Lens V consist of ice poor loam and showed a wavy contact to the covering peat. As a whole the cryogenic structure of deposits is defined by position and dynamics of a polygonal pond at the left.



Fig. 9-14: Structure of the frozen part of pit 11KH-2907-9 (Latin numbers are explained in the text).

Samples were not taken at this site but a logger was installed in this place for 44 hours between 30.07. 17:30 to 01.08. 12:00 to measure the temperature at surface of the vegetation cover, in the pond water, at the pond bottom and in the active layer (Figs. 9-15 and 9-16).

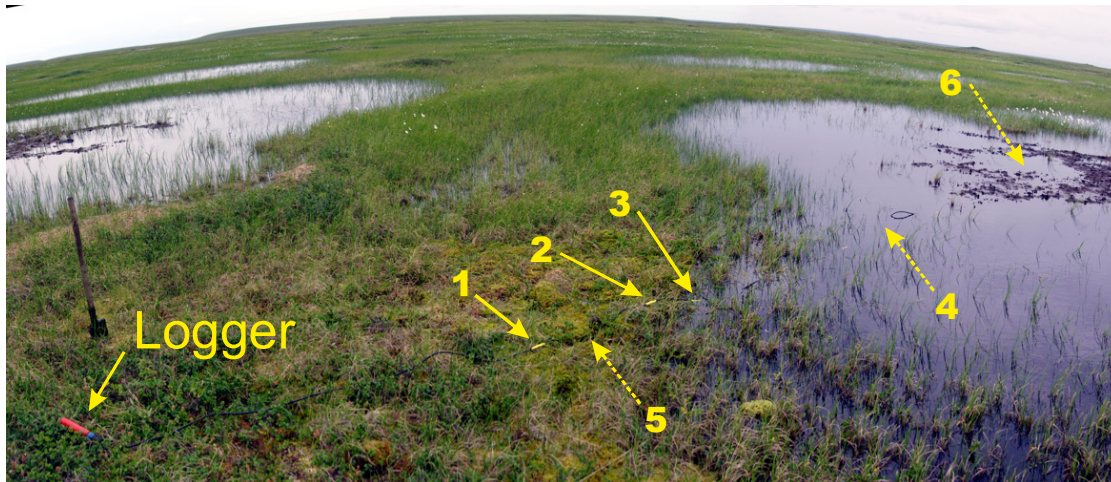


Fig. 9-15: Sites of temperature logger sensors (see also Fig. 9-16).

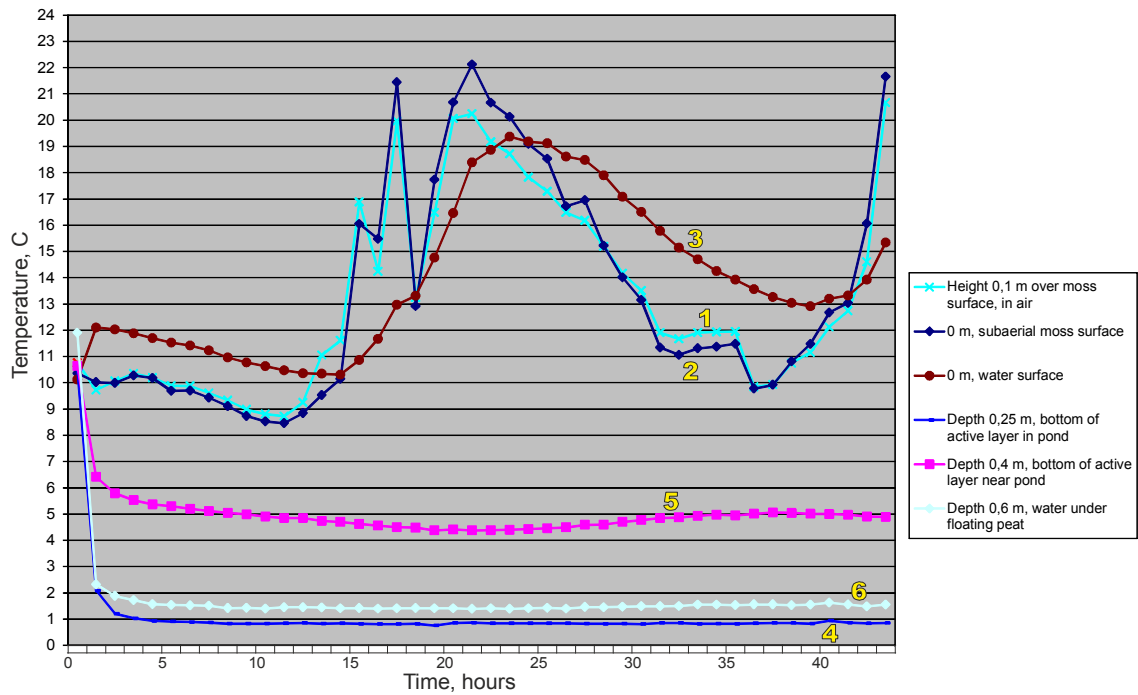


Fig. 9-16: Results of temperature monitoring of ground and water near the pit 11KH-2907-9. Yellow numbers indicate the sensors shown in Fig. 9-15.

9.2.7 Site 11KH-2008-1 (N 70.82047°; E 147.47827°)

In order to study the composition of floodplain deposits, a profile 1 m depth was dug in a step of fresh alluvial deposit (Figs. 9-17 and 9-18) at the first meander upstream the Berelekh River near the station Kytalyk (see Fig. 2-3).



Fig. 9-17: Overview of small outcrop 11KH-2008-1 of modern alluvial deposits.

Description of the studied alluvial sequence from above:

- Horizon 1, depth 0-1 cm: Brown-grey middle-grained sand with silt covering partly the modern alluvial surface (sample 11KH-2008-1-1).
 - Horizon 2, depth 1-35 cm: Grey silt with lenses of plant detritus (2 to 5 mm thick, 5 cm to several decimeters long). Inclined fine-bedding, wavy, each lamina is about 1 mm thick. Between 6 and 22 cm depth, the silt was weakly ochre colored, which was deeper only observed near the lenses of plant detritus and along subvertical fissures that continue 20 to 50 cm further down. The colored zone was 5 to 6 mm wide and the fissures were 1 cm wide in the upper segment and thinning downward (sample 11KH-2008-1-2).
 - Horizon 3, depth 35 to 100 cm: Alternation of silt with lenses of brown-grey fine-sand, horizontal or weakly cross-bedded. The number of plant detritus layers increased downward (sample 11KH-2008-1-3).
- The lowermost part between 75 and 96 cm depth was very wet.

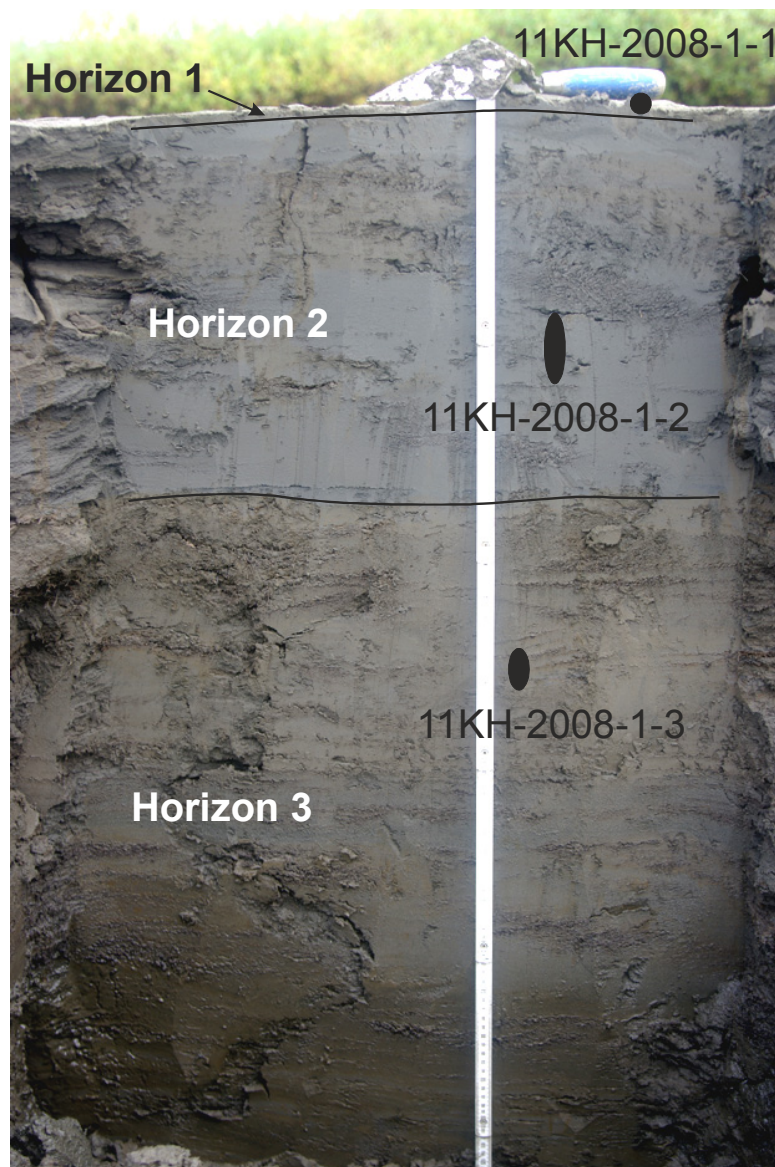


Fig. 9-18: Small outcrop 11KH-2008-1 of modern alluvial deposits.

10. MOSS COLLECTION

Andrea Schneider

One focus during field work in Kytalyk was the collection of local moss species (Figs. 10-1 and 10-2). The mosses were taken from diverse sites around Kytalyk in a tundra environment with different geomorphological and hydrological conditions such as:

- a NE-exposed Yedoma-ridge,
- two different levels of an alas depression,
- wall and central depressions of low-centred polygons,
- submerged growing mosses from polygon ponds,
- the monitoring site KYT-1ite (see chapter 3).

The mosses have been sampled randomly from various sites (appendix 4) and have been included in a vegetation transect across our monitoring site. Qualitative vegetation records and active layer measurements have been performed for each site. We excluded floodplain areas to avoid isotopic influences from both water and sediment transported by the Berelekh River during spring floods. All moss samples are air-dried and packed in paper bags.

The aim of the investigations is to receive an overview about moss species and their spatial habitat dimensions especially in polygonal landscapes. We will establish a collection of mosses and moss assemblages to compare different locations and habitat conditions (e.g. Khatanga and Kytalyk). The modern datasets will support to reconstruct palaeo-environmental conditions, especially changes in hydrological settings of fossil polygonal structures and their micro-relief.

A particular focus is concentrated on the group of *Amblystegiaceae*, which is the dominant moss community in arctic and subarctic ecosystems. In some cases, they can be distinguished by biomolecular characteristics only. Another point of interest focuses submerged growing moss species. They can perform photosynthesis under pond ice in spring and autumn. Therefore, they are an important group to represent seasonal environmental conditions for a longer time span than other species. Isotopic analyses ($\delta^{15}\text{N}/\delta^{13}\text{C}$) of the moss samples will be performed to compare the isotopic composition of species growing under different habitat conditions.



Fig. 10-1 A: Example of a moss community, with *Aulacomnium turgidum*



Fig. 10-1 B: *Sphagnum*-community with *Sphagnum squarrosum* (light green plant in the center with toothed leaflets and sporophytes)



Fig. 10-2: Different moisture conditions in a flat, elongated depression near KYT-27 (Yedoma top region), reflected by different moss species: *Sphagnum* cf. *squarrosum* is growing in the wettest places in the center and is replaced by other mosses and vascular plants along the drier margin.

11. CRYOLITHOLOGICAL STUDIES IN THE MIDDLE BERELEKH AREA

Vladimir Tumskoy & Evgenya Zhukova

11.1 Introduction

During the period from August 2nd to 16th field research was conducted upwards the Berelekh River. The main goal was the study of Quaternary deposits on the Dzhelon-Sise Highland. In Landsat7 ETM+ satellite images on the surface of Dzhelon-Sise roundish negative forms are well visible on the central part of a watershed (Fig. 11-1). They are assumed to be small thermokarst depressions (alases) that have not developed to large basins due to good drainage conditions on top of the Dzhelon-Sise Highland. The presence of alases indicates the existence of Yedoma Ice Complex on the height surface of Dzhelon-Sise, which earlier was not known. To check this assumption, the study on Dzhelon-Sise Highland has been undertaken.

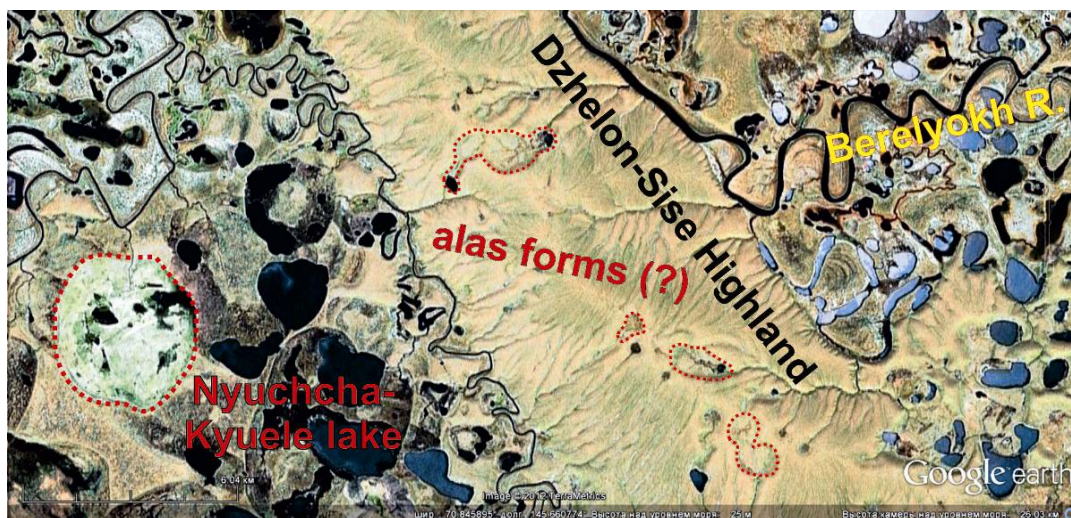


Fig. 11-1: Supposed alase forms on top of Dzhelon-Sise Highland according to remote sensing data interpretation.

Additional studies of alase depressions along the field trip (Fig. 11-2) have been conducted around the lake Dzhardakh near to northern edge of the Dzhelon-Sise Highland and in the lake Nyuchcha-Kyuele located west of the Dzhelon-Sise. The transport during this field trip was carried out by rubber boat (Fig. 11-3). The distance in one direction along the Berelekh River (from the station Kytalyk to the lake Nyuchcha-Kyuele) amounts about 160 km. During the first half of August the river was passed practically without limitation due to a high water level. After falling of water level it was necessary to follow the river waterway since it started to be shallower.

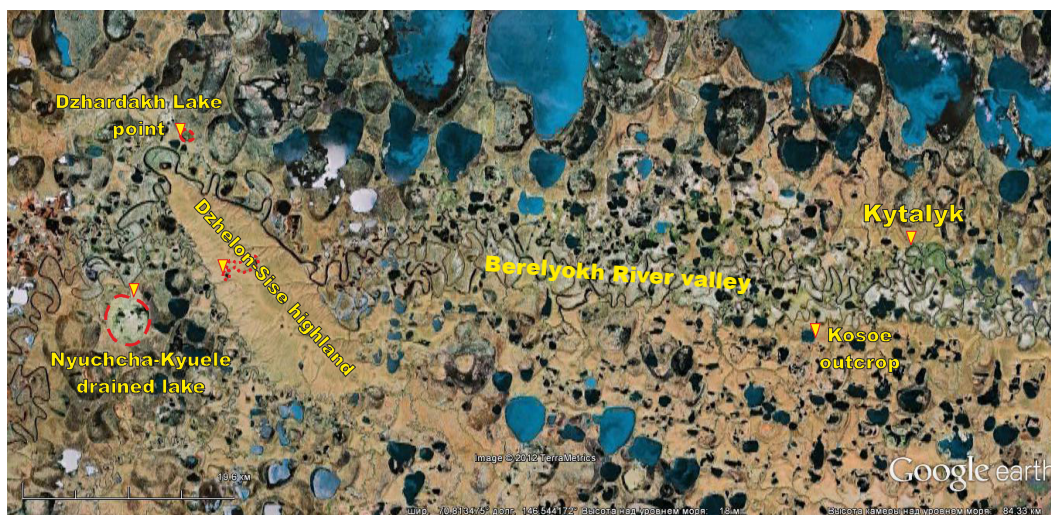


Fig. 11-2: Positions of the study sites during the field trip along the middle reach of the Berelekh River. Dotted lines indicate the alas rims.



Fig. 11-3: Motor-driven rubber boat in field trip.

11.2 Dzhardakh Lake area

The lake Dzhardakh is a residual lake in an alas depression, located north of the Berelekh River meander framing the Dzhelon-Sise Highland. To the southeast, three alas depressions (labeled as western, southern and northern) are connected through channels with the Berelekh River. These depressions were formed in the similar level of 6 m above the Berelekh River. This level was probably not flooded during high waters because fishing cabins were found there. Satellite images show that this level represents a relatively high alas level of an old wide alas of ten kilometers in diameter. The three alas depressions represent drained secondary thermokarst lakes. The western depression is now almost completely occupied by a deep lake, which did not totally freeze up down to the bottom during winter and is therefore used for fishing. The southern depression is partially occupied by a lake. The northern depression was recently drained and in its southern part a small residual lake occurs that is connected with a lake in the southern depression and further with the Berelekh River. A small Yedomahill of 20 m height remains east of the three depressions.



Fig. 11-4: Overview of the northern alas depression with the shrub stripe and the old grass stripes along the rim edge.

The main study field of modern permafrost conditions was conducted on the bottom of recently drained lake, which occupies most of the southern part in the northern alas depression. The drained part of the alas looks quiet homogenous. Shrubs of 1.5 to 2 m height exist along a 5 m high edge, while the largest part of the alas surface is covered by fresh grass (Fig. 11-4). On distance of 10-20 m from the edge, a zone of an old grass cover, which has been brought down, probably marked the bank-line position of the drained lake some years ago. In distance of about 150 meters from this old grass strip and behind a 0.4-0.5 m high surface, grass grows in a shallow lake. The water near this edge is 0.3 m deep. Sedge grows in the water up to a depth

of 0.6 to 0.7 m. The lake bottom is very muddy and viscously. The measured water mineralization amounted 17 to 22 ppm.

Polygonal nets do not exist on the drained thermokarst lake bottom and ice-wedges are not found there. However, the morphology of the northern alas rim and the surface micro relief indicate the presence of ice-wedges on the old alas level. The active layer was 0.3 to 0.35 m deep on August, 5th and 6th. Three pits were dug there through the active layer (Figs. 11-5a, b, c), which were filled by ground water during about 5 to 10 minutes. This water had mineralization of 280 to 290 ppm. Samples were not taken from these pits.

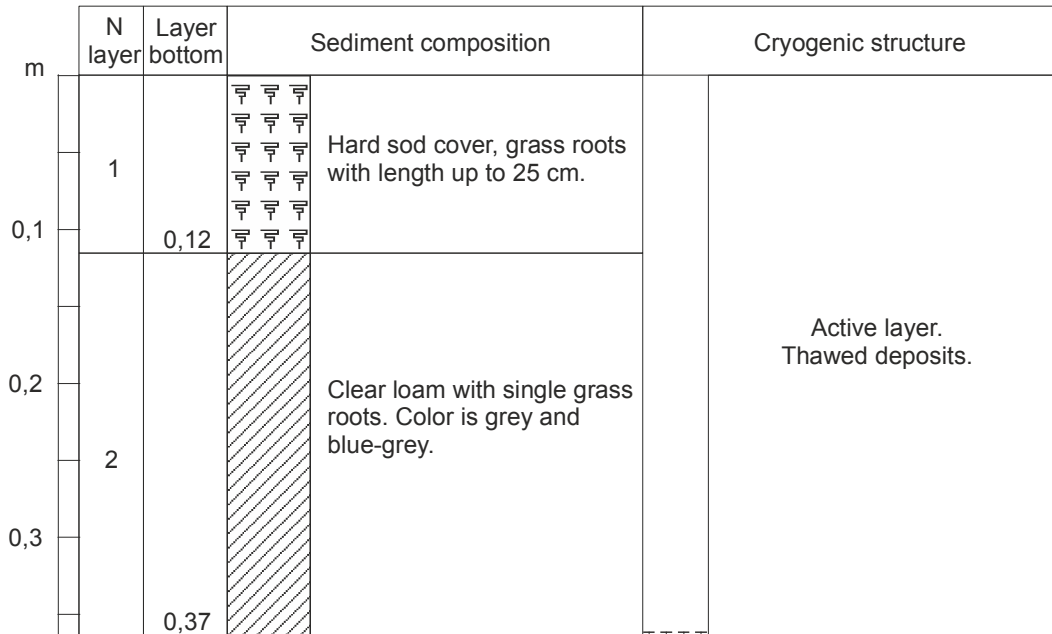


Fig. 11-5a: Stratigraphy of pit 1 (11B-0508-3) in the northern alas depression near lake Dzardakh, (N 70.91767°, E 145.64698°)

11. Middle Berelekh area

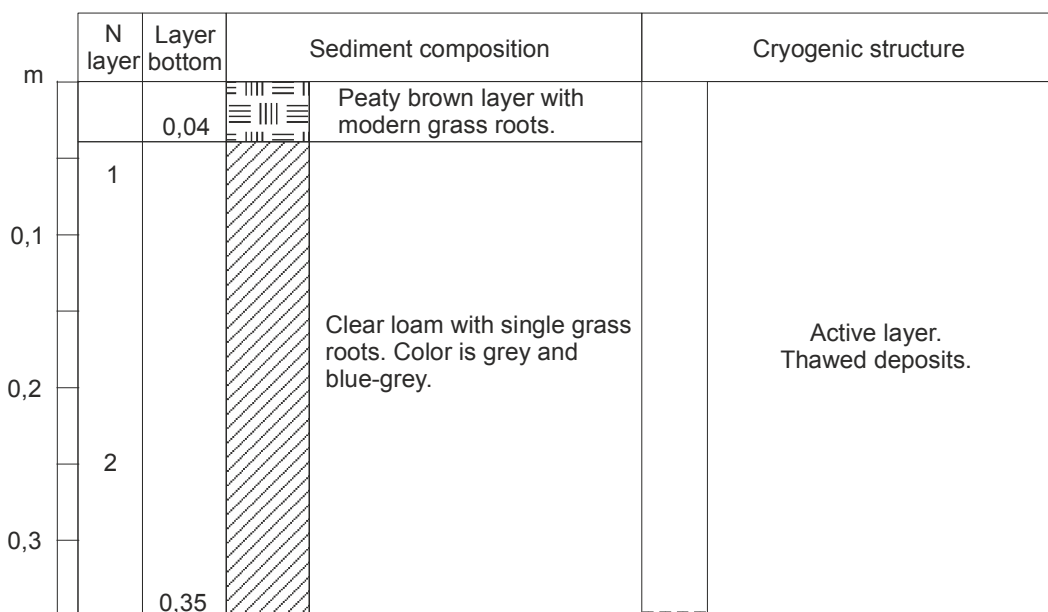


Fig. 11-5b: Stratigraphy of pit 2 (11B-0508-4) in the northern alas depression near lake Dzardakh, (N 70.91753°, E 145.64458°).

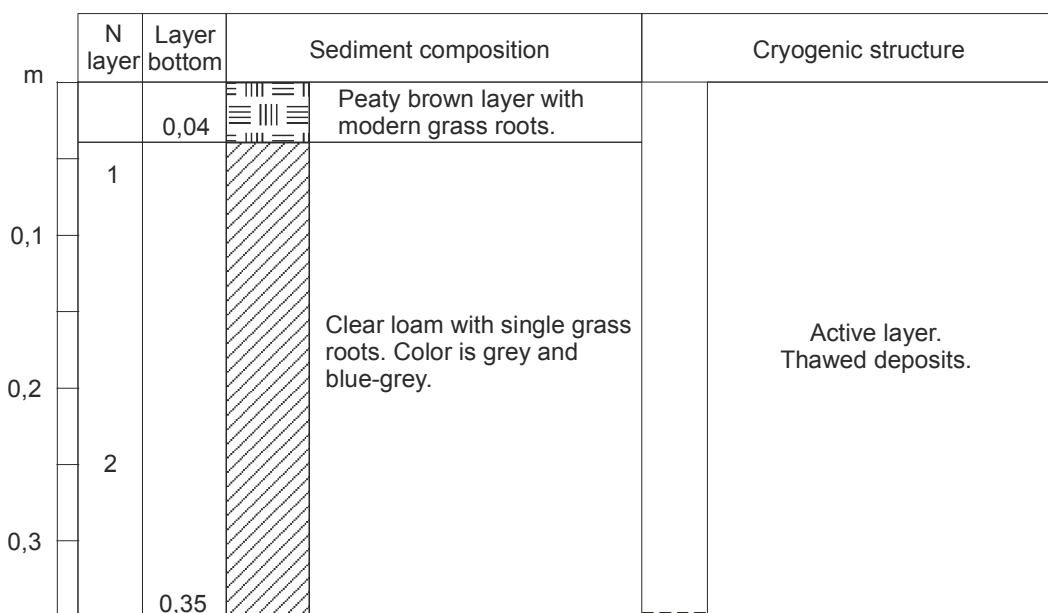


Fig. 11-5c: Stratigraphy of pit 3. (11B-0508-2) in the northern alas depression near lake Dzardakh (N 70.91727°, E 145.64270°).

11.3 Nyuchcha-Kyuele drained lake

The drained lake Nyuchcha-Kyuele is located 6 km west of the Dzhelon-Sise Highland (Fig. 11-2), within an old alas plain about 6 to 8 m height above the Berelekh River level. The meridional oriented alas depression has a size of 4 × 4.4 km. In an older topographic map from 1971 the lake covers almost the entire depression. The lake was drained between 1970 and 1980. According to local residents of the settlement Berelekh, the drained territory was used as grassland for haymaking in the mid-eighties. Lake draining occurred through a channel which cut the old alas plain. Rests of a camp with wind engine, a mowing machine, fuel tanks and bases of wooden tent constructions have remained near the beginning of the channel. Thus, the current state of the alas bottom was formed only during last 30 years.

There are still some small residual lakes in the alas depression (Fig. 11-1). The major field work was conducted near to the beginning of the drainage channel. Two main alas levels, a lower and an upper level, were distinguished. The lower level is grass covered with a polygonal network expressed by water-filled trenches above thawing ice wedges. Dark green juicy sedge grows in depressions, while sward is growing in polygonal centers. The polygonal net has a 5- to 6-edge pattern, with polygon diameters of about 20 m. Over ice wedges the water is 10-15 cm deep and the active layer is 25-40 cm deep (measured on August, 7th). In about 100 m distance from a terrain edge the surface character of the lower alas level changes. The width of sedge strips increases from about 0.5-1 m to 2-2.5 m and the sedge becomes higher (up to 0.5-0.6 m). The water depth above thawing ice wedges increases to 25-30 cm, and the active layer thickness amounts 30-50 cm. The structure of the upper permafrost horizons of lower alas level has been studied in the short boreholes BH-0808-1 and BH-0808-2 (Figs. 11-6, 11-7).

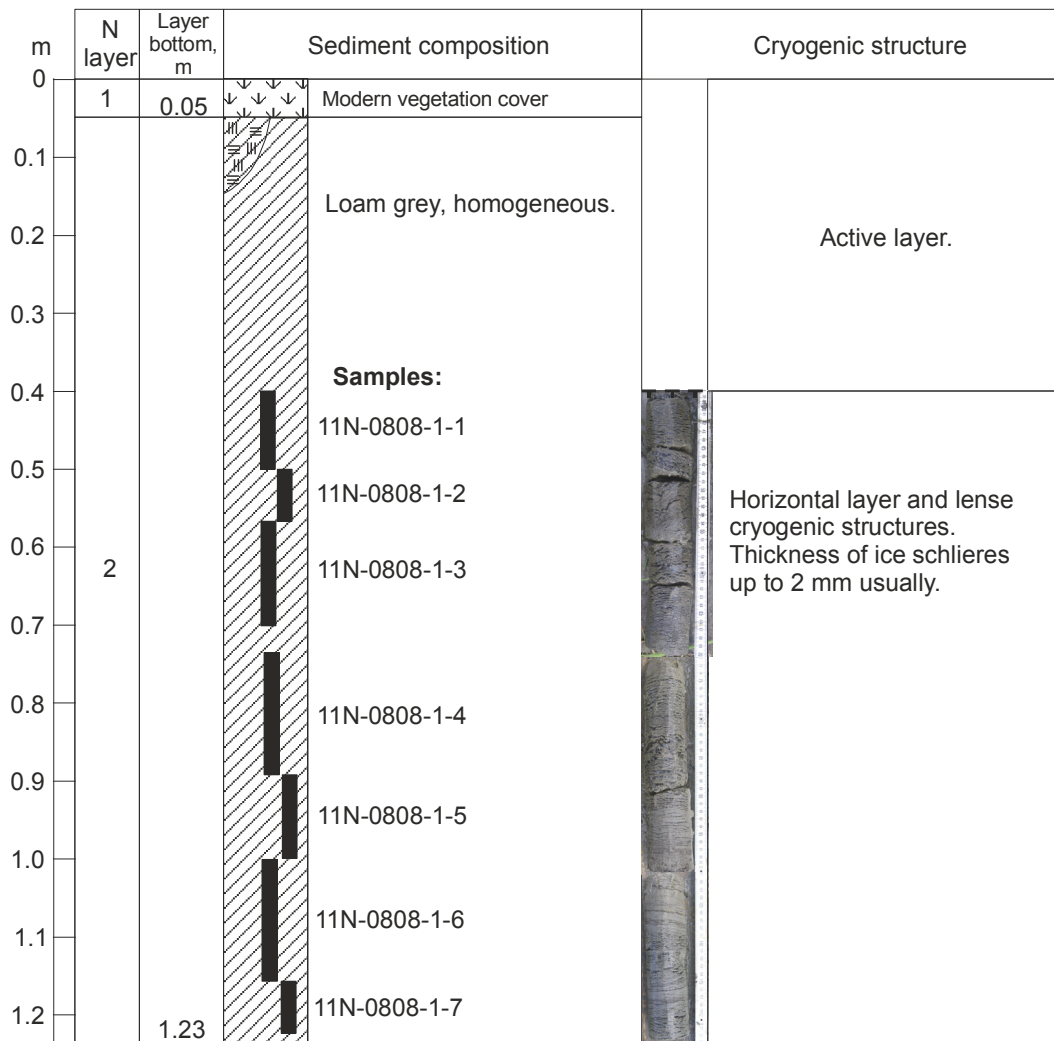


Fig. 11-6: Borehole BH-0808-1. with sample sites Lower level of Nyuchcha-Kyuele alas. Polygon center. GPS point 11N-0808-1 (N 70.78600°, E 145.53232°).

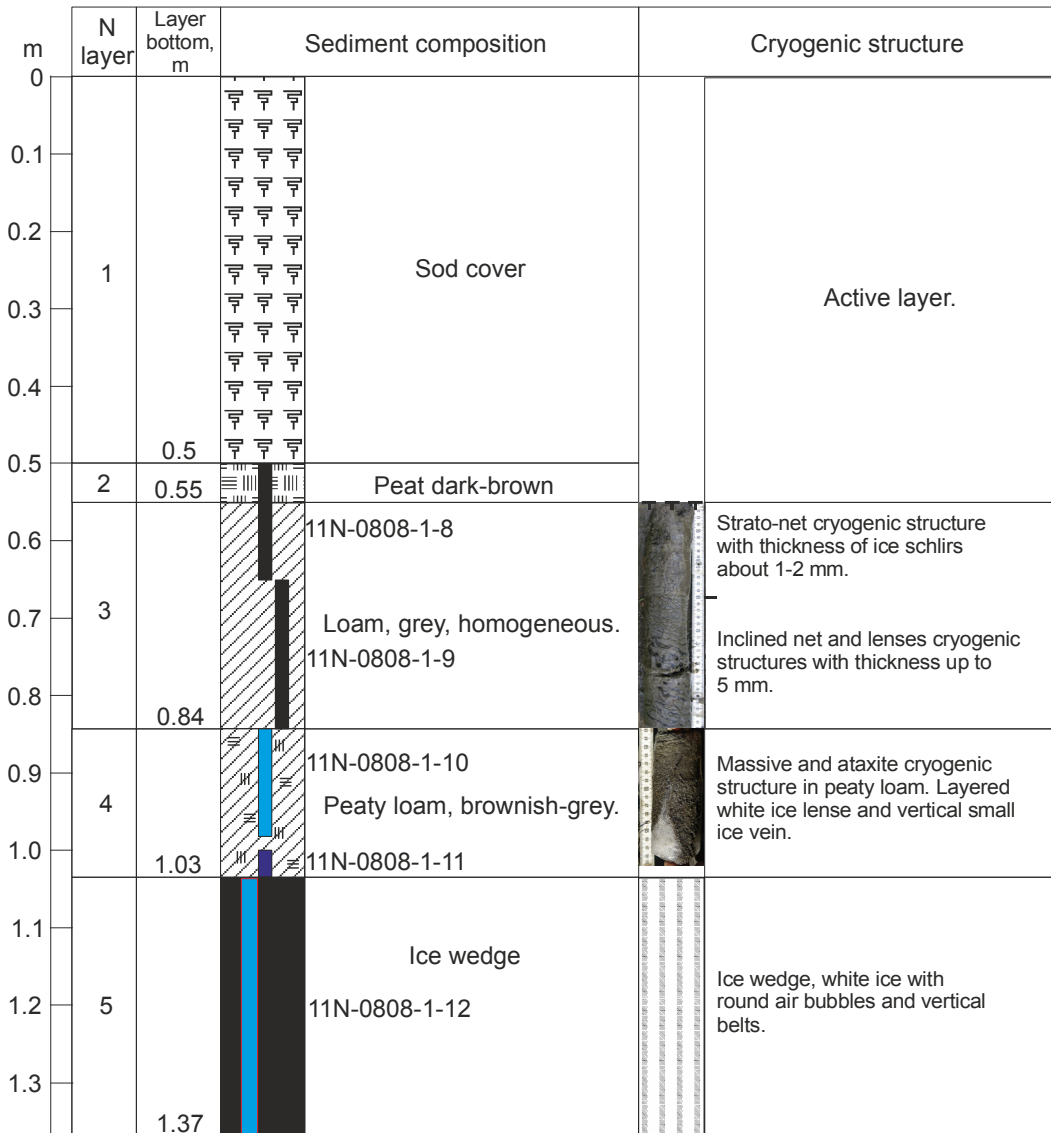


Fig. 11-7: Borehole BH-0808-2. Lower level of Nyuchcha-Kyuele alas. Trench above an ice wedge, located 6 m from the site BH-0808-1.

The 10 m wide transition zone along the slope to the upper level is covered by 2 to 2.5 m high shrubs. The height of the upper alas level edge increases eastward along northern alas rim from 0.5-1 to 3-3.5 m. At the northeast alas end, the upper level edge is about 6.5-7 m high, which decreases again further to the southeast along the alas rim. The upper alas level is covered by moss and lichen and seldom by single low shrubs. The polygonal micro-relief is expressed in form of linear 1 to 1.5 m wide trenches over thawing ice wedges. The tetragonal network is oriented with an angle of 60° to rims. Polygons have sizes of 15×20 to 20×20 m, however approximately the half is dissected by frost cracks into polygons of higher order (size 10×10 m). The structure of the upper permafrost horizon in the upper alas level was studied on borehole BH-1008-1 (Fig. 11-8).

11. Middle Berelekh area

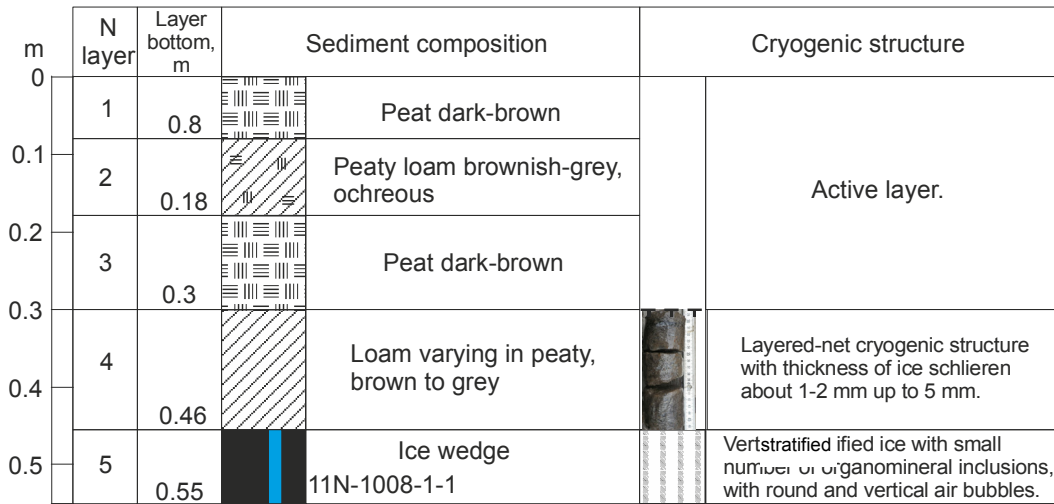


Fig. 11-8: Borehole BH-1008-1. High level of Nyuchcha-Kyuele alas. A linear depression over an ice wedge.

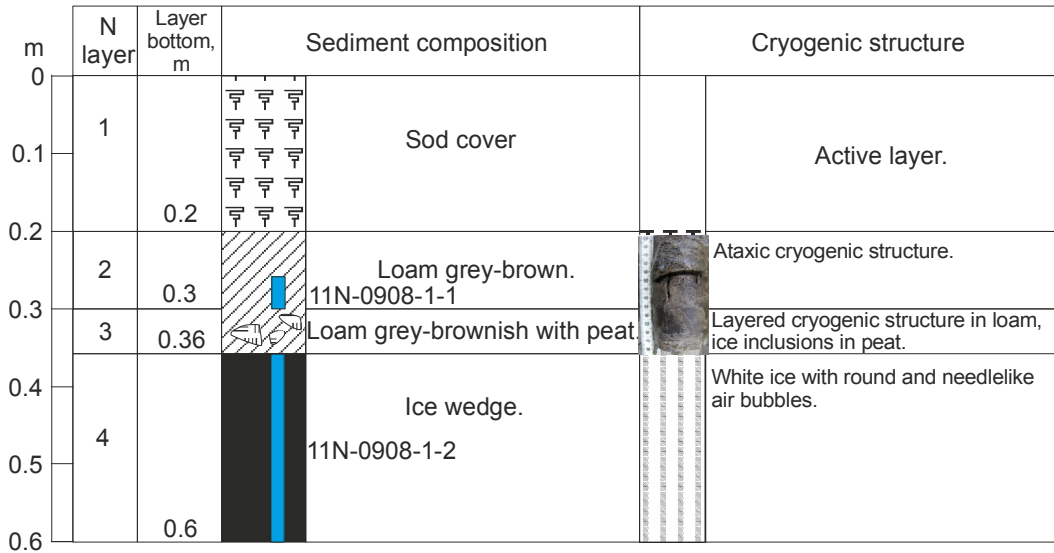


Fig. 11-9: Borehole BH-0908-1. High level of Nyuchcha-Kyuele alas. A trench above an ice wedge.

The highest point of upper alas level is located about 2.5-3 m over the bottom surface at the top of a small flat hill from which the surface smoothly decreases from relative height of 1-2 m over the lower alas level. Apparently, this is results of long-term heaving on a few meters. Similar forms were found on the east rim of the Nyuchcha-Kyuele alas as well as in the Kytalyk alas. They could be considered as an initial pingo stage. The structure of the upper domed part was studied in boreholes BH-0908-1 and BH-0908-2 (Figs 11-9, 11-10).

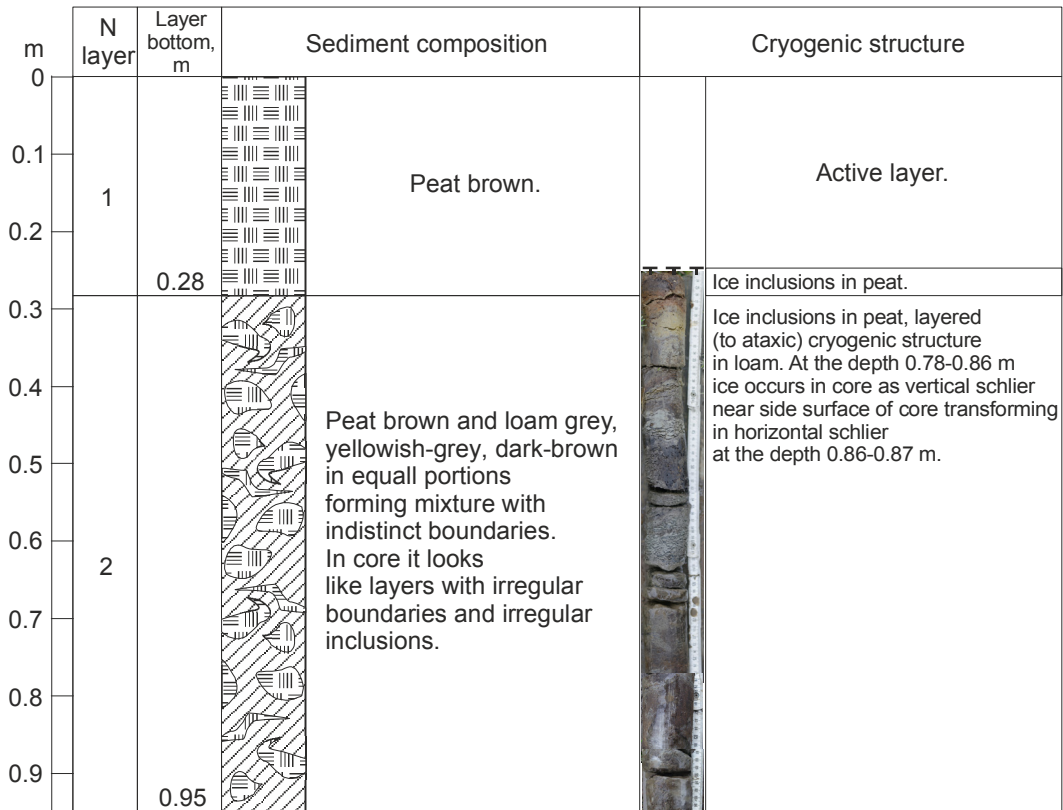


Fig. 11-10: Borehole BH-0908-2. High level of Nyuchcha-Kyuele alas, center of a polygon located in 10 m distance from BH-0908-1.

At the top of this long-term heaving form a second low hill (1-1.5 m high) of about 20×20 m size exists. In the middle of it there passes a ditch depth to 1.5 m which is traced as depression over one of ice wedge (Fig. 11-11). In a lateral wall of a pit an about 0.5 m thick ice lens was exposed (Fig. 11-12). The active layer thickness was 0.3 m.



Fig. 11-11: Top of the long-term heaving form with deep crack (site 11N-0708-3 PINGO, N 70.78623°, E 145.54583°).



Fig. 11-12: Site 11N-0708-3 PINGO. Pit on top of a frost mound with a lens of massive ice. The white numbers are number of layers described in the text below.

Description of the profile 11N-0708-3 PINGO:

- Layer 1: 0.1 m thick; modern vegetation cover; peat and green moss; dwarf willow, *Ledum palustre*; woody roots of up to 1 mm in diameter.
- Layer 2. 0.2 m thick, brown peat in the upper 15 cm; less decomposed; peat black in the lower 5 cm, 2 cm thick lens of gray loam at the contact between both sublayers.
- Layer 3. 0.15 m thick; gray loamy peat with 2 cm large black peat inclusions; ataxic cryostructure, roundish of 2 to 3 mm in diameter, inclusions of pure ice with air bubbles.
- Layer 4. 0.2 to 0.4 m thick; large ice lens; sharp flat roof. The upper 5 to 6 cm thick part of white and ochre ice is oriented parallel to the roof; layered structures are visible due to non-uniform inclusion of mineral blur and mineral-organic substance, and numerous air bubbles (0.2 to 1 mm in diameter). The lower part of 20 cm consisted of transparent gray ice, where upper 2-5 cm contains an increased number of air bubbles and separate inclusions of peat fragments of 1×1 to 1×2 cm size. The purest ice was seen in the center of the ice lens. At the bottom- small air bubbles are vertically chain-like oriented. The rough bottom is defined by character of the top of layer 5.
- Layer 5: > 0.1 m thick; ice with brown peat inclusions; probably a peat lens that was frozen under completely water-saturated conditions.

11.4 The Dzhelon-Sise Highland

11.4.1 Thermo-erosional valley of the site 11D-1308-1

(N 70.80823, E 145.72930)

Holocene valley deposits were exposed in a small thermo-erosional valley. Such valleys exist on the western slope of Dzhelon-Sise down in the Ary-Mas River and to the east down in the Berelekh River. The exposure on the left side of the studied valley is 4.2 m high. Here, two horizons organic material are separated by a sandy layer (Fig. 11-13).

- Layer 1: 0.3 m thick modern sod cover.
- Layer 2: 0.7 m thick, gray-brown ochre loam with numerous modern roots.
- Layer 3: 0.6 m thick, allochthonous peat with grass remains and woody roots up to 5-15 mm in diameter in the upper part; vertical 0.5 m long wedge-like structures in the lower part.
- Layer 4: 1.7 m thick, gray and ochre loam and sandy loam; numerous 5 to 10 cm thick up to 50 cm long lenses of gravely sand compose the lower 0.5 to 0.7 m of section. In places these lenses are cross-bedded.
- Layer 5: visible thickness about 0.9; lower horizon lenses of autochthonous peaty material and numerous woody roots of 3-5 cm in diameter.

Samples for AMS-dating were taken from horizons with allochthonous peat (1308-1 BГ – detritus from wedge-like structure in the base of the upper horizon, 1308-1 HГ – peat from a roof of the lower horizon, Figs. 11-13).

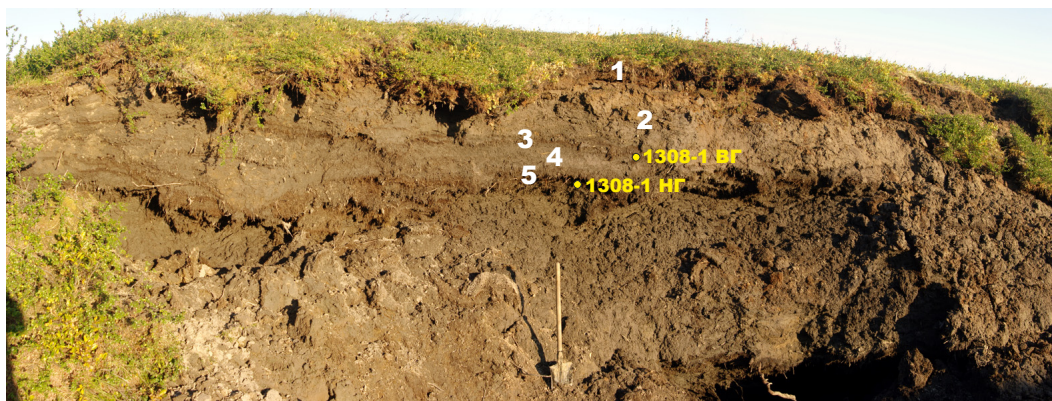


Fig. 11-13: Outcrop of thermo-erosional deposits in site 11D-1308-1. White numbers indicate the numbers of layers; yellow dots are location of AMS-samples.

11.4.2 Alas depressions and Yedoma exposures on top of the Dzhelon-Sise Highland

Site 11D-1308-2 (N 70.80440°, E 145.76137°)

An anonymous lake on the western slope of the Dzhelon-Sise highland (450 to 500 m wide) is located in the southeast part of a small thermokarst depression (700 m in diameter, Fig. 11-14). A small stream drains the lake to the Ary-Mas River (GPS point was located in stream spring). The depth of the alas depression is about 30 m. At the southern edge of the lake a Yedoma hill is eroded where ice wedges and a baydzharakh micro relief are visible.



Fig. 11-14: Overview of the anonymous thermokarst lake on the Dzelon-Sise watershed.

Three additional alas depression are located in higher levels northeast from the alas with the anonymous thermokarst lake mentioned above. All of them are connected by small streams. The largest depression (1.4 km long) is located on a watershed. Further west there is a depression with small lake and a small exposure of ground ices. The stream from this lake flows down to the east into the Berelekh River. Similar thermokarst depressions of smaller sizes are located to the southeast near watershed of Dzhelon-Sise.

Yedoma Ice Complex deposits were studied in three places around the anonymous lake.

1. Site 11D-1308-7 (N 70.80537°, E 145.76973°)

This was the lowermost accessible level for sampling on the east bank of the lake. The sampling height was about 8 m above the lake level (a.l.l.). A small fragment of a ground column was exposed in a landslip place. The deposits consist of gray-

brownish silty loam with lens-like layered cryostructure and ice lens thickness of about 3 to 4 mm. A sample (11D-1308-7-1) was taken there.

2 Site 11D-1408-2 (N 70.80243°, E 145.76838°)

This exposure represents the top of a thermo-cirque above the lake while most of this exposure is closed by taluses and landslips. The Yedoma surface (11.4 m a.l.l.) is lowered by a thermo-erosional valley. Five samples of silty loams were taken on a thermokarst mound (baydzharakh, Fig. 11-15): 11D-1408-2-1 – 9 m a.l.l., 11D-1408-2-2 – 9.3 m a.l.l., 11D-1408-2-3 – 9.6 m a.l.l., 11D-1408-2-4 – 9.9 m a.l.l., 11D-1408-2-5 – 10.2 m a.l.l..

In addition, a small epigenetic ice wedge (sample 11D-1408-2-6) and a 1.2 m wide syngenetic ice wedge (samples 11D-1408-2-7 to 11D-1408-2-10) were sampled at about 9-10 m a.l.l.



Fig. 11-15: Ice Complex exposure of site 11D-1408-2.

3. Site 11D-1408-3 (N 70.80315, E 145.76420)

A few ice wedges between thermokarst mounds are exposed in 9.6 m a.l.l. at the southwest bank of the thermokarst lake near headstream which draining the lake to the Ary-Mas River. Ice wedge were sampled for isotopic analysis: (samples 11D-1408-3-1 to 11D-1408-3-3).

4. Site 11D-1408-1 (N 70.80385°, E 145.78578°)

A gentle slope of the Yedoma hill continues behind the lake bank with thermokarst mounds. This slope declined to a broad gully with a flat several ten meters wide bottom. Modern ravines affect a backward thermo-erosion in the upper streams. The rain-wash from slopes as well as melt-water formed a small waterfall of 1.5-2 m height at steep walls in the stream spring. Thermo-erosional processes expose the polygonal ice wedge network on the bottom of the gully as well as the valley deposits

of probably Holocene age. Ice wedges were exposed in one of the thermo-wells in the upper stream of the thermo-erosional valley (Fig. 11-16). The ice wedges are covered by sod layer and 0.4-0.6 m thick peaty loam containing wood rests (2 cm in diameter). Five ice-wedge samples (11D-1408-1-1 to 11D-1408-1-5) were taken in one level from 1 to 2 ice wedges. The ice wedges were light gray, stripped and contain small inclusions of ground and muddy films. Elementary ice veins of 5-8 mm width are badly visible.



Fig. 11-16: Modern thermo-erosional ravine on the surface of Dzhelon-Sise.

11.5. The outcrop «Kosoe» in a lake depression near the Berelekh River

The exposure “Kosoe” is a Yedoma site located at the east bank of an anonymous lake 1.4 km far from the Markova channels (Figs. 11-2, 11-17).



Fig. 11-17: “Kosoe” outcrop site 11B-2508-2OUTCROP (N 70.75055°, E 147.24580°)

The height of the Yedoma surface is 25 m a.l.l.. The major part of the exposure is covered by landslips and completely grass covered. In the upper part between 15.8 and 25 m a.l.l. the steep wall of ice wedges and frozen ground columns was exposed. The section was described and sampled from below upwards by combining several ground column parts (Tab. 11-1). In general, the sequences could be divided in several cryogenic cycles.

- 1st cryogenic cycle:

The lower part of the southern ground column (named ГС1) is composed of gray silty loam with a banded cryostructure. The ice bands were 3 to 4 cm thick with an interspace of 5 to 6 cm. Loamy deposits at 17.4 m a.l.l. are characterized by banded cryostructure with ice bands of 1 to 2-3 cm thickness and lens-like layered or reticulate cryostructure between the ice bands.

- 2nd cryogenic cycle:

Deposits at 18.4 m a.l.l. characterize the lower part of a following cryogenic cycle. Above the contact, a light-gray loam with small peat inclusions is characterized by a cellular and wavy-layered cryostructure. A sample for radiocarbon dating was collected from a 0.5 m long radial oriented peaty loam inclusion in the uppermost part of this cryogenic cycle. Samples from 11B-2508-2-12 to 16 are ice from a Yedoma ice wedges at about 19 m a.l.l.

- 3rd cryogenic cycle:

Between 20.5 and 21.4 m a.l.l. ochre-gray silty loam with banded cryostructure occurs. The ice bands were 1 to 2 cm thick (up to 8 cm at 20.5 m a.l.l.). The distance between the ice bands amounts 40 cm and more. In the interval of 20 to 21 m a.l.l. the cryostructure was more complicated. A weakly reticulated cryostructure between ice bands was observed in the bottom part while the cryostructure above was micro lens-like or thin reticulate.

Above 21.4 m a.l.l. a strongly peaty loam occurred with wedge-shaped ledges of 0.4 m length (Fig. 11-18). The cryogenic structure of this layer is dominantly massive with rare separate ice lenses. In wedge-shaped edges are well developed ice lenses occur with thicknesses from 2-3 mm to 1.5 cm. Above 21.5 m a.l.l. the study was carried out along the ground column ГС3. The third cryogenic cycle terminates approximately at height of 22 m.

- 4th cryogenic cycle:

The cover layer on the top of the Yedoma sequence at about 24 m a.l.l. was 0.8-1 m thick



Fig. 11-18: Ground column GC3 (detail of outcrop “Kosoe”), 20.5-22 m a.l.l.

Tab. 11-1: Sample collection of the Yedoma exposure “Kosoe” (Salinity analysis with Conductometer COM-100, by NaCl).

Sample	height (m a.l.l.)	sediment	Ground ice	Salinity (ppm)
11B-2508-2-1 (GC1)	16.2	silty loam		740
11B-2508-2-2 (GC1)	16.8	silty loam		290
11B-2508-2-3 (GC1)	17.4	loam		680
11B-2508-2-4 (GC1)	18.4	loam		290
11B-2508-2-5 (GC1)	18.7	peaty loam inclusion		
11B-2508-2-6 (GC2)	20.5		ice layer	130
11B-2508-2-7 (GC2)	20.6	loam		490
11B-2508-2-8 (GC2)	21.6	loam		
11B-2508-2-9 (GC3)	21.6	peat for ¹⁴ C		
11B-2508-2-12 to 16	19		Yedoma ice wedge	
11B-2508-2-18	21.6		textural ice	
11B-2508-2-10 (GC3)	22.1	loam		460
11B-2508-2-11 (GC3)	22.6	loam		450
11B-2508-2-17	22.9		epigenetic ice wedge in GC3	
11B-2508-2-19 (GC4)	24	loam		

REFERENCES

- Beyens L., Chardez D. (1986a). Testate Amoebae Populations from Moss and Lichen Habitats in the Arctic. *Polar Biol.*, 5, 165-173.
- Beyens L., Chardez D. (1986b). Testate Amoebae Communities of Aquatic Habitats in the Arctic. *Polar Biol.*, 6, 197-205.
- Beyens L., Chardez D., de Baere D., de Bock P. (1992). The testate amoebae from the Sondre Stromfjord region (West-Greenland): Their biogeographic implications. *Arch. Protistenk.*, 142, 5-13.
- Biasi, C., Meyer, H., Rusalimova, O., Hämmerle, R., Kaiser, C., Baranyi, C., et al. (2008). Initial effects of experimental warming on carbon exchange rates, plant growth and microbial dynamics of a lichen-rich dwarf shrub tundra in Siberia. *Plant and Soil*, 307(1-2), 191-205.
- Bobrov A.A., Andreev A.A., Schirrmeister L., Siegert C., (2004). Testate amoebae Protozoa: Testacealobosea and Testaceafilosea) as bioindicators in the Late Quaternary deposits of the Bykovsky Peninsula, Laptev Sea, Russia. *Palaeogeography, Palaeoclimatology, Palaeoecology*, 209, 165–181.
- Bowman. R.A., Cole, C.V. (1978). An Exploration Method for Fractionation of Organic Phosphorus from Grassland Soils. *Soil Science*, 125(2), 95-101.
- CAVM Team (2003). Circumpolar Arctic Vegetation Map, Scale 1:7.500.000. Conservation of Arctic Flora and Fauna (CAFF) Map No.1. U.S. Fish and Wildlife Service, Anchorage, Alaska. <http://www.geobotany.uaf.edu/cavm/finalcavm/index.html>.
- Chapin, F.S., Barsdate, R.J., Barèl, D. (1978). Phosphorus Cycling in Alaskan Coastal Tundra : A Hypothesis for the Regulation of Nutrient cycling. *Oikos*, 31(2), 189-199.
- Charman D.J. (1997). Modelling hydrological relationships of testate amoebae (Protozoa: Rhizopoda) on New Zealand peatlands. *J. Royal Soc. of New Zealand*, 27, 465-483.
- Czerepanov, S.K. (1995). Vascular plants of Russia and adjacent states (The former USSR). Cambridge, Cambridge University Press.
- De Klerk, P, Joosten, H. (2007). Short-lived vegetational and environmental change within the Preboreal open vegetation phase in the Biebrza upper basin (NE Poland). *Quaternary Science Reviews*, 26, 1975-1988.
- De Klerk, P., Nikolay N. D., Karpov S., Minke, M., Joosten, H. (2011). Short-term dynamics of a low-centred ice-wedge polygon near Chokurdakh (NE Yakutia, NE Siberia) and climate change during the last ca 1250 years. *Quaternary Science Reviews*, 30 (21-22), 3013-3031.
- Donner, N., Minke, M., de Klerk, P. , Joosten, H. (2009). Patterns in polygon mires in NE Yakutia (NE Siberia): the role of vegetation and water. In: Lindholm, T. & Heikkilä, R. (eds.): Conservation, Biodiversity and Restoration of Mires. *Suomen Ympäristö* 19, 1-12
- Geocryological Map of the USSR, 1991. 1 : 2,500,000.

- Ivanoff, D.B., Reddy, K.R., Robinson, S. (1998). Chemical Fractionation of Organic Phosphorus in Selected Histosols. *Soil Science*, 163(1), 36-45.
- Joosten, H., de Klerk, P. (2007a). DAMOCLES: a DASHing MONolith Cutter for fine sectioning of peats and sediments into Large Slices. *Boreas*, 36, 76-81.
- Joosten, H., de Klerk, P. (2007b). In search of finiteness: the limits of fine-resolution palynology of Sphagnum peat. *The Holocene* 17: 1025-1033.
- Kaplina, T.N., Sher, A.V., Giterman, R.E., Zazhigin, V.S., Kiselev, S.V., Lozhkin, A.V., Nikitin, V.P. (1980). Oporny razrez pleystotsenovykh otlozheniy na reke Allaikha (nizov'ya Indigirki) (Key section of Pleistocene deposits on the Allaikha river (lower reaches of the Indigirka). In: Bulletin of Commission on Quaternary Period research, USSR Academy of Sciences, No. 50, pp. 73-95 (in Russian).
- Lavrushin, Yu.A., (1963). Allyuvii ravninnykh rek subarkticheskogo poyasa i periglyatsialnykh oblastey materikovykh oledeneniy (Alluvium of plain rivers of the subarctic zone and periglacial region of inland glaciers). Proceedings of Geological Institute of AN SSSR, 87, 264 pp. (in Russian).
- Londo, G. (1976). The decimal scale for releves of permanent quadrats. *Vegetatio*, 33/1, 61-64. doi: 10.1007/BF00055300.
- Mattheeussen R., Ledeganck P., Vincke S., B. Van de Vijver, Nijs I., Beyens, L. (2005). Habitat Selection of Aquatic Testate Amoebae Communities on Qeqertarsuaq (Disko Island), West Greenland. *Acta Protozoologica*, 44, 253–263.
- McGuire, A.D., Chapin III, F.S., Wirth, C., Apps, M., Bhatti, J., Callaghan, T.V., Christensen, T.R., Clein, J.S., Fukuda, M., Maximov, T., Onuchin, A., Shvidenko, A., et al. (2007). Responses of high latitude ecosystems to global change: potential consequences for the climate system. In: J. G. Canadell, Pataki, D.E., and L. F. Pitelka (eds.). *Terrestrial Ecosystems in a Changing World*. London, Springer, pp. 297-310.
- Minke, M., Donner, N., Karpov, N.S., de Klerk, P., Joosten, H. (2007a). Distribution, diversity, development and dynamics of polygon mires: examples from NE Yakutia (NE Siberia). *Peatlands International 2007* (1), 36-40.
- Minke, M., Donner, N., Karpov, N.S., Seifert, N., Joosten, H. (2007b). A window to the soul: biotic/abiotic feedback mechanisms in polygon mire ecosystems. In: B. I. Ivanov, Maximov, T.C., Maksimov, A.P., Konovov, A.V. (eds.) *Influence of climatic and ecological changes on permafrost ecosystems. Proceedings of the third international conference "The role of permafrost ecosystems in global climate change"*. YSC Publishing House SB RAS, Yakutsk: 115-121.
- Minke, M., Donner, N., Karpov, N., de Klerk, P., Joosten, H. (2009). Patterns in vegetation composition, surface height and thaw depth in polygon mires in the Yakutian Arctic (NE Siberia): A microtopographical characterisation of the active layer. *Permafrost and Periglacial Processes* 20: 357-368.
- Mochanov, Y.A., Fedoseeva, S.A. (1996). Berelekh, Allakhovsk Region. In *American Beginnings: The Prehistory and Palaeoecology of Beringia*, edited by F. H. West. University of Chicago Press, Chicago.

- Mukhin, N.I., Tolstov, A.N. (1960). Nekotorye dannye po gidrologii r. Eloni (Some data about Elon' river hydrology). Trudy Instituta Merzlotovedeniya im, V.A. Obrucheva (papers of the permafrost institute "V.A. Obruchev"), Vol XVII (Ocherki po regional'noi i istoricheskoi kriologii), 76-77 (in Russian).
- Ovander, M.G., Rybakova, N.O. (1985). Paleogene and Neogene sections of Dzhelon-Sise upland (lower Indigirka River area). Doklady Akademii Nauk SSSR, 282 (2), 412-416 (in Russian).
- Pitulko; V.V. (2011). The Berelekh Quest: A Review of Forty Years of Research in the Mammoth Graveyard in Northeast Siberia.- *Geoarchaeology: An.* 26 (1), 5–32.
- Rivas-Martínez, S. (2007). Global bioclimatics. Data set. Available online at <http://www.globalbioclimatics.org> from Phytosociological Research Center, Madrid, Spain.
- Romanovskii, N.N., (1977). Formirovanie poligonal'no-zhil'nykh struktur (Formation of polygonal-wedge systems). Nauka, Novosibirsk, 215 pp. (in Russian).
- Scheffer, F., Schachtschabel, P. (2002). Lehrbuch der Bodenkunde (15th ed.). Heidelberg: Spektrum Akademischer Verlag, 593 S.
- Schuur, E.A.G., Bockheim, J., Canadell, J.G., Euskirchen, E.B.C., Goryachkin, S.V., et al. (2008). Vulnerability of Permafrost Carbon to Climate Change : Implications for the Global Carbon Cycle. *BioScience*, 58(8), 701-714.
- Schuur, E.A.G., Vogel, J.G., Crummer, K G., Lee, H., Sickman, J.O., Osterkamp, T.E. (2009). The effect of permafrost thaw on old carbon release and net carbon exchange from tundra. *Nature*, 459, 556-559.
- Serreze, M.C., Walsh, J.E., Chapin III, F.S., Osterkamp, T., Dyurgerov, M., Romanovsky, V., Oechel, W.C., Morison, J., Zhang Barry, T.R.G. (2000). Observational evidence of recent change in the northern high-latitude environment. *Climatic Change* 46, 159-207.
- Shishov L.L., Tonkonogov V.D., Lebedeva I I., Gerasimova M.I. (2004). Classification and diagnostics of soils of Russia. Moscow., Publ. "Oecumene". (in Russian).
- Soil Survey Staff (2010). Keys to Soil Taxonomy. 10th ed., Washington, D.C.: United States Department of Agriculture & Natural Resources Conservation Service.
- Sturm, M., Schimel, J., Michaelson, G., Welker, J.M., Oberbauer, S. F., Liston, G.E., et al. (2005). Winter Biological Processes Could Help Convert Arctic Tundra to Shrubland. *BioScience*, 55(1), 17. American Institute of Biological Sciences.
- Trappeniers, K., Kerckoorde van, A., Chardez, D., Beyens, L. (2002). Testate Ameobae Assemblages from Soils in the Zackenberg Area, Northeast Greenland. *Arctic, Antarctic and Alpine Research*, 34(1), 94-101.
- VDLUFA (1991). Methodenbuch 1. Darmstadt: Verband Deutscher Landwirtschaftlicher Untersuchungs- und Forschungsanstalten.
- van Everdingen, R.O. (1998). Multi-language glossary of permafrost and related ground-ice terms. Boulder, CO: National Snow and Ice Data Center/World Data Center for Glaciology, 233 pp.
- Vereshchagin, N.K. (1977). The Berelyokh mammoth "cemetery". In: Proceedings of the Zoological institute USSR Academy of Sciences, 72, 5-50 (in Russian).

- Vereshchagin, N.K., Ukraintseva, V.V. (1985). The origin and stratigraphy of Berelyokh mammoth "burial ground". In: Proceedings of the Zoological institute USSR Academy of Sciences, 131, 104-113 (in Russian).
- Viehberg, F.A. (2002). A new and simple method for qualitative sampling of meiobenthos communities. *Limnologica* 32: 350-351.
- Vincke, S.B., Van de Vijver, I, Mattheeussen R., Beyens L. (2004). Freshwater testate amoebae communities from Ile de la Possession (Crozet Archipelago, Subantarctica). *Arctic, Antarctic and Alpine Research*, 36(4), 584-590.
- Vincke, S., Van de Vijver, B, Nijs, I., Beyens. L. (2006). Changes in the Testacean Community Structure Along Small Soil Profiles. *Acta Protozoologica*, 45, 395-406.
- Wagner, D., Gattinger, A., Embacher, A., Pfeiffer, E.-M., Schlöter, M., Lipski, A. (2007). Methanogenic activity and biomass in Holocene permafrost deposits of the Lena Delta, Siberian Arctic and its implication for the global methane budget. *Global Change Biology*, 13, 1089-1099.
- Warner, B.G., Charman, D.J. (1994). Holocene soil moisture changes on a peatland in northwestern Ontario based on fossil testate amoebae (Protozoa) analysis. *Boreas*, 23, 270-279.
- Weintraub, M.N., Schimel, J.P. (2005). Nitrogen Cycling and the Spread of Shrubs Control Changes in the Carbon Balance of Arctic Tundra Ecosystems. *BioScience*, 55, 408-415.
- Wetterich, S., Schirrmeister, L., Kholodov, A. (2011). The joint Russian-German expedition BERINGIA/KOLYMA 2008 during the International Polar Year (IPY) 2007/2008. *Berichte zur Polar- und Meeresforschung (Reports on Polar and Marine Research)*, Bremerhaven, Alfred Wegener Institute for Polar and Marine Research, 636, 48 p., ISSN: 1866-3192.
- Wille, C., Kutzbach, L., Sachs, T., Wagner, D, Pfeiffer, E-M. (2008). Methane Emission from Siberian Arctic Polygonal Tundra: Eddy Covariance Measuring and Modeling. *Global Change Biology*, 14, 1395-1408.

APPENDIX 1 – STUDY SITES

Lutz Schirrmeister

Tab. A 1-1: Coordinates of study sites in the Kytalyk area

Name	Date	° E	° N
Ecological study sites (chapters 3, 4)			
KYT-1	19.07.2011	147,48299	70,83121
KYT-2	21.07.2011	147,47839	70,83291
KYT-3	23.07.2011	147,48895	70,84306
KYT-4 / GPS 24	23.07.2011	147,48555	70,84312
KYT-5	03.08.2011	147,48596	70,82958
KYT-6	27.07.2011	147,44064	70,82832
KYT-7	28.07.2011	147,49527	70,86152
KYT-8	03.08.2011	147,48248	70,83157
KYT-9	04.08.2011	147,46181	70,82761
KYT-10	04.08.2011	147,44827	70,83604
KYT-11	04.08.2011	147,44356	70,83910
KYT-12	06.08.2011	147,42291	70,84752
KYT-13	06.08.2011	147,40939	70,84760
KYT-14	12.08.2011	147,47955	70,83120
KYT-15	12.08.2011	147,47595	70,83173
KYT-16	13.08.2011	147,47943	70,84522
KYT-17 / GPS 201	13.08.2011	147,47131	70,84276
KYT-18	15.08.2011	147,47542	70,81393
KYT-19	15.08.2011	147,48856	70,81246
KYT-20	16.08.2011	147,47833	70,81631
KYT-21	16.08.2011	147,47942	70,81596
KYT-22	18.08.2011	147,47485	70,81786
KYT-23	18.08.2011	147,47600	70,81617
KYT-24	20.08.2011	147,48322	70,81973
KYT-25	22.08.2011	147,52426	70,82465
KYT-26	22.08.2011	147,52097	70,82375
KYT-27	24.08.2011	147,47778	70,82645
Limnological study sites (chapter 5)			
GPS 128/LBR	31.07.2011	147,416105	70,848262
GPS 38/1	27.07.2011	147,421981	70,832817
LBL	31.07.2011	147,402300	70,846880
LBR	31.07.2001	147,420210	70,847560
GPS 34	26.07.2011	147,479429	70,845223
GPS 201	09.08.2011	147,471316	70,842756
GPS 24/KYT-4	23.07.2011	147,485552	70,843118
GPS 26	26.07.2011	147,476907	70,834470
GPS 25	26.07.2011	147,473240	70,834950

Name	Date	° E	° N
Model polygon LHC-11 (chapter 6)			
LHC-11		147,48115	70,83069
Pedological study sites (chapter 7)			
KYTF1		147,4826944	70,8311944
KYTF2		147,4813333	70,8319444
KYTF3		147,4746944	130,352667
KYTF4		147,4775278	70,8320556
KYTF5		147,4542778	70,8432778
KYFT6		147,4956389	70,8621111
KYTF7		147,45775	70,8459722
YED1		147,4506111	70,8403611
Permafrost exposures (Chapter 8)			
11-KH-2607-1	26.07.2011	147,49153	70,82689
11 KH 2807-1	28.07.2011	147,49753	70,860300
11 KH 3007-1	30.07.2011	147,43876	70,83180
Drill holes and pits (Chapter 9)			
11-KH-2707-1	27.07.2011	147,47849	70,83162
11-KH-2307-1/2/3/4	23.07.2011	147,48115	70,83069
11-KH-2107-1/2	21.07.2011	147,48557	70,82887
11KH-2008-1	20.08.2011	147,47827	70,82047
11KH-1907-1	19.07.2011	147,48263	70,83127
11KH-2107-1	21.07.2011	147,48498	70,82920
11KH-2407-1	24.07.2011	147,48454	70,82595
11KH-2807	28.07.2011	147,49753	70,860300
11KH-2907-2	29.07.2011	147,48752	70,83922
11KH-2907-9 BUGOR	29.07.2011	147,48587	70,84235
11KH-3007-1LOGGER	30.07.2011	147,48715	70,84261
11KH-2208-3	22.08.2011	147,56277	70,83652
11KH-2308-2-PINGO	23.08.2011	147,48583	70,80215
11KH-2308-7 POLY	23.08.2011	147,47545	70,79857

APPENDIX 2

List of hydrobiological samples

Andrea Schneider

Tab. A 2-1: General characteristics, sampling depths and hydrobiological samples of the monitoring site KYT-1.

No.	Date	Water depth [cm]	Thaw depth center [cm]	Thaw depth wall ([1] [cm]	Thaw depth T2 [cm]	Thaw depth M [cm]	Sample depth, hydrochemistry [cm]	Sample depth, exhauster [cm]	Ostracodes	Phytoplankton	Zooplankton	Makrozoobenthos	Sediment	Testate amoebae	Isotopes	Hydrochemistry
1-1	19/07/11	21	40	20 - 30	no data	no data	20	20	x	x	x	x	x	x	x	x
1-2	24/07/11	28	45	20 - 25	no data	no data	15	30	x	x	x	x			x	x
1-3	28/07/11	35	50	20 - 25	no data	no data	15	30	x	x	x	x			x	x
1-4	01/08/11	40	48	19 - 25	no data	no data	15	30	x	x	x	x			x	x
1-5	05/08/11	37.5	47.5	22	43	22	15	37	x	x	x	x		x	x	x
1-6	09/08/11	32	55	22 - 25	42 - 45	22 - 25	15	25	x	x	x	x			x	x
1-7	13/08/11	33	55	25	45	23	15	30	x	x	x	x			x	x
1-8	17/08/11	31	58	22	43	24	15	30	x	x	x	x			x	x
1-9	21/08/11	39	52	22 - 25	45 - 47	25 - 28	15	30	x	x	x	x			x	x
1-10	25/08/11	36	55	25	45	25	15	36	x	x	x	x	x	x	x	x

Tab. A 2-2: Physico-chemical features of the monitoring site KYT-1.

* Values for NH_4^+ , NO_3^- and PO_4^{3-} are related to the molecular weight of N and P. Negative or missing values occur from the detection limits in the spectral photometer (Hach Lange DR 2800).

No.	T Air [°C] Detection limit	T Water [°C]	EC [$\mu\text{S}/\text{cm}$]	pH (WTW)	* NH_4^+ [mg/l] 0.015 mg/l	* NO_3^- [mg/l] 0.23 mg/l	* PO_4^{3-} [mg/l] 0.05 mg/l	O ₂ [mg/l]	Alk [mmol/l]	Aci [mmol/l]	total hard [°dH]
1-1	17.2	19.0	23	6.2	0.039	0.278	no data	8.4	0.4	0.4	1.5 (0.3 mmol/l)
1-2	15.4	17.8	17	5.9	no data	no data	no data	8.4	0.4	0.4	1.5 (0.3 mmol/l)
1-3	19.2	17.9	21	6.4	no data	no data	no data	6.0	0.4	0.4	2.5 (0.4 mmol/l)
1-4	13.2	17.6	21	5.6	0.078	0.458	no data	8.4	0.4	0.4	0.5 (0.4 mmol/l)
1-5	18.2	13.5	18	6.3	0	0.393	0	7.2	0.4	0.4	3.5 (0.5 mmol/l)
1-6	7.0	19.0	26	7.6	0.019	0.454	0	9.8	0.4	0.4	3.5 (0.6 mmol/l)
1-7	8.5	8.7	18	6.1	0.010	0.401	0	9.8	0.4	0.4	4.0 (0.4 mmol/l)
1-8	4.5	8.0	21	6.5	0.004	0.492	0	10.0	0.4	0.4	4.0 (0.7 mmol/l)
1-9	5.5	7.3	21	6.2	0.028	0.383	no data	10.8	0.4	0.4	4.5 (0.7 mmol/l)
1-10	8.4	7.2	21	6.0	0.048	0.403	0	8.0	0.4	0.4	3.5 (0.6 mmol/l)

Tab. A 2-3: Location, type, and general characteristics of the studied ponds and lakes KYT-2 to 27. LC – Intrapolygon pond in low-centered polygon. I – Interpolygon pond. NP - Non-polygonal pond. T – Thermokarst lake. A – Alas. Y- Yedoma. F – Floodplain.

Pond No.	Date	Coordinates	Type	Area	Size of the water body (m)	Water depth (cm)	Thaw depth center (cm)	Thaw depth wall (cm)
KYT-2	21/07/11	70.83291°N 147.47839°E	LC	A	20.5 x 12.7	70	no data	30 - 35
KYT-3	23/07/11	70.84306°N 147.48895°E	I	A	20.9	50	40	30 - 35
KYT-4	23/07/11	70.84312°N 147.48555°E	LC	A	20.8	32	40	30 - 35
KYT-5	03/08/11	70.82958°N 147.48596°E	LC	A	20.4 x 16.5	> 1 m	no data	17 - 20
KYT-6	27/07/11	70.82832°N 147.44064°E	LC	A	18	15	35 - 45	30 - 32
KYT-7	28/07/11	70.86152°N 147.49527°E	LC	A	12.8 x 8.9	29	38 - 40	20-22
KYT-8	03/08/11	70.83157°N 147.48248°E	I	A	15 x 7	45 - 50	30	25 - 28
KYT-9	04/08/11	70.82761°N 147.46181°E	NP	Y	5.9	22	40	30 - 50
KYT-10	04/08/11	70.83604°N 147.44827°E	NP	Y	10 x 1.5	15 - 20	40 - 50	40 cm
KYT-11	04/08/11	70.83910°N 147.44356°E	I	A	10 x 25	20 - 30	42	40 - 45
KYT-12	06/08/11	70.84752°N 147.42291°E	T	A	7 x 10	40	35 - 40	45 - 50
KYT-13	06/08/11	70.84760°N 147.40939°E	NP	A	5 - 10 x 25	45	40	margin: 28 - 35
KYT-14	12/08/11	70.83120°N 147.47955°E	I	A	24.6 x 18.6	60 - 75	15 - 25	22 - 30
KYT-15	12/08/11	70.83173°N 147.47595°E	LC	A	7.7 x 8.2	20	40 - 45	50 - 60
KYT-16	13/08/11	70.84522°N 147.47943°E	LC	A	14 x 19	35	50	40
KYT-17	13/08/11	70.84276°N 147.47131°E	LC	A	8 x 6.5	30	53	65
KYT-18	15/08/11	70.81393°N 147.47542°E	I	F	15 x 7	55	20	48 - 52
KYT-19	15/08/11	70.81246°N 147.48856°E	NP	F	ca. 50	margin: 70	margin: 50	margin: 50
KYT-20	16/08/11	70.81631°N 147.47833°E	I	F	10 x 4	55	45	46 - 50
KYT-21	16/08/11	70.81596°N 147.47942°E	I	F	7 x 5.5	50	35	52
KYT-22	18/08/11	70.81786°N 147.47485°E	I	F	9.3 x 7.7	50	25	50 - 60
KYT-23	18/08/11	70.81617°N 147.47600°E	LC	F	10.3 x 8.5	50	35	51-52

Pond	Date	Coordinates	Type	Area	Size of the water body	Water depth	Thaw depth center	Thaw depth wall
KYT-24	20/08/11	70.81973°N 147.48322°E	NP	F	20 x 35 m	2 m from margin: 50 - 60	2 m from margin: 20 - 40	margin: 45 - 50
KYT-25	22/08/11	70.82465°N 147.52426°E	LC	F	10 x 12	2 m from margin: 70	2 m from margin: 40	45 - 60
KYT-26	22/08/11	70.82375°N 147.52097°E	LC	F	10 x 16	1 m from margin: 70	1 m from margin: 30	45
KYT-27	24/08/11	70.82645°N 147.47778°E	NP	Y	6.5 x 4.5	42	33	40

Tab. A 2-4: Sampling depths and hydrobiological samples of the studied ponds and lakes KYT-2 to 27.

Pond No.	Sample depth hydrochemistry (cm)	Sample depth sediments (cm)	Sample depth exhauster (cm)	Sediment	Ostracodes	Phytoplankton	Zooplankton	Makrozoobenthos (qual./quant.)	Testate amoebes	Isotopes	Hydrochemistry	Short core
KYT-2	20	50	50	x	x	x	x	x	x	x	x	/
KYT-3	20	50	50	x	x	x	x	x	x	x	x	x (2)
KYT-4	20	30	30	x	x	x	x	x	x	x	x	x
KYT-5	20	80	30 - 80	x	x	x	x	x	x	x	x	x (2)
KYT-6	15	15	15	x	x	x	x	x	x	x	x	x
KYT-7	10	29	25	x	x	x	x	x	x	x	x	x
KYT-8	15	45 - 50	45 - 50	x	x	x	x	x	x	x	x	x (2)
KYT-9	15	22	20	x	x	x	x	x	x	x	x	/
KYT-10	15	15 - 20	15	x	x	x	x	x	x	x	x	/
KYT-11	10	30	30	x	x	x	x	x	x	x	x	/
KYT-12	10	40	40	x	x	x	x	x	x	x	x	x
KYT-13	15	45	45	x	x	x	x	x	x	x	x	x
KYT-14	10	75	75	x	x	x	x	x	x	x	x	/
KYT-15	10	20	20	x	x	x	x	x	x	x	x	/
KYT-16	10	35	35	x	x	x	x	x	x	x	x	x
KYT-17	10	30	30	x	x	x	x	x	x	x	x	x
KYT-18	15	55	55	x	x	x	x	x	x	x	x	/
KYT-19	15	70	70	x	x	x	x	x	x	x	x	/
KYT-20	15	55	55	x	x	x	x	x	x	x	x	/
KYT-21	10	50	50	x	x	x	x	x	x	x	x	/
KYT-22	10	50	50	x	x	x	x	x	x	x	x	/
KYT-23	10	50	50	x	x	x	x	x	x	x	x	/
KYT-24	10	40	40	x	x	x	x	x	x	x	x	/
KYT-25	10	50	50	x	x	x	x	x	x	x	x	/
KYT-26	10	50	50	x	x	x	x	x	x	x	x	/
KYT-27	10	40	40	x	x	x	x	x	x	x	x	/

Tab. A 2-5: Physico-chemical features of the studied ponds and lakes KYT-2 to 27.

* Values for NH_4^+ , NO_3^- and PO_4^{3-} are related to the molecular weight of N and P. Negative or missing values occur from the detection limits in the spectral photometer (Hach Lange DR 2800).

Pond No.	T Air (°C)	T Water (°C)	EC (µS/cm)	pH (wtw)	* NH_4^+ (mg/l)	* NO_3^- (mg/l)	* PO_4^{3-} (mg/l)	O_2 (mg/l)	Alkalinity (mmol/l)	Acidity (mmol/l)	total hardness (°dH)
Detection limit					0.015 mg/l	0.23 mg/l	0.05 mg/l				
KYT-2	25.0	19.5	53	5.6	0.003	0.402	0.286	7.0	0.8	0.4	1.5 (0.2 mmol/l)
KYT-3	12.6	14.8	23	5.5	0.024	0.188	0.044	10.0	0.3	0.4	2.5 (0.4 mmol/l)
KYT-4	11.8	16.1	20	5.6	0.045	0.245	0.010	8.2	0.2	0.4	3 (0.5 mmol/l)
KYT-5	7.5	8.6	25	6.4	0.048	0.523	0.012	8.2	0.4	0.4	3.0 (0.5 mmol)
KYT-6	18.0	23.5	153	6.4	0.041	0.118	no data	7.6	1.6	0.4	4.2 (0.6 mmol/l)
KYT-7	19.1	21.9	21	6.8	0.028	0.730	no data	6.6	0.2	0.4	3.0 (0.5 mmol)
KYT-8	7.3	8.5	34	6.7	0.042	0.518	0.067	8.4	0.4	0.4	3.5 (0.6 mmol/l)
KYT-9	18.0	8.9	28	6.2	0.030	0.792	0.013	6.4	0.4	0.4	2.5 (0.4 mmol/l)
KYT-10	16.5	11.8	36	6.2	0.023	0.776	0.021	5.4	0.4	0.6	2.5 (0.4 mmol/l)
KYT-11	18.5	13.4	42	6.3	0.029	0.563	0.010	8.6	0.4	0.6	4.0 (0.6 mmol/l)
KYT-12	16.7	13.9	20	6.4	0.006	0.303	0.014	8.8	0.4	0.4	3.0 (0.4 mmol/l)
KYT-13	16.2	13.9	23	6.3	0.005	0.341	0.013	6.2	0.4	0.4	3.0 (0.4 mmol/l)
KYT-14	6.7	7.2	28	5.8	0.128	0.621	no data	7.2	0.4	0.4	5.5 (0.8 mmol/l)
KYT-15	6.4	9.0	31	5.8	0.003	0.681	0	9.6	0.4	0.4	3.0 (0.5 mmol)
KYT-16	8.2	9.0	22	6.2	0.019	0.710	0.003	8.6	0.6	0.4	5.0 (0.8 mmol/l)
KYT-17	7.8	10.6	31	6.4	0.004	0.170	0	10.0	0.4	0.4	5.0 (0.8 mmol/l)
KYT-18	9.9	8.1	29	6.3	0.002	0.358	0.002	10.0	0.4	0.4	4.5 (0.8 mmol/l)
KYT-19	no data	10.6	61	6.6	<0.004	0.220	0.039	11.6	0.8	0.4	7.5 (1.3 mmol/l)
KYT-20	11.5	8.1	22	6.2	0.003	0.518	0.035	9.4	0.4	0.4	4.0 (0.7 mmol/l)
KYT-21	12.1	10.2	19	6.3	0.034	0.428	0.079	8.6	0.4	0.4	3.5 (0.6 mmol/l)
KYT-22	13.6	10.0	29	6.5	0.033	0.170	no data	8.8	0.4	0.4	4.0 (0.7 mmol/l)
KYT-23	12.4	10.0	35	6.7	0.023	0.203	no data	9.4	0.4	0.4	4.0 (0.7 mmol/l)

Pond No.	T Air (°C)	T Water (°C)	EC (µS/cm)	pH (wtw)	*NH ₄ ⁺ (mg/l)	*NO ₃ ⁻ (mg/l)	*PO ₄ ³⁻ (mg/l)	O ₂ (mg/l)	Alkalinity (mmol/l)	Acidity (mmol/l)	total hardness (°dH)
Detection limit					0.015 mg/l	0.23 mg/l	0.05 mg/l				
KYT-24	7.1	10.6	44	6.6	0.012	0.181	no data	9.2	0.8	0.4	5.0 (0.8 mmol/l)
KYT-25	5.2	6.0	37	7.0	0.027	0.042	0	11.8	0.6	0.4	6.5 (1.2 mmol/l)
KYT-26	5.0	5.5	28	7.1	0.022	0.264	0.055	10.0	1.0	0.4	6.5 (1.2 mmol/l)
KYT-27	5.8	7.8	20	6.3	0.025	0.524	0	10.0	0.4	0.4	3.5 (0.6 mmol/l)

APPENDIX 3 - LIST OF PLANT TAXA (VEGETATION TRANSECT KYT-1)

Andrea Schneider

Tab. A 3-1: Plant taxa at the single positions in the vegetation transect across the monitoring site KYT-1 at 09/08/2011 (Fig. 3-16), surface cover and cover in percent per taxa after Londo (1976).

Position	Surface	%	Taxa	Cover (%)	Thaw depth (cm)
1	Cover total	90	Moss total	75	58.5
	Water	10	<i>Eriophorum angustifolium</i>	30	
	Litter	10	<i>Carex aquatilis</i> ssp. <i>stans</i>	5	
			<i>Poaceae</i>	3	
			<i>Potentilla palustris</i>	0.1	
			<i>Vaccinium vitis-idaea</i>	0.1	
			<i>Caltha palustris</i>	0.1	
			Lichen total	0	
2	Cover total	100	<i>Vaccinium vitis-idaea</i>	40	32
	Water	0	Moss total	40	
	Litter	10	<i>Ledum palustre</i>	30	
			Lichen total	20.1	
			<i>Betula nana</i>	20	
			<i>Carex aquatilis</i> ssp. <i>stans</i>	5	
			<i>Poaceae</i>	5	
			<i>Eriophorum vaginatum</i>	3	
3	Cover total	90	Moss total	100	35
	Water	10	<i>Carex aquatilis</i> ssp. <i>stans</i>	20	
	Litter	10	<i>Salix</i> sp.	15	
			<i>Ledum palustre</i>	10	
			<i>Potentilla palustris</i>	3	
			<i>Vaccinium vitis-idaea</i>	1	
			<i>Carex chordorrhizza</i>	1	
			<i>Betula nana</i>	0.1	
Lichen total	0				
4	Cover total		Moss total	10	49.5
	Water	100	<i>Carex aquatilis</i> ssp. <i>stans</i>	5	
	Litter	0	<i>Potentilla palustris</i>	0.1	
			Lichen total	0	
5	Cover total		Moss total	20	63
	Water	100	<i>Carex aquatilis</i> ssp. <i>stans</i>	10	
	Litter	0	Lichen total	0	

Position	Surface	%	Taxa	Cover (%)	Thaw depth (cm)
6	Cover total		Moss total	80	64
	Water	100	<i>Eriophorum angustifolium</i>	30	
	Litter	0	<i>Carex aquatilis</i> ssp. <i>stans</i>	10	
			<i>Salix</i> sp.	3	
			<i>Potentilla palustris</i>	0.1	
			Lichen total	0	
7	Cover total	90	Moss total	100	48
	Water	10	<i>Eriophorum angustifolium</i>	30	
	Litter	10	<i>Carex aquatilis</i> ssp. <i>stans</i>	10	
			<i>Salix</i> sp.	5	
			<i>Betula nana</i>	1	
			<i>Potentilla palustris</i>	1	
			Lichen total	0	
8	Cover total	100	<i>Betula nana</i>	50	27.5
	Water	0	Moss total	37	
	Litter	10	<i>Vaccinium vitis-idaea</i>	20	
			Lichen total	5.1	
			<i>Poaceae</i>	3	
			<i>Carex aquatilis</i> ssp. <i>stans</i>	3	
9	Cover total	100	<i>Betula nana</i>	60	33
	Water	0	Moss total	48	
	Litter	10	<i>Ledum palustre</i>	30	
			<i>Salix</i> cf. <i>myrtiloides</i>	3	
			Lichen total	2	
10	Cover total	100	<i>Betula nana</i>	90	26.5
	Water	0	Moss total	15	
	Litter	20	<i>Poaceae</i>	3	
			<i>Salix</i> sp.	1	
			Lichen total	0	
11	Cover total	80	<i>Betula nana</i>	50	33.5
	Water	20	Moss total	42	
	Litter	20	<i>Eriophorum angustifolium</i>	30	
			<i>Salix</i> sp.	1	
			Lichen total	0	
12	Cover total	90	<i>Eriophorum angustifolium</i>	50	47.5
	Water	10	Moss total	26	
	Litter	20	<i>Salix</i> sp.	1	
			Lichen total	0.1	

Position	Surface	%	Taxa	Cover (%)	Thaw depth (cm)
13	Cover total	100	Moss total	100	48
	Water	0	<i>Eriophorum angustifolium</i>	30	
	Litter	10	<i>Potentilla palustris</i>	20	
			<i>Salix</i> sp.	1	
			<i>Hierochloe</i> sp.	0.1	
			<i>Luzula</i> sp.	0.1	
			Lichen total	0	
14	Cover total	80	Moss total	55	44
	Water	20	<i>Potentilla palustris</i>	40	
	Litter	0	<i>Eriophorum angustifolium</i>	20	
			<i>Carex aquatilis</i> ssp. <i>stans</i>	5	
			<i>Betula nana</i>	3	
			<i>Salix</i> sp.	1	
			Lichen total	0	
15	Cover total	100	Moss total	76	37
	Water	0	<i>Betula nana</i>	30	
	Litter	10	<i>Potentilla palustris</i>	3	
			<i>Carex aquatilis</i> ssp. <i>stans</i>	3	
			Lichen total	1	
16	Cover total	100	<i>Betula nana</i>	90	31.5
	Water	0	Moss total	22	
	Litter	10	<i>Ledum palustre</i>	20	
			<i>Salix</i> sp.	3	
			<i>Poaceae</i>	3	
			Lichen total	2	
			<i>Eriophorum vaginatum</i>	1	
			<i>Pyrola rotundifolia</i>	1	

APPENDIX 4 - LIST OF MOSS AND LICHEN SAMPLES

Andrea Schneider

Sample code	Location*	Coordinates	Date	Associated vegetation	Thaw depth (cm)	Remarks
KYT R-1	KYT-27 (Yedomas)	70.82645°N 147.47778°E	24/08 /2011	<i>Betula nana</i> , <i>Carex aquatilis</i> ssp. <i>stans</i> , <i>Eriophorum vaginatum</i> , <i>Ledum palustre</i> , <i>Pedicularis lapponicus</i> , <i>Rubus chamaemorus</i> , <i>Salix</i> sp., <i>Sphagnum</i> spp., <i>Vaccinium vitis-idaea</i>	40	
KYT R-2	Monitoring site	70.83121°N 147.48299 °E	05/08 /2011	<i>Betula nana</i> , <i>Ledum palustre</i> , <i>Salix</i> cf. <i>myrtilloides</i>	33	
KYT R-3	KYT-27 (Yedomas)	70.82645°N 147.47778°E	24/08 /2011	<i>Betula nana</i> , <i>Carex aquatilis</i> ssp. <i>stans</i> , <i>Eriophorum vaginatum</i> , <i>Ledum palustre</i> , <i>Pedicularis lapponicus</i> , <i>Rubus chamaemorus</i> , <i>Salix</i> sp., <i>Sphagnum</i> spp., <i>Vaccinium vitis-idaea</i>	40	Re-named sample (formerly KYT R-5 which was twice)
KYT R-4	KYT-27 (Yedomas)	70.82645°N 147.47778°E	24/08 /2011	<i>Betula nana</i> , <i>Carex aquatilis</i> ssp. <i>stans</i> , <i>Eriophorum vaginatum</i> , <i>Ledum palustre</i> , <i>Pedicularis lapponicus</i> , <i>Rubus chamaemorus</i> , <i>Salix</i> sp., <i>Sphagnum</i> spp., <i>Vaccinium vitis-idaea</i>	40	
KYT R-5	Monitoring site	70.83121°N 147.48299 °E	05/08 /2011	<i>Betula nana</i> , <i>Ledum palustre</i> , <i>Salix</i> cf. <i>myrtilloides</i>	33	
KYT R-6	Monitoring site (1)	70.83121°N 147.48299 °E	09/08 /2011	<i>Caltha palustris</i> , <i>Carex aquatilis</i> ssp. <i>stans</i> , <i>Eriophorum angustifolium</i> , <i>Poaceae</i> , <i>Potentilla palustris</i> , <i>Vaccinium vitis-idaea</i>	58.5	<i>Sphagnum</i> sp., cover 0.1%
KYT R-7	Monitoring site	70.83121°N 147.48299 °E	05/08 /2011	<i>Betula nana</i> , <i>Carex aquatilis</i> ssp. <i>stans</i> , <i>Eriophorum vaginatum</i> , <i>Ledum palustre</i> , <i>Poaceae</i> , <i>Vaccinium vitis-idaea</i>	32	
KYT R-8	Floodplain		14/08 /2011	<i>Betula nana</i> , <i>Carex</i> spp., <i>Eriophorum vaginatum</i> , <i>Salix</i> sp., <i>Pyrola rotundifolia</i>	42-49	ca. 1000m in the E of the station
KYT R-9	Floodplain		14/08 /2011	<i>Betula nana</i> , <i>Carex</i> spp., <i>Eriophorum vaginatum</i> , <i>Salix</i> sp., <i>Pyrola rotundifolia</i>	42-49	ca. 1000m in the E of the station
KYT R-10	Kytalyk field station	70.4928°N 147.2923°E	09/08 /2011	<i>Carex</i> spp., <i>Eriophorum vaginatum</i> , <i>Poaceae</i> , <i>Rubus chamaemorus</i> , <i>Salix</i> sp.	42-49	
KYT R-11	Floodplain		14/08 /2011	<i>Betula nana</i> , <i>Carex</i> spp., <i>Eriophorum vaginatum</i> , <i>Salix</i> sp., <i>Pyrola rotundifolia</i>	42-49	ca. 1000m in the E of the station
KYT R-12	KYT-16 (Alas)	70.84522°N 147.47943°E	13/08 /2011	<i>Caltha palustris</i> , <i>Carex aquatilis</i> ssp. <i>stans</i> , <i>Carex chordorrhiza</i> , <i>Eriophorum angustifolium</i> , <i>Ledum</i>	40	

Sample code	Location*	Coordinates	Date	Associated vegetation	Thaw depth (cm)	Remarks
				<i>palustre</i> , <i>Pedicularis</i> cf. <i>lapponicus</i> , <i>Poaceae</i> , <i>Potentilla palustris</i> , <i>Salix</i> sp., <i>Sphagnum</i> spp., <i>Vaccinium vitis-idaea</i>		
KYT R-13	KYT-16 (Alas)	70.84522°N 147.47943°E	13/08 /2011	<i>Caltha palustris</i> , <i>Carex aquatilis</i> ssp. <i>stans</i> , <i>Carex chordorrhizza</i> , <i>Eriophorum angustifolium</i> , <i>Ledum palustre</i> , <i>Pedicularis</i> cf. <i>lapponicus</i> , <i>Poaceae</i> , <i>Potentilla palustris</i> , <i>Salix</i> sp., <i>Sphagnum</i> spp., <i>Vaccinium vitis-idaea</i>	40	
KYT R-14						Missing sample
KYT R-15	KYT-16 (Alas)	70.84522°N 147.47943°E	13/08 /2011	<i>Caltha palustris</i> , <i>Carex aquatilis</i> ssp. <i>stans</i> , <i>Carex chordorrhizza</i> , <i>Eriophorum angustifolium</i> , <i>Ledum palustre</i> , <i>Pedicularis</i> cf. <i>lapponicus</i> , <i>Poaceae</i> , <i>Potentilla palustris</i> , <i>Salix</i> sp., <i>Sphagnum</i> spp., <i>Vaccinium vitis-idaea</i>	40	
KYT R-16						Missing sample
KYT R-17	KYT-16 (Alas)	70.84522°N 147.47943°E	13/08 /2011	<i>Caltha palustris</i> , <i>Carex aquatilis</i> ssp. <i>stans</i> , <i>Carex chordorrhizza</i> , <i>Eriophorum angustifolium</i> , <i>Ledum palustre</i> , <i>Pedicularis</i> cf. <i>lapponicus</i> , <i>Poaceae</i> , <i>Potentilla palustris</i> , <i>Salix</i> sp., <i>Sphagnum</i> spp., <i>Vaccinium vitis-idaea</i>	40	
KYT R-18	KYT-15 (Alas)	70.83173°N 147.47595°E	12/08 /2011	<i>Andromeda polifolia</i> , <i>Betula nana</i> , <i>Carex aquatilis</i> ssp. <i>stans</i> , <i>C. chordorrhizza</i> , <i>C. rotundata</i> , <i>Pedicularis</i> cf. <i>lapponicus</i> , <i>Polygonum viviparum</i> , <i>Utricularia ochroleuca</i> , <i>Salix</i> sp., <i>Sphagnum squarrosum</i> , <i>Sphagnum</i> spp., <i>Vaccinium vitis-idaea</i>	50-60	
KYT R-19	KYT-12 (Alas)	70.84752°N 147.42291°E	06/08 /2011	<i>Carex aquatilis</i> ssp. <i>stans</i> , <i>Eriophorum angustifolium</i> , <i>Potentilla palustris</i> , <i>Sphagnum</i> spp., <i>Salix</i> sp.	45-50	
KYT R-20	Monitoring site	70.83121°N 147.48299 °E	05/08 /2011	<i>Betula nana</i> , <i>Carex aquatilis</i> ssp. <i>stans</i> , <i>Carex chordorrhizza</i> , <i>Potentilla palustris</i> , <i>Ledum palustre</i> , <i>Salix</i> sp., <i>Vaccinium vitis-idaea</i>	35	
KYT R-21	Monitoring site (16)	70.83121°N 147.48299 °E	09/08 /2011	<i>Betula nana</i> , <i>Eriophorum vaginatum</i> , <i>Ledum palustre</i> , <i>Poaceae</i> , <i>Pyrola rotundifolia</i> , <i>Salix</i> sp.	31.5	Moos XII, cover 3%

Sample code	Location*	Coordinates	Date	Associated vegetation	Thaw depth (cm)	Remarks
KYT R-22	Monitoring site (16)	70.83121°N 147.48299 °E	09/08 /2011	<i>Betula nana</i> , <i>Eriophorum vaginatum</i> , <i>Ledum palustre</i> , <i>Poaceae</i> , <i>Pyrola rotundifolia</i> , <i>Salix</i> sp.	31.5	Lichen, cover 3%
KYT R-23	Monitoring site (7)	70.83121°N 147.48299 °E	09/08 /2011	<i>Betula nana</i> , <i>Carex aquatilis</i> ssp. <i>stans</i> , <i>Eriophorum angustifolium</i> , <i>Potentilla palustris</i> , <i>Salix</i> sp.	48	Moos I, cover 1%
KYT R-24						Missing sample
KYT R-25	Monitoring site (16)	70.83121°N 147.48299 °E	09/08 /2011	<i>Betula nana</i> , <i>Eriophorum vaginatum</i> , <i>Ledum palustre</i> , <i>Poaceae</i> , <i>Pyrola rotundifolia</i> , <i>Salix</i> sp.	31.5	Moos XIII, cover 3%
KYT R-26	Monitoring site (11)	70.83121°N 147.48299 °E	09/08 /2011	<i>Betula nana</i> , <i>Eriophorum angustifolium</i> , <i>Salix</i> sp.	33.5	Moos X, cover 10%
KYT R-27	Monitoring site (8)	70.83121°N 147.48299 °E	09/08 /2011	<i>Betula nana</i> , <i>Carex aquatilis</i> ssp. <i>stans</i> , <i>Poaceae</i> , <i>Vaccinium vitis-idaea</i>	27.5	Moss V, cover 30%
KYT R-28	Monitoring site (8)	70.83121°N 147.48299 °E	09/08 /2011	<i>Betula nana</i> , <i>Carex aquatilis</i> ssp. <i>stans</i> , <i>Poaceae</i> , <i>Vaccinium vitis-idaea</i>	27.5	Moss II, cover 1%
KYT R-29	Floodplain		14/08 /2011	<i>Betula nana</i> , <i>Carex</i> spp., <i>Eriophorum vaginatum</i> , <i>Salix</i> sp., <i>Pyrola rotundifolia</i>	42-49	ca. 1000m in the E of the station
KYT R-30	Monitoring site	70.83121°N 147.48299 °E	09/08 /2011			<i>Sphagnum</i> sp.
KYT R-31	Monitoring site (9)	70.83121°N 147.48299 °E	09/08 /2011	<i>Betula nana</i> , <i>Ledum palustre</i> , <i>Salix</i> cf. <i>myrtilloides</i>	33	Moss VI, cover 20%
KYT R-32	Monitoring site (1)	70.83121°N 147.48299 °E	09/08 /2011	<i>Caltha palustris</i> , <i>Carex aquatilis</i> ssp. <i>stans</i> , <i>Eriophorum angustifolium</i> , <i>Poaceae</i> , <i>Potentilla palustris</i> , <i>Vaccinium vitis-idaea</i>	58.5	<i>Sphagnum</i> sp., cover 3%
KYT R-33	Monitoring site (1)	70.83121°N 147.48299 °E	09/08 /2011	<i>Caltha palustris</i> , <i>Carex aquatilis</i> ssp. <i>stans</i> , <i>Eriophorum angustifolium</i> , <i>Poaceae</i> , <i>Potentilla palustris</i> , <i>Vaccinium vitis-idaea</i>	58.5	<i>Sphagnum</i> sp., cover 70%
KYT R-34	Monitoring site (2)	70.83121°N 147.48299 °E	09/08 /2011	<i>Betula nana</i> , <i>Carex aquatilis</i> ssp. <i>stans</i> , <i>Eriophorum vaginatum</i> , <i>Ledum palustre</i> , <i>Poaceae</i> , <i>Vaccinium vitis-idaea</i>	32	Lichen, cover 20%
KYT R-35	Monitoring site (2)	70.83121°N 147.48299 °E	09/08 /2011	<i>Betula nana</i> , <i>Carex aquatilis</i> ssp. <i>stans</i> , <i>Eriophorum vaginatum</i> , <i>Ledum palustre</i> , <i>Poaceae</i> , <i>Vaccinium vitis-idaea</i>	32	<i>Aulacomnium</i> ?, cover 20%
KYT R-36	Monitoring site (2)	70.83121°N 147.48299 °E	09/08 /2011	<i>Betula nana</i> , <i>Carex aquatilis</i> ssp. <i>stans</i> , <i>Eriophorum vaginatum</i> , <i>Ledum palustre</i> , <i>Poaceae</i> , <i>Vaccinium vitis-idaea</i>	32	<i>Stephanocladus</i> ?, cover 30%

Sample code	Location*	Coordinates	Date	Associated vegetation	Thaw depth (cm)	Remarks
KYT R-37	Monitoring site (8)	70.83121°N 147.48299 °E	09/08 /2011	<i>Betula nana</i> , <i>Carex aquatilis</i> ssp. <i>stans</i> , <i>Poaceae</i> , <i>Vaccinium vitis-idaea</i>	27.5	Moss III, cover 1%
KYT R-38	Monitoring site (8)	70.83121°N 147.48299 °E	09/08 /2011	<i>Betula nana</i> , <i>Carex aquatilis</i> ssp. <i>stans</i> , <i>Poaceae</i> , <i>Vaccinium vitis-idaea</i>	27.5	Moss IV, cover 10%
KYT R-39	KYT-17 (Alas)	70.84276°N 147.47131°E	13/08 /2011	<i>Andromeda polifolia</i> , <i>Betula nana</i> , <i>Carex aquatilis</i> ssp. <i>stans</i> , <i>Carex chordorrhizza</i> , <i>Eriophorum angustifolium</i> , <i>Pedicularis</i> cf. <i>lapponicus</i> , <i>Polygonum viviparum</i> , <i>Potentilla palustris</i> , <i>Ranunculus pallasii</i> , <i>Salix</i> sp.	65	10 cm below water surface
KYT R-40	KYT-15 (Alas)	70.83173°N 147.47595°E	12/08 /2011	<i>Andromeda polifolia</i> , <i>Betula nana</i> , <i>Carex aquatilis</i> ssp. <i>stans</i> , <i>C. chordorrhizza</i> , <i>C. rotundata</i> , <i>Pedicularis</i> cf. <i>lapponicus</i> , <i>Polygonum viviparum</i> , <i>Utricularia ochroleuca</i> , <i>Salix</i> sp., <i>Sphagnum squarrosum</i> , <i>Sphagnum</i> spp., <i>Vaccinium vitis-idaea</i>	50-60	
KYT R-41	KYT-13 (Alas)	70.84760°N 147.40939°E	06/08 /2011	<i>Betula nana</i> , <i>Eriophorum angustifolium</i> , <i>Eriophorum vaginatum</i> , <i>Ledum palustre</i>	28-35	
KYT R-42	KYT-16 (Alas)	70.84522°N 147.47943°E	13/08 /2011	<i>Caltha palustris</i> , <i>Carex aquatilis</i> ssp. <i>stans</i> , <i>Carex chordorrhizza</i> , <i>Eriophorum angustifolium</i> , <i>Ledum palustre</i> , <i>Pedicularis</i> cf. <i>lapponicus</i> , <i>Poaceae</i> , <i>Potentilla palustris</i> , <i>Salix</i> sp., <i>Sphagnum</i> spp., <i>Vaccinium vitis-idaea</i>	40	Polytrichum?
KYT R-43	KYT-27 (Yedomas)	70.82645°N 147.47778°E	24/08 /2011	<i>Betula nana</i> , <i>Carex aquatilis</i> ssp. <i>stans</i> , <i>Eriophorum vaginatum</i> , <i>Ledum palustre</i> , <i>Pedicularis lapponicus</i> , <i>Rubus chamaemorus</i> , <i>Salix</i> sp., <i>Sphagnum</i> spp., <i>Vaccinium vitis-idaea</i>	40	
KYT R-44	Monitoring site		05/08 /2011	<i>Carex aquatilis</i> ssp. <i>stans</i> , <i>Potentilla palustris</i>	49.5	
KYT R-45	Monitoring site (9)	70.83121°N 147.48299 °E	09/08 /2011	<i>Betula nana</i> , <i>Ledum palustre</i> , <i>Salix</i> cf. <i>myrtilloides</i>	33	
KYT R-46	Monitoring site (12)	70.83121°N 147.48299 °E	09/08 /2011	<i>Eriophorum angustifolium</i> , <i>Salix</i> sp.	47.5	Lichen, cover 0.1%
KYT R-47	Monitoring site (9)	70.83121°N 147.48299 °E	09/08 /2011	<i>Betula nana</i> , <i>Ledum palustre</i> , <i>Salix</i> cf. <i>myrtilloides</i>	33	Lichen, cover 1%
KYT R-48	Monitoring site (11)	70.83121°N 147.48299 °E	09/08 /2011	<i>Betula nana</i> , <i>Eriophorum angustifolium</i> , <i>Salix</i> sp.	33.5	Moss VIII, cover 3%
KYT R-49	Monitoring site (11)	70.83121°N 147.48299 °E	09/08 /2011	<i>Betula nana</i> , <i>Eriophorum angustifolium</i> , <i>Salix</i> sp.	33.5	Moss IX, cover 5%

Sample code	Location*	Coordinates	Date	Associated vegetation	Thaw depth (cm)	Remarks
KYT R-50	KYT-27 (Yedomas)	70.82645°N 147.47778°E	24/08 /2011	<i>Betula nana</i> , <i>Carex aquatilis</i> ssp. <i>stans</i> , <i>Eriophorum vaginatum</i> , <i>Ledum palustre</i> , <i>Pedicularis lapponicus</i> , <i>Rubus chamaemorus</i> , <i>Salix</i> sp., <i>Sphagnum</i> spp., <i>Vaccinium vitis-idaea</i>	40	
KYT R-51	Monitoring site	70.83121°N 147.48299 °E	05/08 /2011	<i>Betula nana</i> , <i>Carex aquatilis</i> ssp. <i>stans</i> , <i>Eriophorum vaginatum</i> , <i>Ledum palustre</i> , <i>Poaceae</i> , <i>Vaccinium vitis-idaea</i>	32	
KYT R-52	Monitoring site	70.83121°N 147.48299 °E	05/08 /2011	<i>Betula nana</i> , <i>Carex aquatilis</i> ssp. <i>stans</i> , <i>Eriophorum vaginatum</i> , <i>Ledum palustre</i> , <i>Poaceae</i> , <i>Vaccinium vitis-idaea</i>	32	
KYT R-53	Monitoring site	70.83121°N 147.48299 °E	05/08 /2011	<i>Betula nana</i> , <i>Carex aquatilis</i> ssp. <i>stans</i> , <i>Poaceae</i> , <i>Vaccinium vitis-idaea</i>	27.5	
KYT R-54	KYT-27 (Yedomas)	70.82645°N 147.47778°E	24/08 /2011	<i>Betula nana</i> , <i>Carex aquatilis</i> ssp. <i>stans</i> , <i>Eriophorum vaginatum</i> , <i>Ledum palustre</i> , <i>Pedicularis lapponicus</i> , <i>Rubus chamaemorus</i> , <i>Salix</i> sp., <i>Sphagnum</i> spp., <i>Vaccinium vitis-idaea</i>	40	
KYT R-55	Floodplain		14/08 /2011	<i>Betula nana</i> , <i>Carex</i> spp., <i>Eriophorum vaginatum</i> , <i>Salix</i> sp., <i>Pyrola rotundifolia</i>	42- 49	ca. 1000m in the E of the station
KYT R-56	Monitoring site	70.83121°N 147.48299 °E	05/08 /2011	<i>Betula nana</i> , <i>Carex aquatilis</i> ssp. <i>stans</i> , <i>Eriophorum vaginatum</i> , <i>Ledum palustre</i> , <i>Poaceae</i> , <i>Vaccinium vitis-idaea</i>	32	
KYT R-57	KYT-27 (Yedomas)	70.82645°N 147.47778°E	24/08 /2011	<i>Betula nana</i> , <i>Carex aquatilis</i> ssp. <i>stans</i> , <i>Eriophorum vaginatum</i> , <i>Ledum palustre</i> , <i>Pedicularis lapponicus</i> , <i>Rubus chamaemorus</i> , <i>Salix</i> sp., <i>Sphagnum</i> spp., <i>Vaccinium vitis-idaea</i>	40	
KYT R-58	Kytalyk field station	70.4928°N 147.2923°E	25/08 /2011	<i>Carex</i> spp., <i>Eriophorum vaginatum</i> , <i>Poaceae</i> , <i>Rubus chamaemorus</i> , <i>Salix</i> sp.		
KYT R-59	Kytalyk field station	70.4928°N 147.2923°E	25/08 /2011	<i>Carex</i> spp., <i>Eriophorum vaginatum</i> , <i>Poaceae</i> , <i>Rubus chamaemorus</i> , <i>Salix</i> sp.		
KYT R-60	KYT-17 (Alas)	70.84276°N 147.47131°E	13/08 /2011	<i>Andromeda polifolia</i> , <i>Betula nana</i> , <i>Carex aquatilis</i> ssp. <i>stans</i> , <i>Carex chordorrhiza</i> , <i>Eriophorum angustifolium</i> , <i>Pedicularis</i> cf. <i>lapponicus</i> , <i>Polygonum viviparum</i> , <i>Potentilla palustris</i> , <i>Ranunculus pallasii</i> , <i>Salix</i> sp.	40	
KYT R-61	Monitoring site (2)	70.83121°N 147.48299 °E	09/08 /2011	<i>Betula nana</i> , <i>Carex aquatilis</i> ssp. <i>stans</i> , <i>Eriophorum vaginatum</i> ,	32	Lichen, cover 0,1%

Sample code	Location*	Coordinates	Date	Associated vegetation	Thaw depth (cm)	Remarks
				<i>Ledum palustre</i> , <i>Poaceae</i> , <i>Vaccinium vitis-idaea</i>		
KYT R-62	KYT-27 (Yedoma)	70.82645°N 147.47778°E	24/08 /2011	<i>Betula nana</i> , <i>Carex aquatilis</i> ssp. <i>stans</i> , <i>Eriophorum vaginatum</i> , <i>Ledum palustre</i> , <i>Pedicularis lapponicus</i> , <i>Rubus chamaemorus</i> , <i>Salix</i> sp., <i>Sphagnum</i> spp., <i>Vaccinium vitis-idaea</i>	40	Submerged growing moss
KYT R-63	Monitoring site (15)	70.83121°N 147.48299 °E	09/08 /2011	<i>Betula nana</i> , <i>Carex aquatilis</i> ssp. <i>stans</i> , <i>Potentilla palustris</i>	37	Moss XI, cover 40%
KYT R-64	KYT-17 (Alas)	70.84276°N 147.47131°E	13/08 /2011	<i>Andromeda polifolia</i> , <i>Betula nana</i> , <i>Carex aquatilis</i> ssp. <i>stans</i> , <i>Carex chordorrhizza</i> , <i>Eriophorum angustifolium</i> , <i>Pedicularis</i> cf. <i>lapponicus</i> , <i>Polygonum viviparum</i> , <i>Potentilla palustris</i> , <i>Ranunculus pallasii</i> , <i>Salix</i> sp.	65	
KYT R-65	Floodplain		14/08 /2011	<i>Betula nana</i> , <i>Carex</i> spp., <i>Eriophorum vaginatum</i> , <i>Salix</i> sp., <i>Pyrola rotundifolia</i>	42- 49	ca. 1000m in the E of the station
KYT R-66	KYT-27 (Yedoma)	70.82645°N 147.47778°E	24/08 /2011	<i>Betula nana</i> , <i>Carex aquatilis</i> ssp. <i>stans</i> , <i>Eriophorum vaginatum</i> , <i>Ledum palustre</i> , <i>Pedicularis lapponicus</i> , <i>Rubus chamaemorus</i> , <i>Salix</i> sp., <i>Sphagnum</i> spp., <i>Vaccinium vitis-idaea</i>	40	
KYT R-67	KYT-27 (Yedoma)	70.82645°N 147.47778°E	24/08 /2011	<i>Betula nana</i> , <i>Carex aquatilis</i> ssp. <i>stans</i> , <i>Eriophorum vaginatum</i> , <i>Ledum palustre</i> , <i>Pedicularis lapponicus</i> , <i>Rubus chamaemorus</i> , <i>Salix</i> sp., <i>Sphagnum</i> spp., <i>Vaccinium vitis-idaea</i>	40	Submerged, 10 cm below water surface
KYT R-68	Floodplain		14/08 /2011	<i>Betula nana</i> , <i>Carex</i> spp., <i>Eriophorum vaginatum</i> , <i>Salix</i> sp., <i>Pyrola rotundifolia</i>	42- 49	ca. 1000m in the E of the station
KYT R-69	Floodplain		14/08 /2011	<i>Betula nana</i> , <i>Carex</i> spp., <i>Eriophorum vaginatum</i> , <i>Salix</i> sp., <i>Pyrola rotundifolia</i>	42- 49	ca. 1000m in the E of the station
KYT R-70	Floodplain		14/08 /2011	<i>Betula nana</i> , <i>Carex</i> spp., <i>Eriophorum vaginatum</i> , <i>Salix</i> sp., <i>Pyrola rotundifolia</i>	42- 49	ca. 1000m in the E of the station
KYT R-71	Floodplain		14/08 /2011	<i>Betula nana</i> , <i>Carex</i> spp., <i>Eriophorum vaginatum</i> , <i>Salix</i> sp., <i>Pyrola rotundifolia</i>	42- 49	ca. 1000m in the E of the station
KYT R-72	Floodplain		14/08 /2011	<i>Betula nana</i> , <i>Carex</i> spp., <i>Eriophorum vaginatum</i> , <i>Salix</i> sp., <i>Pyrola rotundifolia</i>	42- 49	ca. 1000m in the E of the station
KYT R-73	Floodplain		15/08 /2011	<i>Betula nana</i> , <i>Carex</i> spp., <i>Eriophorum vaginatum</i> , <i>Salix</i> sp., <i>Pyrola rotundifolia</i>	42- 49	ca. 1000m in the E of the station

Sample code	Location*	Coordinates	Date	Associated vegetation	Thaw depth (cm)	Remarks
KYT R-74	Floodplain		15/08 /2011	<i>Betula nana</i> , <i>Carex</i> spp., <i>Eriophorum vaginatum</i> , <i>Salix</i> sp., <i>Pyrola rotundifolia</i>	42-49	ca. 1000m in the E of the station
KYT R-75	Monitoring site (8)	70.83121°N 147.48299 °E	09/08 /2011	<i>Betula nana</i> , <i>Carex aquatilis</i> ssp. <i>stans</i> , <i>Poaceae</i> , <i>Vaccinium vitis-idaea</i>	27.5	Lichen, cover 0,1%

APPENDIX 5 - PLANT COLLECTION AND PEAT CORES FROM LHC-11

Annette Teltewskoi

Tab. A 5-1: List of plant collection from the model polygon LHC 11

No	Layer	Species	Family	Herbarium	Species of the study site	Reference material
1	herb	<i>Arctagrostis latifolia</i>	Poaceae	1	1	
2	herb	<i>Bistorta major</i>	Polygonaceae	2		
3	herb	<i>Bistorta viviparum</i>	Polygonaceae	3		
4	herb	<i>Caltha palustris</i>	Ranunculaceae	4	2	
5	herb	<i>Carex chordorrhiza</i>	Cyperaceae	5	3	1
6	herb	<i>Carex concolor (Carex aquatilis ssp. stans)</i>	Cyperaceae	6	4	2
7	herb	<i>Carex rotundata</i>	Cyperaceae	7	5	3
8	herb	<i>Carex sp. *</i>	Cyperaceae	8		4
9	herb	<i>Comarum palustre</i>	Rosaceae	9	6	
10	herb	<i>Dryas octopetala</i>	Rosaceae	10		
11	herb	<i>Eriophorum angustifolium</i>	Cyperaceae	11	7	5
12	herb	<i>Eriophorum vaginatum</i>	Cyperaceae	12	8	6
13	herb	<i>Glyceria declinata</i>	Poaceae	13		
14	herb	<i>Hierochloë pauciflora</i>	Poaceae	14	9	
15	herb	<i>Pedicularis lapponica</i>	Scrophulariaceae	15	10	
16	herb	<i>Pedicularis sp.</i>	Scrophulariaceae	16	11	
17	herb	<i>Pedicularis sp.</i>	Scrophulariaceae	17	12	
18	herb	<i>Poaceae*</i>	Poaceae	18	13	
19	herb	<i>Pyrola rotundifolia</i>	Pyrolaceae	19		
20	herb	<i>Ranunculus lapponicus</i>	Ranunculaceae	20		
21	herb	<i>Ranunculus pallasii</i>	Ranunculaceae	21		
22	herb	<i>Rumex arcticus</i>	Polygonaceae	22	14	
23	herb	<i>Saxifraga cernua</i>	Saxifragaceae	23	15	
24	herb	<i>Saxifraga hirculus</i>	Saxifragaceae	24		
25	herb	<i>Saxifraga punctata</i>	Saxifragaceae	25		
26	herb	<i>Stellaria peduncularis</i>	Caryophyllaceae	26		
27	herb	<i>Tofieldia pusilla</i>	Liliaceae	27		
28	herb	<i>Utricularia ochroleuca</i>	Lentibulariaceae	28	16	
29	herb	<i>Utricularia vulgaris</i>	Lentibulariaceae	29	17	
30	herb	<i>Valeriana capitata</i>	Valerianaceae	30		
31	shrub	<i>Andromeda polyfolia</i>	Ericaceae	31	18	7
32	shrub	<i>Arctous alpina</i>	Ericaceae	32		8
	shrub	<i>Betula exilis (Betula nana ssp. exilis)</i>	Betulaceae	33	19	9
33						
34	shrub	<i>Duschekia sp.* (Alnaster)</i>	Betulaceae,	34		10

No	Layer	Species	Family	Herbarium	Species of the study site	Reference material
35	shrub	<i>Empetrum nigrum</i>	Empetraceae	35		11
36	shrub	<i>Ledum decumbens</i>	Ericaceae	36	20	12
37	shrub	<i>Rubus chamaemorus</i>	Rosaceae	37	21	13
38	shrub	<i>Salix myrtilloides</i>	Salicaceae	38	22	14
39	shrub	<i>Salix</i> sp. *	Salicaceae	39	23	15
40	shrub	<i>Vaccinium uliginosum</i>	Ericaceae	40	24	16
41	shrub	<i>Vaccinium vitis-idaea</i>	Ericaceae	41	25	17

*determination will follow in Greifswald

Tab. A 5-2: List of peat cores from the model polygon

Name of the peat profile	length	position	coordinates (yx)
LHC-11 j14,30	35 cm	center central depression	j14,30
LHC-11 j14,80	35 cm	central depression	j14,80
LHC-11 j17,80	60 cm	inner margin expanded ridge	j17,80
LHC-11 j18,80	120 cm	center expanded ridge	j18,80
LHC-11 j19,50	42 cm	outer margin expanded ridge	j19,50
LHC-11 j20,10	29 cm	collapsed expanded ridge	j20,10
LHC-11 j21,20	33 cm	collapsed wedge ridge	j21,20

APPENDIX 6 - DATA OF SOIL STUDIES (FIELD ANALYTICS)

Fabian Beerman

Since reliable water content data are only available for the samples from the peat cores, data of the water content and amounts of nutrients, calculated on the basis of the dry weights of the soils are only presented for these samples.

Tab. A 6-1: Analytical data of soil profiles of the eight different polygons are presented. Nutrient values are presented as measured values in extracts of CaCl_2 (NH_4^+ & NO_3^-) and Na_2HCO_3 (PO_4^{3-}), respectively.

Sample name	Nr	Date	pH	EC ($\mu\text{S/cm}$)	NH_4^+ (mg/l)	NO_3^- (mg/l)	PO_4^{3-} (mg/l)
KYTF 1.1. Oi	1	19.07.11	4.0	96	0.09	1.01	0.19
KYTF 1.1. Oe	2	19.07.11	4.3	59	0.50	0.90	0.06
KYTF 1.1. Bg	3	19.07.11	5.1	22	0.60	0.13	0.04
KYTF 1.2. Oi	4	19.07.11	4.4	49	0.35	0.52	0.10
KYTF 1.2. Oe	5	19.07.11	4.6	39	0.81	0.68	0.14
KYT 1.2 frozen ground	6	19.07.11	5.0	24	0.69	0.29	0.12
KYT 1.3. Oi	7	19.07.11	4.6	26	0.16	0.09	0.05
KYTF 1.3. Oe	8	19.07.11	4.9	13	1.10	0.10	0.05
KYTF 1.3. Bg	9	19.07.11	5.1	20	1.22	0.14	0.05
KYTF 1.4. Oi	10	19.07.11	5.3	25	0.12	0.33	0.28
KYTF 1.4. Oe	11	19.07.11	5.3	27	0.41	0.29	0.09
KYTF 2.1. Oe	15	20.07.11	4.2	49	0.25	0.48	0.12
KYTF 2.1. Oa	16	20.07.11	4.6	23	0.46	0.33	0.22
KYTF 2.1. Bg (jj?)	17	20.07.11	5.2	9	0.16	0.06	0.07
KYTF 2.2. Oi	18	20.07.11	4.2	40	0.22	0.84	0.09
KYTF 2.2. Oa	19	20.07.11	4.4	278	0.44	0.42	0.06
KYTF 2.2. frozen	20	20.07.11	4.9	24	0.33	0.50	0.06
KYTF 1.4. Bg	21	20.07.11	5.2	28	0.55	0.31	0.06
KYTF 2.3. Oi	22	23.07.11	4.9	23	0.42	0.32	0.04
KYTF 2.3. Oe	23	23.07.11	5.4	17	0.69	-0.10	0.04
KYTF 2.3. Oa	24	23.07.11	5.5	23	0.66	0.48	0.06
KYTF 2.3. Bg	25	23.07.11	5.8	31	0.51	0.22	0.17
KYTF 2.4. Oi	26	23.07.11	5.6	9	0.64	0.24	0.05
KYTF 2.4. Oe	27	23.07.11	5.6	20	0.67	0.38	0.04
KYTF 2.4. Oa	28	23.07.11	5.7	26	0.93	0.32	0.10
KYTF 2.5. Oi	29	23.07.11	5.7	10	0.67	0.24	0.04
KYTF 2.5. Oe	30	23.07.11	5.5	14	0.34	0.11	0.05
KYTF 2.6. Oi	31	23.07.11	5.4	20	0.51	0.18	0.06
KYTF 2.6. Oe	32	23.07.11	5.5	21	0.70	0.48	0.11
KYTF 2.6. Bg	33	23.07.11	5.8	36	1.05	0.11	0.12
KYTF 3.1. Oi	34	24.07.11	4.4	49	0.47	0.33	0.06

Sample name	Nr	Date	pH	EC ($\mu\text{S/cm}$)	NH_4^+ (mg/l)	NO_3^- (mg/l)	PO_4^{3-} (mg/l)
KYTF 3.1. Oe/Oa	35	24.07.11	5.4	16	1.20	0.60	0.05
KYTF 3.1. Bg	36	24.07.11	5.3	11	0.93	0.10	-0.05
KYTF 3.2. Oi	37	24.07.11	3.8	108	0.83	1.51	0.15
KYTF 3.2. Oe	38	24.07.11	4.2	44	0.67	0.54	0.05
KYTF 3.2. Oa	39	24.07.11	4.5	29	0.40	0.62	0.07
KYTF 3.3. Oi	40	24.07.11	4.3	33	0.57	0.57	0.10
KYTF 3.3. Oa	41	24.07.11	4.8	22	0.57	0.58	0.15
KYTF 3.3. Bg	42	24.07.11	4.9	18	1.76	0.34	0.12
KYTF 3.4.Oi	43	24.07.11	4.6	31	0.38	0.42	0.04
KYTF 3.4. Oe	44	24.07.11	4.8	16	0.72	0.46	0.09
KYTF 3.4. Bg	45	24.07.11	5.3	32	0.39	0.44	0.05
KYTF 4.1. Oi	46	25.07.11	4.1	99	0.34	0.61	0.07
KYTF 4.1. Oe	47	25.07.11	5.0	37	0.38	0.52	0.06
KYTF 4.1. frozen	48	25.07.11	5.4	49	0.35	0.30	0.04
KYTF 4.2. Oi	49	25.07.11	5.5	27	0.64	0.20	0.03
KYTF 4.2. Oe	50	25.07.11	5.3	25	0.66	0.47	0.05
KYTF 4.2. Oa	51	25.07.11	5.3	28	1.02	0.48	-0.06
KYTF 4.2. Bg	52	25.07.11	5.4	34	2.54	0.07	0.14
YED1 Ah	53	27.07.11	7.4	46	0.00	0.10	0.04
YED 1 Bgjj	54	27.07.11	7.5	39	0.20	0.13	0.10
KYTF 5.1. Oi	55	27.07.11	4.1	127	1.14	4.15	0.46
KYTF 5.1. Oe	56	27.07.11	4.5	39	0.04	0.54	0.09
KYTF 5.1. Oea	57	27.07.11	5.0	34	0.79	0.44	0.24
KYTF 5.1. Bg	58	27.07.11	5.1	13	0.13	0.09	0.62
KYTF 6.1. Oi	59	29.07.11	4.6	25	0.16	0.18	0.03
KYTF 6.1. Oie	60	29.07.11	4.5	26	0.24	0.39	0.01
KYTF 6.2. Oa	62	29.07.11	4.4	30	0.10	0.67	0.18
KYTF 6.2. Bh	63	29.07.11	5.0	13	0.07	0.16	0.06
KYTF 6.3. Oe	64	29.07.11	4.9	25	0.14	0.40	0.00
KYTF 6.3. Oi	65	29.07.11	5.4	28	0.33	0.87	0.03
KYTF 6.3. Oea	66	29.07.11	4.7	24	0.02	0.18	0.00
KYTF 6.4. Oi	67	29.07.11	5.1	19	1.60	0.81	0.07
KYTF 6.4. Oe	68	29.07.11	5.0	22	0.85	1.37	0.04
KYTF 6.4. Bg	69	29.07.11	5.8	42	0.48	0.33	0.04
KYTF 7.1. Oa	78	30.07.11	5.6	39	-0.14	0.39	0.11
KYTF 7.1. Oe	79	30.07.11	4.9	29	0.29	0.45	0.14
KYTF 7.1. Bgjj	80	30.07.11	5.2	20	0.18	0.13	0.06
KYTF 7.1. Bg	81	30.07.11	5.5	58	0.00	0.11	0.09
KYTF 7.2. Oi	82	30.07.11	4.2	63	0.79	5.81	0.23
KYTF 7.2. Oa	83	30.07.11	4.8	22	0.17	0.27	0.07
KYTF 7.2. Oe	84	30.07.11	5.0	15	0.16	0.89	0.04
KYTF 7.2. Bg	85	30.07.11	5.4	28	0.19	0.14	0.10
KYTF 7.3. Oi1 dunkel	86	04.08.11	5.6	55	1.13	0.22	0.09
KYTF 7.3. Oi2 hell	87	04.08.11	5.5	31	0.78	0.30	0.07
KYTF 7.3. Oa	88	04.08.11	5.3	22	0.40	0.47	0.07
KYTF 7.3. Bg	89	04.08.11	6.0	24	0.14	0.08	0.09

Sample name	Nr	Date	pH	EC ($\mu\text{S/cm}$)	NH_4^+ (mg/l)	NO_3^- (mg/l)	PO_4^{3-} (mg/l)
KYTF 7.4. Oe	90	04.08.11	5.3	23	0.35	0.30	0.08
KYTF 7.4. Oa	91	04.08.11	5.6	17	0.16	0.30	0.07
KYTF 7.4. Bg	92	04.08.11	5.7	27	0.12	0.21	0.06
KYTF 7.5. Oe	93	04.08.11	5.4	21	0.44	0.35	0.05
KYTF 7.5. Oa	94	04.08.11	5.7	31	0.29	0.47	0.10
KYTF 5.2. Oi	95	04.08.11	4.0	61	0.24	0.89	0.40
KYTF 5.2. Oa	96	04.08.11	4.5	25	0.12	0.87	0.11
KYTF 5.2. Bh	97	04.08.11	5.0	14	0.38	0.10	0.25
KYTF 5.3. Oi sph	98	04.08.11	4.5	32	0.0	0.26	0.06
KYTF 5.3. Oa	99	04.08.11	5.0	38	0.67	0.46	0.08
KYTF 5.4. Oe	100	04.08.11	5.1	16	0.27	0.25	0.05
KYTF 5.4. Oa	101	04.08.11	5.2	31	0.51	0.67	0.08
KYTF 5.4. Bg	102	04.08.11	5.5	52	1.87	0.18	0.06
KYTF 8.1. Oi	174	13.08.11	5.8	44	0.14	0.19	0.08
KYTF 8.1. Oe	175	13.08.11	6.1	17	0.25	0.31	0.03
KYTF 8.1. Bg	176	13.08.11	6.3	17	0.10	0.01	0.09
KYTF 8.2. Oi	177	13.08.11	5.9	22	0.21	0.33	0.05
KYTF 8.2. Oe1 braun	178	13.08.11	5.8	22	0.27	0.23	0.06
KYTF 8.2. Oe2 rötlich	179	13.08.11	5.7	16	0.33	0.23	0.03
KYTF 8.2. Oa	180	13.08.11	5.6	16	0.44	0.35	0.05
KYTF 8.2. Bg	181	13.08.11	6.1	17	0.26	0.08	0.03
KYTF 8.3.Oi	182	13.08.11	5.5	26	0.35	0.31	0.08
KYTF 8.3. Oe	183	13.08.11	5.5	15	0.0	0.21	0.02
KYTF 8.3. Oa	184	13.08.11	5.4	21	0.0	0.39	0.01
KYTF 8.4. Oe	185	13.08.11	5.5	14	0.34	0.22	0.01
KYTF 8.4. Oa	186	13.08.11	5.3	16	0.21	0.18	0.06
KYTF 3.4. Oi (2)	187	16.08.11	4.5	27	0.19	0.27	0.05
KYTF 3.4. Oa (2)	188	16.08.11	4.9	18	0.57	0.60	0.04
KYTF 3.4. Bg (2)	189	16.08.11	6.2	22	1.69	0.09	0.03
YED 2 Ah	233	18.08.11	4.1	39	0.17	0.67	0.10
YED2 Bhjj2	234	18.08.11	5.7	10	0.0	0.23	0.87
KYTF 4.1. Oi (2)	235	18.08.11	4.3	32	0.0	0.27	0.01
KYTF 4.1. Oe (2)	236	18.08.11	5.4	17	0.02	0.37	0.08
KYTF 4.1. Oa (2)	237	18.08.11	5.5	15	0.06	0.58	0.03
YED 2 Bhjj1	238	18.08.11	5.5	10	0.0	0.08	0.10
KYTF 1.1. (2) Oi	252	23.08.11	4.0	37	0.15	0.55	0.18
KYTF 1.1. (2) Oe	253	23.08.11	4.6	25	0.05	0.46	0.01
KYTF 1.1. (2) Bg	254	23.08.11	5.6	7	0.0	-0.01	0.16
KYTF 1.2. (2) Oi	255	23.08.11	4.3	36	0.09	0.61	0.10
KYTF 1.2. (2) Oe	256	23.08.11	5.4	18	0.76	0.52	0.13
KYTF 1.2. (2) Bg	257	23.08.11	5.8	21	1.17	0.11	0.21
KYTF 1.3. (2) Oi Sph	258	23.08.11	4.9	26	0.04	0.16	0.04
KYTF 1.3. (2) Oa	259	23.08.11	5.4	20	0.95	0.67	0.12
KYTF 1.3. (2) Bg	260	23.08.11	5.9	10	1.03	0.12	0.15
KYTF 1.3. (2) Oe	261	23.08.11	5.4	12	0.40	0.24	0.11
KYTF 1.4. (1) Oi	262	23.08.11	5.5	13	0.0	0.21	0.20
KYTF 1.4. (2) Oa	263	23.08.11	5.5	24	0.0	0.48	0.11

Tab. A 6-2: Analytical Data of the intensively investigated model polygon (LHC-11) are presented. Nutrient values are presented as measured values in extracts of CaCl_2 (NH_4^+ and NO_3^-) and Na_2HCO_3 (PO_4^{3-}), respectively.

Sample name	Nr	Date	pH	EC ($\mu\text{S/cm}$)	NH_4^+ (mg/l)	NO_3^- (mg/l)	PO_4^{3-} (mg/l)
HR 1 Oi	103	06.08.11	4.2	27	0.09	0.70	0.11
HR1 Oe	104	06.08.11	4.5	43	0.09	0.61	0.05
HR 1 Oa	105	06.08.11	5.0	19	0.23	0.36	0.06
HR 5 Oi	106	06.08.11	5.3	11	2.66	0.29	0.02
HR5Oe	107	06.08.11	5.2	15	0.58	0.35	0.03
HR5 Oa	108	06.08.11	5.1	21	1.11	0.65	0.10
HR9 Oi	109	06.08.11	5.3	16	0.15	0.24	0.06
HR9 Oe	110	06.08.11	5.3	14	0.15	0.22	0.08
HR9 Oa	111	06.08.11	5.1	13	0.52	0.43	0.07
HR13 Oi	112	06.08.11	5.2	17	0.18	0.23	0.07
HR13 Oe	113	06.08.11	5.2	17	0.31	0.19	0.37
HR13 Oa	114	06.08.11	5.3	10	0.75	0.50	0.05
HR17 Oi	115	06.08.11	4.0	43	0.15	1.00	0.07
HR17 Oa	116	06.08.11	4.8	19	0.19	0.49	0.08
HR17 Oe	117	06.08.11	5.3	17	0.12	0.30	0.02
HR21 Oi	118	06.08.11	5.2	9	0.56	0.27	0.05
HR21 Oe	119	06.08.11	5.2	13	0.61	0.35	0.04
HR21 Oa	120	06.08.11	5.2	15	0.17	0.42	0.06
HM1 Oe	121	07.08.11	5.6	57	0.60	0.46	0.03
HM1 Oa	122	07.08.11	5.7	21	0.47	0.44	0.06
HM5 Oa	123	07.08.11	5.7	24	0.34	0.35	0.04
HM5 Bg	124	07.08.11	6.2	50	1.10	0.19	0.11
HM5 Oi	125	07.08.11	5.9	17	0.47	0.28	0.04
HM9 Oi	126	07.08.11	5.4	21	0.31	0.20	0.07
HM9 Oe	127	07.08.11	5.4	25	0.83	0.55	0.06
HM9 Oa	128	07.08.11	5.8	37	1.46	0.37	0.08
HM9 Bg	129	07.08.11	6.0	71	2.73	0.12	0.10
Hm13 Oi	130	07.08.11	4.8	36	0.61	0.61	0.16
HM13 Oe	131	07.08.11	5.2	16	0.30	0.28	0.03
HM13Oa	132	07.08.11	5.4	12	0.28	0.52	0.03
HM17 Oi	133	07.08.11	4.1	94	0.17	0.71	0.12
HM17 Bhgjj	134	07.08.11	4.9	27	0.21	0.68	0.01
HM17 Bhg	135	07.08.11	5.2	19	0.24	0.46	0.08
HM21 Oi	136	07.08.11	5.3	13	0.13	0.14	0.03
HM21 Oe	137	07.08.11	5.4	20	0.33	0.21	0.04
HM21 Oa	138	07.08.11	5.6	20	0.21	0.63	0.04
HH1 Oe	139	07.08.11	5.6	9	0.28	0.21	0.04
HH1 Oa	140	07.08.11	5.5	19	0.12	0.39	0.08
HH17 Oi	141	08.08.11	5.2	43	0.31	0.34	0.03
HH17 Oe	142	08.08.11	5.4	24	0.46	0.46	0.04
HH17 Oa	143	08.08.11	5.6	25	0.53	0.95	0.02
HH14 Oe	144	08.08.11	5.7	22	0.61	0.50	0.03
HH14 Oa	145	08.08.11	5.8	25	0.0	0.90	0.01
HH9 Oi	146	08.08.11	5.2	20	0.10	0.43	0.28
HH9 Bh	147	08.08.11	5.6	51	0.0	0.71	0.06

Sample name	Nr	Date	pH	EC ($\mu\text{S/cm}$)	NH_4^+ (mg/l)	NO_3^- (mg/l)	PO_4^{3-} (mg/l)
HH9 Bg	148	08.08.11	5.8	27	0.0	0.41	0.06
HH9 Oe	149	08.08.11	5.5	39	0.24	0.61	0.04
HH5 Oi Sph	150	08.08.11	5.4	38	0.41	0.41	0.08
HH5 Oi Betula	151	08.08.11	5.7	26	0.19	0.55	0.04
HH5 Oa	152	08.08.11	5.9	28	0.20	0.34	0.06
HH21 Oi Bet	153	08.08.11	5.9	14	0.21	0.31	0.03
HH21 Oe (gleyic)	154	08.08.11	5.8	25	0.07	0.30	0.11
HH21 Oa	155	08.08.11	5.7	31	0.05	0.35	0.05
HC1 Oi	156	08.08.11	5.8	27	0.01	0.19	0.05
HC1 Oe	157	08.08.11	5.7	19	0.11	0.32	0.05
HC1 Oa	158	08.08.11	5.8	18	0.16	0.06	0.05
HC21 Oi Sph	159	09.08.11	6.4	10	0.41	0.28	0.03
HC21 Oi Betula	160	09.08.11	6.0	32	0.14	0.29	0.09
HC21 Oa	161	09.08.11	6.2	13	0.93	0.29	0.08
HC21 Bg	162	09.08.11	5.8	48	0.06	0.15	0.08
HC17 Oi Sph	163	09.08.11	6.1	12	0.52	0.16	0.01
HC17 Oe	164	09.08.11	6.0	15	1.13	0.26	0.08
HC17Oi Betula	165	09.08.11	5.8	17	0.32	0.22	0.10
HC17 Oe	166	09.08.11	5.7	29	1.36	0.43	0.09
HC13Oi Betula	167	09.08.11	5.8	18	0.84	0.40	0.04
HC13 Oe/Oa	168	09.08.11	5.8	27	0.0	0.40	0.06
HC13 Bg	169	09.08.11	5.8	47	0.74	0.15	0.08
HC5 Oi Sph	170	09.08.11	5.8	19	0.68	0.50	0.06
HC5 Oe Betula	171	09.08.11	5.7	40	0.93	0.90	0.11
HC5 Oa	172	09.08.11	5.8	12	0.60	0.33	0.07
HC5 Bg	173	09.08.11	5.6	37	0.22	0.69	0.09

Tab. A6-3: Analytical data of the peat cores of the intensively investigated polygon (LHC-11) are presented. Amounts of nutrients are shown in quantity (mol) of N and P, respectively, per dry mass of the soil.

Sample name	Nr	Date	Water content	pH	EC (µS/cm)	NH ₄ ⁺ -N (mmol/kg)	NO ₃ ⁻ -N (mmol/kg)	PO ₄ ³⁻ -P (mmol/kg)
J17.80 0-60 0-5	190	18.08.11	423.08%	4.2	39	0.27	0.66	0.50
J17.80 0-60 5-10	191	18.08.11	438.89%	4.1	40	0.22	0.98	0.48
J17.80 0-60 10-15	192	18.08.11	338.46%	4.5	27	0.15	0.53	0.54
J17.80 0-60 15-20	193	18.08.11	261.54%	5.2	21	0.19	0.14	0.31
J17.80 0-60 20-25	194	18.08.11	290.24%	5.7	19	0.30	0.38	0.28
J17.80 0-60 25-30	195	18.08.11	248.28%	5.6	24	0.09	0.27	0.24
J17.80 0-60 30-35	196	18.08.11	533.33%	5.6	17	0.41	0.92	0.09
J17.80 0-60 35-40	197	18.08.11	700.00%	5.6	17	2.06	0.98	0.26
J17.80 0-60 40-45	198	18.08.11	542.86%	5.6	22	0.77	0.43	0.27
J17.80 0-60 45-50	199	18.08.11	677.78%	5.3	64	2.15	1.24	0.29
J17.80 0-60 50-55	200	18.08.11	675.00%	5.6	33	1.91	0.94	0.54
J17.80 0-60 55-60	201	18.08.11	775.00%	5.5	30	3.10	1.01	0.42
J18.80 0-60 0-5	202	18.08.11	NA	NA	NA	NA	NA	NA
J18.80 0-60 5-10	203	18.08.11	427.27%	4.1	56	0.17	1.46	0.34
J18.80 0-60 10-15	204	18.08.11	468.75%	4.1	47	0.16	1.31	0.56
J18.80 0-60 15-20	205	18.08.11	304.55%	4.8	26	0.18	0.53	0.29
J18.80 0-60 20-25	206	18.08.11	262.07%	5.2	13	0.12	0.16	0.24
J18.80 0-60 25-30	207	18.08.11	320.00%	5.6	18	0.26	0.25	0.33
J18.80 0-60 30-35	208	18.08.11	361.90%	5.8	17	0.21	0.43	0.43
J18.80 0-60 35-40	209	18.08.11	572.73%	5.7	18	0.26	0.77	0.29
J18.80 0-60 40-45	210	18.08.11	500.00%	5.7	18	0.36	0.75	0.19
J18.80 0-60 45-50	211	18.08.11	625.00%	5.4	17	0.76	1.32	0.38
J18.80 0-60 50-55	212	18.08.11	583.33%	5.6	19	1.29	1.24	0.55
J18.80 60-120 60-65	213	18.08.11	661.54%	5.6	17	3.89	0.86	0.35
J18.80 60-120 65-70	214	18.08.11	700.00%	5.6	18	3.84	0.92	0.54
J18.80 60-120 70-75	215	18.08.11	777.78%	5.7	17	4.69	1.35	0.63
J18.80 60-120 75-80	216	18.08.11	850.00%	5.2	16	5.19	1.46	0.63
J18.80 60-120 80-85	217	18.08.11	828.57%	5.4	16	4.42	1.22	0.40
J18.80 60-120 85-90	218	18.08.11	614.29%	5.4	21	3.91	1.43	0.76
J18.80 60-120 90-95	219	18.08.11	714.29%	5.8	18	4.04	1.12	0.94
J18.80 60-120 95-100	220	18.08.11	506.25%	5.6	22	3.47	0.95	0.78
J18.80 60-120 100-105	221	18.08.11	483.33%	5.9	24	3.64	0.84	0.98
J18.80 60-120 105-110	222	18.08.11	466.67%	5.9	19	3.24	0.93	1.05
J18.80 60-120 110-115	223	18.08.11	504.76%	6.0	15	3.10	1.15	1.27
J19.50 0-42 0-5	224	18.08.11	545.45%	4.1	63	0.01	1.18	1.13
J19.50 0-42 5-10	225	18.08.11	450.00%	4.8	40	0.00	0.89	0.63
J19.50 0-42 10-15	226	18.08.11	304.00%	5.0	17	0.00	0.29	0.63
J19.50 0-42 15-20	227	18.08.11	254.55%	5.8	8	0.06	0.31	0.46
J19.50 0-42 20-25	228	18.08.11	456.25%	5.5	10	0.26	1.30	0.61
J19.50 0-42 25-30	229	18.08.11	646.15%	5.5	11	0.19	0.85	0.49
J19.50 0-42 30-35	230	18.08.11	600.00%	5.4	15	0.14	0.56	0.80
J19.50 0-42 35-40	231	18.08.11	588.89%	5.2	14	0.22	0.66	0.84
J19.50 0-42 40-42	232	18.08.11	658.33%	5.2	12	0.33	0.55	1.43
J20.20 0-29 0-5	239	22.08.11	NA	NA	NA	NA	NA	NA
J20.20 0-29 5-10	240	22.08.11	NA	NA	NA	NA	NA	NA

Sample name	Nr	Date	Water content	pH	EC (µS/cm)	NH₄⁺-N (mmol/kg)	NO₃⁻-N (mmol/kg)	PO₄³⁻-P (mmol/kg)
J20.20 0-29 10-15	241	22.08.11	NA	NA	NA	NA	NA	NA
J20.20 0-29 15-20	242	22.08.11	NA	NA	NA	NA	NA	NA
J20.20 0-29 20-25	243	22.08.11	NA	NA	NA	NA	NA	NA
J20.20 0-29 25-29	244	22.08.11	NA	NA	NA	NA	NA	NA
J21.20 0-33 0-5	245	22.08.11	820.00%	5.3	45	0.21	1.76	1.10
J21.20 0-33 5-10	246	22.08.11	1000.00%	5.5	33	0.24	1.41	1.39
J21.20 0-33 10-15	247	22.08.11	1116.67%	5.6	10	0.18	0.64	0.43
J21.20 0-33 15-20	248	22.08.11	683.33%	5.3	15	0.38	0.84	0.66
J21.20 0-33 20-25	249	22.08.11	336.84%	5.3	12	0.21	0.37	0.85
J21.20 0-33 25-30	250	22.08.11	390.00%	5.5	16	0.35	0.48	0.86
J21.20 0-33 30-33	251	22.08.11	365.38%	5.6	8	0.32	0.28	0.45

APPENDIX 7 - SAMPLES FROM PERMAFROST DEPOSITS

Lutz Schirrmeister

Sample code	Date	height (m)	Cryotexture	Sediment	ice grav. (wt%)	ice abs. (wt%)	TI	pH	EC (µS/cm)
Yedoma									
11KH-3007-1-1	30.07	0.15	a.l., unfrozen	grey-brown/light-grey, spotty, partly banded, clayish silty, rooted					
11KH-3007-1-2	30.07.	0.30	horizontal	dark-brown/reddish-brown	102.8	50.7	x		
11KH-3007-1-3	30.07.	0.45	lens-like to coarse lens-like (1-3 mm thick, 2-4 mm long)	cryoturbation structures, matrix gray-brown silt	110.7	52.5	x		
11KH-3007-1-4	30.07.	0.60			150.7	60.1			
11KH-3007-1-6	30.07.	1.20	fine to coarse		134.6	57.4	x	6.8	574
11KH-3007-1-7	30.07.	1.40	lens-like (1-3 mm thick, 1-4 cm long)	grey-brown, no organic visible	54.5	35.3	x		
11KH-3007-1-8	30.07.	1.60			74.6	42.7	x	7.4	622
11KH-3007-1-9	30.07.	1.90			116.3	53.8	x	7.6	998
11KH-3007-1-10	30	2.00		light-brown, grey, black patches (2-5 mm) root	66.7	40.0	x		
11KH-3007-1-11	30.07.	2.15	horizontal		48.5	32.6			
11KH-3007-1-12	30.07.	2.35	micro-lens-like (< 1mm thick, 3-10 mm long)	remains (?), numerous vertical thin roots	50.4	33.5			
11KH-3007-1-13	30.07.	2.55			76.6	43.4			
11KH-3007-1-15	24.08.	4.20		grey-brown, single black patches (< 1mm), single grass roots, small wood remains	48.1	32.5	x		
11KH-3007-1-16	24.08.	4.40	micro-lens-like to massive		58.6	36.9	x		
11KH-3007-1-17	24.08.	4.60			58.5	36.9	x		

Sample code	Date	depth (m)	Cryotexture	Sediment	ice grav. (wt%)	ice abs. (wt%)	TI	pH	EC (µS/cm)
Pingo									
11KH-2807-1-1	28.7.	4.25	unfrozen	grey-brown, active layer, loamy, rootlets, aggregates 2-3 mm large, pedogenic altered lake deposits					
11KH-2807-1-2	28.07.	3.95	unfrozen	brownish, partly coloured by iron-hydroxide, silty fine-sand, lake deposits, horizontal bedded, crumbly (1-5 cm blocks)					
11KH-2807-1-3	28.07.	3.55	Diagonal,		83.3	45.5			
11KH-2807-1-4	28.07.	3.15	lattice,		75.5	43.0			
11KH-2807-1-5	28.07.	2.75	probably postcryogenic		50.8	33.7			
11KH-2807-1-6	28.07.	2.35	structures,	grey-brown, clayish fine-silt,	39.1	28.1			
11KH-2807-1-7	28.07.	2.05	size of ice veins (1-3	1-3 mm thick	62.4	38.4			
11KH-2807-1-8	28.07.	1.65	mm wide, 5-	plant detritus	48.4	32.6			
11KH-2807-1-9	28.07.	1.25	10 cm long)	layers, ripple-bedding	54.4	35.3			
11KH-2807-1-10	28.07.	0.85	and sediment blocks are increasing downward		45.2	31.1			
11KH-2807-1-11	28.07.	0.55			47.9	32.4			
11KH-2807-1-12	28.07.	0.15	lens-like, horizontal	brownish, altered lake deposits	88.1	46.8	x	5.7	442
11KH-2807-1-13	28.07.	0.05	see 11KH-2807-1-3 to 1-10	see 11KH-2807-1-3 to 1-11	48.0	32.4			
Ice cellar									
11KH-2607-1-1	26.07.		massive	light brownish grey, silt			x	6.1	995
Drill sites									
KYT-1 Drill-1	19.07.	0.25-0.33	not frozen	alas deposits; silty loam, brownish-grey					
KYT-1 Drill-2	19.07.	0.39-0.45	cellular-net cryogenic structure	alas deposits; silty loam, brownish-grey					
KYT-1 Drill-3	19.07.	0.48-0.52	net cryogenic structure (ice lenses up to 2-3 mm thick)	alas deposits; silty loam, brownish-grey					

Sample code	Date	depth (m)	Cryotexture	Sediment	ice grav. (wt%)	ice abs. (wt%)	TI	pH	EC (µS/cm)
KYT-1 Drill-4	19.07.	0.52-0.565	net cryogenic structure (ice lens thickness up to 2-3 mm)	alas deposits; silty loam, brownish-grey					
KYT-1 Drill-5	19.07.	0.565-0.585	net cryogenic structure (ice lens thickness up to 2-3 mm)	alas deposits; silty loam, brownish-grey					
KYT-1 Drill-6	19.07.	0.585-0.65	net cryogenic structure (ice lens thickness up to 2-3 mm)	alas deposits; silty loam, brownish-grey					
Pits									
11KH-2107-2-2	21.07.		Net-like, ice lenses 1.5 mm thick,	grey, silty, loam					
11KH-2707-1-1	27.07.	0.92-0.96	porphiric cryogenic structure	alas deposits, peat brown					
11KH-2707-1-2	27.07.	0.96-1.01	porphiric cryogenic structure	alas deposits, peat brown					
11KH-2707-1-3	27.07.	1.01-1.05	porphiric cryogenic structure	alas deposits, peat brown					
11KH-2008-1-1	20.08.	0-0.01	not frozen	aluvial deposits of Berelekh, sand					
11KH-2008-1-2	20.08.	0.18-0.27	not frozen	aluvial deposits of Berelekh, loamy sand					
11KH-2008-1-3	20.08.	0.5-0.55	not frozen	aluvial deposits of Berelekh, loamy sand					

APPENDIX 8 - LIST OF WATER, ICE AND RAIN SAMPLES

Lutz Schirrmeister, Andrea Schneider & Evgenya Zhukova

(IW - ice wedge, TI - texture ice, PW - pond water, R - rain, RW - River water)

Sample code	Date	Type	distance (cm)	Isotopes	Cations	Anions	back-up solid fraction	pH	EC
Ice cellar									
11KH-2607-1-1	26.07.2011	TI						6.1	995
11KH-2607-1-2	26.07.2011	IW		x			x	7.2	633
11KH-2607-1-3	26.07.2011	IW		x	x	x	x	7.4	41
11KH-2607-1-4	26.07.2011	IW		x	x	x	x	7.1	73
11KH-2607-1-5	26.07.2011	IW		x			x	6.9	65
11KH-2607-1-6	26.07.2011	IW		x			x	6.8	49
11KH-2607-1-7	26.07.2011	IW		x			x	6.8	35
11KH-2607-1-8	26.07.2011	IW		x			x	6.7	30
11KH-2607-1-9	26.07.2011	IW		x			x	6.5	61
11KH-2607-1-10	26.07.2011	IW		x			x	6.6	45
11KH-2607-1-11	26.07.2011	IW		x			x	6.7	39
11KH-2607-1-12	26.07.2011	IW		x			x	6.6	29
11KH-2607-1-13	26.07.2011	IW		x			x	6.5	28
11KH-2607-1-14	26.07.2011	IW		x			x	6.5	29
11KH-2607-1-15	26.07.2011	IW		x			x	6.4	32
11KH-2607-1-16	26.07.2011	IW		x			x	6.4	30
11KH-2607-1-17	26.07.2011	IW		x			x	6.4	28
11KH-2607-1-18	26.07.2011	IW		x			x	6.7	36
11KH-2607-1-19	26.07.2011	IW		x	x	x	x	7.3	32
11KH-2607-1-20	26.07.2011	IW		x	x	x		7.3	27
11KH-2607-1-21	26.07.2011	IW		x	x	x		7.2	29
11KH-2607-1-22	26.07.2011	IW		x			x	7.0	39
11KH-2607-1-23	26.07.2011	IW		x			x	6.7	35
11KH-2607-1-24	26.07.2011	IW		x	x	x	x	6.8	32
11KH-2607-1-25	26.07.2011	IW		x			x	6.6	30
11KH-2607-1-26	26.07.2011	IW		x			x	6.5	44
11KH-2607-1-27	26.07.2011	clear ice		x	x	x		6.6	16
11KH-2607-1-28	26.07.2011	clear ice		x	x	x		6.9	7
11KH-2607-1-29	26.07.2011	clear ice		x	x	x	x	6.9	7
11KH-2607-1-30	26.07.2011	ice crystal		x				6.5	16
Pingo exposure									
11KH-2807-1-12		TI		x				5.7	442

Sample code	Date	Type	distance (cm)	Isotopes	Cations	Anions	back-up fraction	pH	EC
Yedoma exposure									
11KH-3007-2-1	30.07.2011	IW (Holocene)	10	x					
11KH-3007-2-2	30.07.2011	IW (Holocene)	10	x					
11KH-3007-2-3	30.07.2011	IW (Yedoma)	10	x					
11KH-3007-2-4	30.07.2011	IW (Yedoma)	10	x					
11KH-3007-2-5	30.07.2011	IW (Yedoma)	10	x					
11KH-3007-2-6	30.07.2011	IW (Yedoma)	10	x					
11KH-3007-2-7	30.07.2011	IW (Yedoma)	20	x					
11KH-3007-2-8	30.07.2011	IW (Yedoma)	20	x					
11KH-3007-2-9	30.07.2011	IW (Yedoma)	20	x					
11KH-3007-2-10	30.07.2011	IW (Yedoma)	20	x					
11KH-3007-2-11	30.07.2011	IW (Yedoma)	20	x					
11KH-3007-2-12	30.07.2011	IW (Yedoma)	20	x					
11KH-3007-2-13	30.07.2011	IW (Yedoma)	20	x					
11KH-3007-2-14	30.07.2011	IW (Yedoma)	20	x					
11KH-3007-2-15	30.07.2011	IW (Yedoma)	20	x					
11KH-3007-2-16	30.07.2011	IW (Yedoma)	20	x					
11KH-3007-2-17	30.07.2011	IW (Yedoma)	20	x					
11KH-3007-2-18	30.07.2011	IW (Yedoma)	20	x					
11KH-3007-2-19	30.07.2011	IW (Yedoma)	20	x					
11KH-3007-2-20	30.07.2011	IW (Yedoma)	20	x					
11KH-3007-1-2	30.07.2011	TI		x					
11KH-3007-1-3	30.07.2011	TI		x					
11KH-3007-1-5	30.07.2011	TI		x			6.5	588	
11KH-3007-1-6	30.07.2011	TI		x			6.8	574	
11KH-3007-1-7	30.07.2011	TI		x					
11KH-3007-1-8	30.07.2011	TI		x			7.4	622	
11KH-3007-1-9	30.07.2011	TI		x			7.6	998	
11KH-3007-1-10	30.07.2011	TI		x					
11KH-3007-1-14	30.07.2011	TI		x					
11KH-3007-1-15	30.07.2011	TI		x					
11KH-3007-1-16	30.07.2011	TI		x					
11KH-3007-1-17	30.07.2011	TI		x					

Sample code	Date	Type	distance (cm)	Isotopes	Cations	Anions	back-up soils fraction	pH	EC
Pond water									
KYT-2	21.7.2011	PW		x	x	x	x	5.6	53
KYT-3	23.7.2011	PW		x	x	x	x	5.5	23
KYT-4	23.7.2011	PW		x	x	x	x	5.6	20
KYT-5	3.8.2011	PW		x	x	x	x	6.4	25
KYT-6	27.7.2011	PW		x	x	x	x	6.4	153
KYT-7	28.7.2011	PW		x	x	x	x	6.8	21
KYT-8	3.8.2011	PW		x	x	x	x	6.7	34
KYT-9	4.8.2011	PW		x	x	x	x	6.2	28
KYT-10	4.8.2011	PW		x	x	x	x	6.2	36
KYT-11	4.8.2011	PW		x	x	x	x	6.3	42
KYT-12	6.8.2011	PW		x	x	x	x	6.4	20
KYT-13	6.8.2011	PW		x	x	x	x	6.3	23
KYT-14	12.8.2011	PW		x	x	x	x	5.8	28
KYT-15	12.8.2011	PW		x	x	x	x	5.8	31
KYT-16	13.8.2011	PW		x	x	x	x	6.2	22
KYT-17	13.8.2011	PW		x	x	x	x	6.4	31
KYT-18	15.8.2011	PW		x	x	x	x	6.3	29
KYT-19	15.8.2011	PW		x	x	x	x	6.6	61
KYT-20	16.8.2011	PW		x	x	x	x	6.2	22
KYT-21	16.8.2011	PW		x	x	x	x	6.3	19
KYT-22	18.8.2011	PW		x	x	x	x	6.5	29
KYT-23	18.8.2011	PW		x	x	x	x	6.7	35
KYT-24	20.8.2011	PW		x	x	x	x	6.6	44
KYT-25	22.8.2011	PW		x	x	x	x	7.0	37
KYT-26	22.8.2011	PW		x	x	x	x	7.1	28
KYT-27	24.8.2011	PW		x	x	x	x	6.3	20
KYT-1-1	19.7.2011	PW		x	x	x	x	6.2	23
KYT-1-2	24.7.2011	PW		x	x	x	x	5.9	17
KYT-1-3	28.7.2011	PW		x	x	x	x	6.4	21
KYT-1-4	1.8.2011	PW		x	x	x	x	5.6	21
KYT-1-5	5.8.2011	PW		x	x	x	x	6.3	18
KYT-1-6	9.8.2011	PW		x	x	x	x	7.6	26
KYT-1-7	13.8.2011	PW		x	x	x	x	6.1	18
KYT-1-8	17.8.2011	PW		x	x	x	x	6.5	21
KYT-1-9	21.8.2011	PW		x	x	x	x	6.2	21
KYT-1-10	25.8.2011	PW		x	x	x	x	6.0	21

Sample code	Date	Type	distance (cm)	Iso-topes	Cations	Anions	back-up fraction	pH	EC
Kytalyk Rainwater									
(1)	22.7.11 17:00			x					
(2)	23.7.11 23:00			x					
(3)	26.7.11 1:00			x					
(4)	26.7.11 11:00			x					
(5)	26.7.11 18:00			x					
(6a)	28.7.11 2:00			x					
(6b)	29.7.11 10:00	R		x					
(7)	2.8.11 16:20	R		x					
(8)	2.8.11 20:00	R		x					
(9)	6.8.11 19:00	R		x					
(10)	7.8.11 1:00	R		x					
(11)	11.8.11 19:00	R		x					
(12)	12.8.11 10:30	R		x					
(13)	13.8.11 0:30	R		x					
(14)	14.8.11 6:00	R		x					
(15)	18.8.11 9:30	R		x					
(16)	18.8.11 13:00	R		x					
(17)	19.8.11 9:00	R		x					
(18)	20.8.11 8:30	R		x					
(19)	21.8.11 9:00	R		x					
(20)	21.8.11 14:00	R		x					
(21)	22.8.11 0:30	R		x					
Additional samples									
11D-1408-3-2	14.08.2011			x					
11D-1408-3-3	14.08.2011			x					
11D-1408-LAKE	14.08.2011			x					
11N-1008-1-1	10.08.2011			x					
11KH-2308-7-1	23.08.2011			x					
11KH-2408-2-1	24.08.2011			x					
Yedoma lake	24.08.2011	PW		x					
11B-2508-2-6	25.08.2011			x					
11B-2508-2-12	25.08.2011			x					
11B-2508-2-13	25.08.2011			x					
11B-2508-2-14	25.08.2011			x					
11B-2508-2-15	25.08.2011			x					
11B-2508-2-16	25.08.2011			x					
11B-2508-2-17	25.08.2011			x					
11B-2508-2-18	25.08.2011			x					

Sample code	Date	Type	distance (cm)	Iso-topes	Cations	Anions	back-up fraction	pH	EC
11AA-3008-1-3	30.08.2011	TI	7.5 m	x					
11AA-3008-1-4	30.08.2011	TI	9.0 m	x					
11AA-3008-1-6	30.08.2011	TI	10.05 m	x					
11AA-3008-1-13	30.08.2011	IW (shoulder)	10.7 m	x					
11AA-3008-1-14	30.08.2011	IW 2nd generation	10.8 m	x					
11AA-3008-1-15	30.08.2011	IW 1st generation	10.5 m	x					
11AA-3008-1-16	30.08.2011	IW 1st generation	10.5 m	x					
11AA-3008-1-17	30.08.2011	IW 1st generation	10.5 m	x					
11AA-3008-1-18	30.08.2011	IW (top)	10.8 m	x					
11AA-3008-1-19	30.08.2011	IW 1st generation	10.5 m	x					
11AA-3008-1-20	30.08.2011	IW 1st generation	10.5 m	x					
11AA-3008-1-21	30.08.2011	IW 1st generation	10.5 m	x					
11AA-3008-1-22	30.08.2011	IW (top)	10.8 m	x					
KYT-1-IC-1		IW (modern)		x					
KYT-1-IC-2		TI (ice lens)		x					
11KH-2107-1-1	21.07.2011	segregation ice		x				6.4	34
11KH-2107-1-2	21.07.2011	IW		x				6.4	23
11KH-2107-2-1	21.07.2011	IW		x					
11KH-2307-1-1	23.07.2011	TI		x					
LHC-11 J 14,30 -1		IW (center)		x					
LHC-11 J 14,30 -2		IW (center)		x	x	x	x		
LHC-11 J 19,00 -1		IW (wall)		x	x	x			
Alasflüsschen		RW		x	x	x	x	6.3	21
Berelekh-Wasser		RW		x	x	x	x	6.4	22
J1880 Hans Site (LHC 11)		IW (wall)		x					
Hans Palsa		TI (ice lens)	120 cm depth	x					

APPENDIX 9 - WATER SALINITY IN SURFACE WATER AND TEXTURE ICE

(Conductometer COM-100, for NaCl)

Vladimir Tumskoy

Data	Location	Salinity, ppm
Surface water		
20.08.2011	Berelekh water near coast	12
20.08.2011	Ground water on floodplain beach of Berelekh river	114-117
23.08.2011	Berelekh floodplain polygonal ponds	7, 5, 12
18.07.2011	Kytalyk alas, lower level, polygonal ponds (in 3 different ponds)	15, 17, 19
29.07.2011	Kytalyk alas, lower level, polygonal ponds (in 3 different ponds)	13.5, 13, 13.4, 13, 14.3
22.08.2011	Kytalyk area, alas eastward from Kytalyk, lower level, polygonal ponds	10.8, 12
22.08.2011	Kytalyk area, alas eastward from Kytalyk, upper level, polygonal ponds	8.7, 8.3, 7.7, 9.1
18.07.2011	Kytalyk alas, upper level, polygonal ponds	15, 10, 23, 16
05.08.2011	Dzhardakh alas lake, open water	17-18
05.08.2011	Dzhardakh alas lake, pool near the coast	22
05.08.2011	Dzhardakh alas, ground water of active layer	280-290
08.08.2011	Nyuchcha-Kyuele alas, lower level, depression over thawing ice wedge	29.5; 32; 30.1
08.08.2011	Nyuchcha-Kyuele alas, lower level, ground water in active layer near the center of polygon	35.5
13.08.2011	Dzhelon-Sise highland, water in lake	12.5
13.08.2011	Dzhelon-Sise Highland, water in small stream between alases	6
Texture ice of the Yedoma exposure "Kosoe"		
25.08.2011	16.2 m above lake level	740
25.08.2011	16.8 m	290
25.08.2011	17.4 m	680
25.08.2011	18.4 m	290
25.08.2011	20.5 m	130
25.08.2011	20.6 m	490
25.08.2011	22.1 m	460
25.08.2011	22.6 m	450

Die "**Berichte zur Polar- und Meeresforschung**" (ISSN 1866-3192) werden beginnend mit dem Heft Nr. 569 (2008) als Open-Access-Publikation herausgegeben. Ein Verzeichnis aller Hefte einschließlich der Druckausgaben (Heft 377-568) sowie der früheren "**Berichte zur Polarforschung**" (Heft 1-376, von 1981 bis 2000) befindet sich im open access institutional repository for publications and presentations (**ePIC**) des AWI unter der URL <http://epic.awi.de>. Durch Auswahl "Reports on Polar- and Marine Research" (via "browse"/"type") wird eine Liste der Publikationen sortiert nach Heftnummer innerhalb der absteigenden chronologischen Reihenfolge der Jahrgänge erzeugt.

To generate a list of all Reports past issues, use the following URL: <http://epic.awi.de> and select "browse"/"type" to browse "Reports on Polar and Marine Research". A chronological list in declining order, issues chronological, will be produced, and pdf-icons shown for open access download.

Verzeichnis der zuletzt erschienenen Hefte:

Heft-Nr. 641/2012 — "The Expedition of the Research Vessel 'Maria S. Merian' to the South Atlantic in 2011 (MSM 19/2)", edited by Gabriele Uenzelmann-Neben

Heft-Nr. 642/2012 — "Russian-German Cooperation SYSTEM LAPTEV SEA: The Expedition LENA 2008", edited by Dirk Wagner, Paul Overduin, Mikhail N. Grigoriev, Christian Knoblauch, and Dimitry Yu. Bolshiyarov

Heft-Nr. 643/2012 — "The Expedition of the Research Vessel 'Sonne' to the subpolar North Pacific and the Bering Sea in 2009 (SO202-INOPEX)", edited by Rainer Gersonde

Heft-Nr. 644/2012 — "The Expedition of the Research Vessel 'Polarstern' to the Antarctic in 2011 (ANT-XXVII/3)", edited by Rainer Knust, Dieter Gerdes and Katja Mintenbeck

Heft-Nr. 645/2012 — "The Expedition of the Research Vessel 'Polarstern' to the Arctic in 2011 (ARK-XXVI/2)", edited by Michael Klages

Heft-Nr. 646/2012 — "The Expedition of the Research Vessel 'Polarstern' to the Antarctic in 2011/12 (ANT-XXVIII/2)", edited by Gerhard Kattner

Heft-Nr. 647/2012 — "The Expedition of the Research Vessel 'Polarstern' to the Arctic in 2011 (ARK-XXVI/1)", edited by Agnieszka Beszczynska-Möller

Heft-Nr. 648/2012 — "Interannual and decadal variability of sea ice drift, concentration and thickness in the Weddell Sea", by Sandra Schwegmann

Heft-Nr. 649/2012 — "The Expedition of the Research Vessel 'Polarstern' to the Arctic in 2011 (ARK-XXVI/3 - TransArc)", edited by Ursula Schauer

Heft-Nr. 650/2012 — "Combining stationary Ocean Models and mean dynamic Topography Data", by Grit Freiwald

Heft-Nr. 651/2012 — "Phlorotannins as UV-protective substances in early developmental stages of brown algae", by Franciska S. Steinhoff

Heft-Nr. 652/2012 — "The Expedition of the Research Vessel 'Polarstern' to the Antarctic in 2012 (ANT-XXVIII/4)", edited by Magnus Lucassen

Heft-Nr. 653/2012 — "Joint Russian-German Polygon Project East Siberia 2011 - 2014: The expedition Kytalyk 2011", edited by Lutz Schirrmeister, Lyudmila Pestryakova, Sebastian Wetterich and Vladimir Tumskoy